Genetics of *Drosophila* hearing

Dissertation

for the award of the degree

"Doctor rerum naturalium"

Division of Mathematics and Natural Sciences

of the Georg-August-Universität Göttingen

within the doctoral program *Sensory and Motor Neuroscience* (SMN)

of the Georg-August University School of Science (GAUSS)

Submitted by

David Piepenbrock

born in Marburg, Germany, September 29th, 1983

Göttingen, 2013

Members of Thesis Committee

Prof. Dr. Martin Göpfert (Supervisor)

Georg-August-University of Göttingen, Cellular Neurobiology

Prof. Dr. Tobias Moser

Georg-August-University of Göttingen, Otolaryngology, Inner Ear Lab

Prof. Dr. André Fiala

Georg-August-University of Göttingen, Molecular Neurobiology of Behaviour

Oral examination: September 27th, 2013

Herewith I declare that I prepared this doctoral thesis entitled "Genetics of *Drosophila* hearing" on my own, with no other sources and aids than quoted.

_____

David Piepenbrock

Göttingen, August 22nd, 2013

Table of contents

Abstract

By probing Johnston's organ function in mutant fly strains, mutations in forty-four genes that affect *Drosophila* hearing have been identified. This result increases the list of genes that are known for audition by 180 % (forty-four new versus twenty-four old). I defined several auditory categories based on the change in auditory performance: nine mutations severely impaired Johnston's organ function, twenty-nine moderately, and six are hypersensitive. This list of hearing genes includes motor proteins, ion channels, and genes that are involved in response to light. With this surprising result, I screened for contributions of genes of the phototransduction cascade to *Drosophila* hearing, and found that key proteins of the cascade functionally contribute to hearing. Probing correlates of transducer gating revealed that rhodopsins affect mechano-electrical transduction and antibody staining indicates that rhodopsins are expression in Johnston's organ neurons. In addition, my analysis of flies with duplicated NOMPC ankyrin residues foster the hypothesis that ankyrins may act as gating springs that convey mechanical force to transduction channels.

Preface

We perceive our environment with at least five senses (Ernst and Bülthoff 2004): Audition, vision, taste, smell and touch. With these senses we detect: sound, light, taste, smell and pressure. Among these senses, hearing might be the most important one, since it mediates communication. This becomes noticeable when this sense is impaired:

> *"Hearing impairment negatively impacts social communication and carries a strong stigma" due to "communication problems for those with hearing impairment"* (Wahl et al. 2013)[1].

Beside this incentive reason, my motivation arises from the unsolved question which molecular parts transduce sounds into cellular electrochemical signals.

The objective of this doctoral thesis is to foster our understanding about the genetic basis of hearing. Since genes encode the 'blueprint' of molecular structures and pathways (Henry et al. 2010; Moreira et al. 2012), I put them into focus in order to understand the biological processes of hearing.

Hearing

Hearing is a specialized form of mechanosensation, which is widespread amongst organisms ranging from single bacteria, which are able to sense mechanical force, e.g. osmotic pressure (Sukharev and Sachs 2012), to humans who are able to detect sound pressure in a large range of intensities and frequencies.

---

[1] Wahl, H.-W., V. Heyl, P. M. Drapaniotis, K. Hörmann, J. B. Jonas, P. K. Plinkert, and K. Rohrschneider. 2013. Severe Vision and Hearing Impairment and Successful Aging: A Multidimensional View. The Gerontologist. page 2 of 13

Some organs and structures are specialized in sensing mechanical force. The mechanical force acts directly on the organs by deflecting, stretching, or compressing the structure, i.e. a hair or an insect bristle or antenna (Held 1991; Göpfert and Robert 2002). This mechanical deformation is conveyed to mechanosensory neurons (Caldwell and Eberl 2002), that transduce the mechanical force into cellular electrochemical signals. These signals are transmitted to processing brain regions where the information of these signals are analyzed (Munkong and Juang 2008; Tootoonian et al. 2012).

Animals perceive objects by processing sensory information that is encoded in graded signals, the frequency of action potentials, and by comparing inputs of different neurons. Humans use their tactile sense for example to search for keyboard keys to write a thesis. Additionally, we are able to detect mechanical stimuli such as sound. Sound, for example, can be caused by a loudspeaker, where a membrane vibration creates sound pressure and sound particle velocity. Whereas humans detect the sound pressure, insects like the model organism that I used *Drosophila melanogaster* are able to detect the particle velocity (Göpfert and Robert 2002).

Human hearing covers frequencies from circa 20 Hz to 20 kHz within a large intensity range. Our ear drum, the tympanum, detects changes in sound pressure. Vibrations of the tympanum are conveyed by the middle ear bones, the *hammer*, the *incus* and the *stapes*, through the middle ear to the oval window, eliciting a traveling wave in the fluid filled cochlea, the inner ear. Due to the stiffness, mass, and width of the basilar membrane, high frequencies displace more basal parts, whereas low frequencies lead to vibrations in the apical part of the chochlea. This spatial mapping is named 'tonotopy'. Deformations of the *organ of Corti* lead to deflections of inner hair cell stereocilia. This deflection results in the gating of ion channels, which transduce the mechanical force into a cellular electrochemical signal (Hudspeth 1989; Fettiplace and Hackney 2006; Rüdiger and Walter 2007; Olson et al. 2012).

The genetic model organism *Drosophila melanogaster*

I used *Drosophila melanogaster* as a genetic model system in order to investigate the genetic basis of hearing because of its many advantages: *Drosophila* has a short generation cycle, many offspring, is easy to handle, and its genome is fully sequenced. Most importantly though, *Drosophila* is able to hear – it perceives sound via antennal ears. These ears, in turn, are amenable to genetic and functional investigations, offering many opportunities to assess the relation between hearing defects and genes.

Due to the striking similarities between fly and vertebrate hearing, *Drosophila* can be considered as a model to study the genetic basis of hearing. These similarities include the functional equivalence of the auditory transduction and adaptation machineries, the motility of auditory sensory cells, transducer-based force generation, and the expression of homologous genes (Göpfert and Robert 2001; Albert et al. 2007a; Albert et al. 2007b; Kamikouchi et al. 2009). In *Drosophila* and humans alike, hearing is based on dedicated mechano-electrical transduction machineries that seem to

consist of a) a directly gated mechano-electrical transduction channel (MET) and b) a gating spring that connects mechanical stimuli to that channel.

Physiology of *Drosophila* hearing

Different hearing organs occur within insects. E.g. caterpillars sense sound via trichoid sensilla, ants with the subgenual organ in their tibia, butterflies with tympanal organs and dipteran flies such as *Drosophila melanogaster* with its antennal ears (Yack 2004).

Acoustic communication of *Drosophila* is used during courtship and to defend territories (Jonsson et al. 2011). To facilitate courtship, male flies vibrate their wing and produce a 'love song' (Hall 1994; Caldwell and Eberl 2002; Tootoonian et al. 2012). This song is composed of sine and pulse components, whereas the pulse lasts circa 10 ms, the sine has a carrier frequency of circa 160 Hz (Göpfert and Robert 2002; Jonsson et al. 2011).

The antenna of *Drosophila* consists of three segments. The first segment (*scape*) houses muscles that actively position the antenna via the joint between the scape and the pedicel (Mamiya et al. 2011). The second segment (*pedicel*), houses a chordotonal organ, the Johnston's organ, which acts as the auditory sensory organ (Göpfert and Robert 2002). Movements of the joint between second and third segment stretch and relax this organ (Caldwell and Eberl 2002). The third antennal segment (funiculus and arista) serves as a sound receiver (Caldwell and Eberl 2002) that vibrates in response to the particle velocity of sound. In addition to sound, gravity and wind also act on the antenna which can be detected by different neuronal subsets (Kamikouchi et al. 2009; Yorozu et al. 2009).

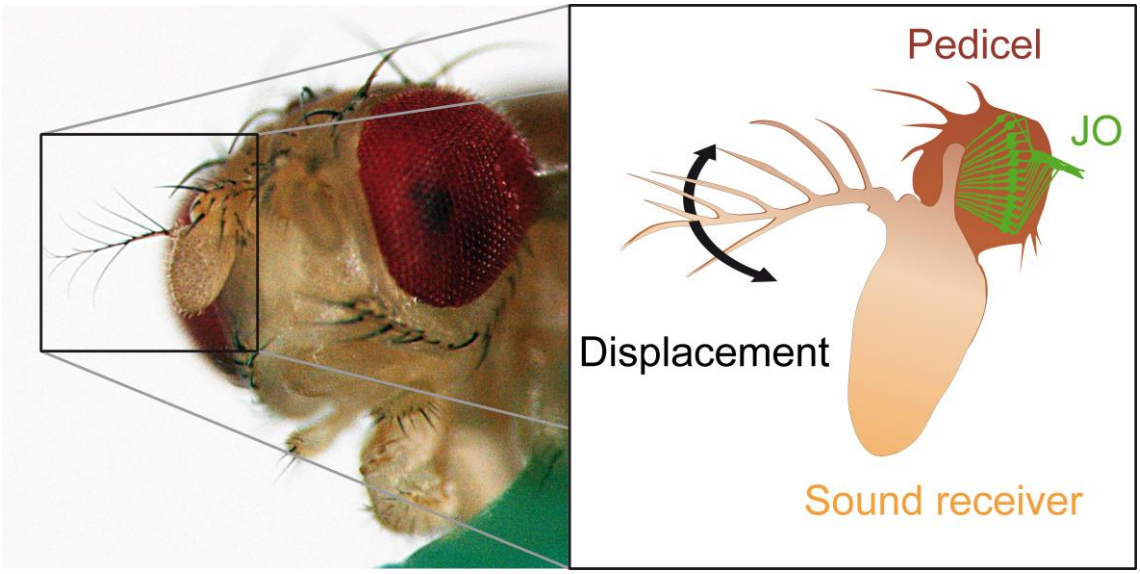

Figure 1: Antennal ear of *Drosophila*

Left: Picture of a *Drosophila* head, with compound eyes (red) and antennal ears (black box) consisting of the feathery arista (circa 0.1 mm in length), and the stiffly bound barrel-shaped funiculus.
Right: Scheme of the *Drosophila* ear (Senthilan and Piepenbrock et al. 2012). The sound receiver consists of the arista and the funiculus, (light brown) and rotates about the

longitudinal axis of the funiculus in response to sound (Caldwell and Eberl 2002). The pedicel houses the Johnston's organ (JO), a chordotonal organ that transduces antennal vibrations into cellular electrochemical signals.

The Johnston's organ is directly connected to the sound receiver. Thus, vibrations of the sound receiver directly stretch and compress the neurons of the Johnston's organ (Caldwell and Eberl 2002). The Johnston's organ consist of circa 200 functional units, the scolopidia (Kamikouchi et al. 2006). Each scolopidium bears two to three ciliated sensory neurons, which are enveloped by supporting cells. A dendritic cap connects the neurons dendrites with the antennal joint (scape – pedicel). The dendrites are surrounded by the endolymph in the scolopale space, which might be K^+ rich (Eberl 1999; Roy et al. 2013; Wiek 2013), and the scolopale rods. The sensory neurons transduce mechanical force into cellular electrochemical signals. These signals are than conveyed to the antennal mechanosensory and motor center in the brain (AMMC) (Kamikouchi et al. 2006). Four major subgroups, of Johnston's organ neurons, can be distinguished: two groups (A and B) serve the sensation of sound, whereas the other two groups (C and E) detect gravity and wind (Kamikouchi et al. 2006; Kamikouchi et al. 2009; Senthilan et al. 2010).

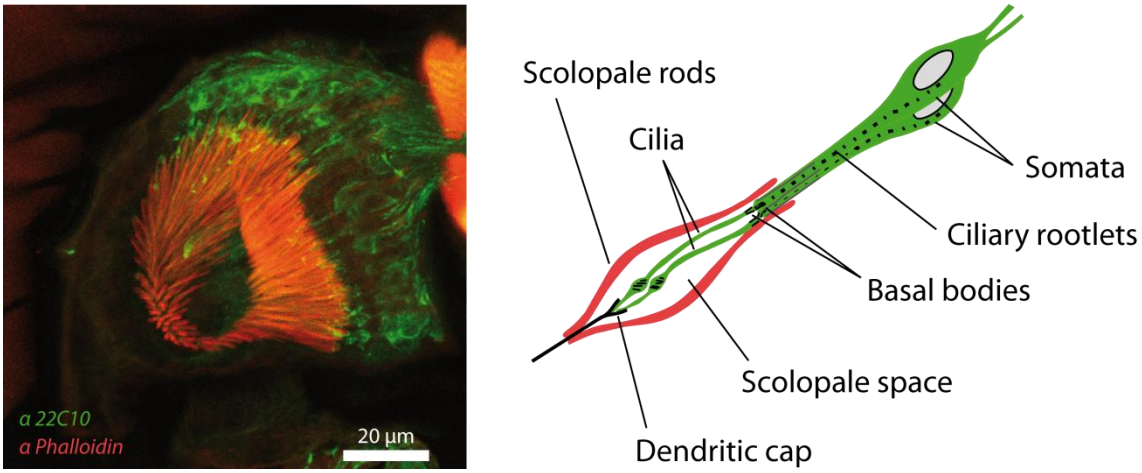

Figure 2: *Drosophila* Johnston's organ

The *Drosophila* Johnston's organ (JO) is housed in the second segment of the antenna, the pedicel. It is comprised of functional units the scolopidia.
Left: Immunohistochemistry picture (by Seol-hee Joo) shows actin rich scolopale rods (red) and sensory neurons (green) that convey through the first antennal segment to the antennal mechanosensory and motor center (AMMC).
Right: Scheme of a scolopidium (Senthilan and Piepenbrock et al. 2012).

The main role of the mechanosensory Johnston's organ is to transduce sound receiver vibrations, into cellular electrochemical signals. This mechano-electrical transduction is mediated by dedicated ion channels, the mechano-electrical transduction channels (MET-channels). These transduction channels open in response to mechanical stimuli. Due to opening and closing of transduction channels the membrane permeability for ions is altered. As a result, the electrochemical membrane potential is changed, which results in a cellular electrochemical signal. In the *Drosophila* ear, mechanosensory neurons are directly connected to the sound receiver, and vibrations of the sound receiver are transmitted to these transduction channels. Due to this direct mechanical coupling of

sound receiver and transduction channels, force transmission is bidirectional. Displacement of the antenna will change the open probability of transduction channels, and vice versa changes of the open probability will move the sound receiver. Force transmission in both ways is thought to be mediated by elastic elements, the 'gating springs'. This transduction apparatus is thought to be connected to molecular motors that amplify movements and are involved in adaptation processes (Ewing 1978; Kamikouchi et al. 2006; Nadrowski et al. 2008; Kamikouchi et al. 2009; Senthilan et al. 2010).

The antennal ear of *Drosophila* is remarkably sensitive to sound. Sensitivity is obtained by a positive feedback amplification that is exerted by Johnston's organ neurons. This amplifier shares all the four hallmarks of the vertebrate cochlear amplifier: (i) nonlinear compression, (ii) frequency-specific amplification, (iii) self-sustained oscillations and (iv) power gain (Nadrowski et al. 2011). Transducer based force generation actively boosts sound evoked displacements of the antenna. This amplification in the *Drosophila* ear can be modeled by a harmonic oscillator coupled with transduction modules. The activity is provided by an interplay of transduction channels and molecular adaptation motors (Göpfert and Robert 2002; Albert et al. 2007b; Nadrowski and Göpfert 2009).

Structure of my study

I have split my thesis into four parts in order to investigate the genetic basis of hearing:

Chapter 1 First, I identified genes, which are required for hearing. Therefore, we screened mutant flies, and characterized corresponding phenotypes.

Chapter 2 The screen identified genes that encode proteins of the phototransduction cascade. I provide an overview about the genes that are known to be involved in sensory perception of light, and address their impact on hearing.

Chapter 3 NOMPC is the bona fide transduction channel. Its ankyrin repeats have been proposed to function as gating springs, of mechano-electrical transduction channels. Flies with duplicated ankyrin residues were made and I analyzed the antennal mechanics.

Experimental approach: Probing Johnston's organ function

To probe the Johnston's organ function and to characterize corresponding alterations due to mutations, affecting parts of the transduction machinery, I probed antennal mechanics and corresponding antennal nerve responses.

The methods described below were established by Jörg Albert, Martin Göpfert, Thomas Effertz and Björn Nadrowski (Albert 2006; Albert et al. 2007b; Effertz et al. 2012).

All physiological recordings in this thesis monitor antennal displacements, in response to different stimuli. Therefore, it is essential to immobilize flies completely, to be able to record antennal vibrations and its response to sound and force steps. Thus, single flies are mounted on top of a plastic rod with wax. In the next step, the antennal joint between first and second segment is fixed with dental glue to rule out muscular motions. This is inevitable because Johnston's organ neurons are located in the second antennal segment and connected to the sound receiving third segment (Albert et al. 2006). Due to this direct coupling of Johnston's organ neurons and the sound receiver, vibrations of this sound receiver reflect neuron motility and movements due to transducer gating.

The procedure to probe the function of the fly's ear includes three steps. Firstly, free fluctuations that represent the thermal noise and active energy contributions due to the motility of Johnston's organ neurons (Göpfert and Robert 2003; Göpfert et al. 2005) are probed; secondly, antennal displacement responses and compound action potentials to pure tones are assessed, and thirdly correlates of transducer gating, are examined.

Antennal free fluctuations

To assess the function of Johnston's organ in *Drosophila* mutant strains I first measured the unconstrained movements of the antenna's tip in absence of stimulation. Being driven by thermal motion and active motions of Johnston's organ neurons, these free fluctuations provide a simple measure of the functional integrity of the fly's ear.

Johnston's organ mechanosensory neurons generate motions, to actively boost antennal vibrations (Göpfert et al. 2003; Göpfert et al. 2005). This drives the sensitivity of the flies ear, by active feedback amplification. This amplification can be even observed in the absence of sound as spontaneous oscillations of the antenna. The 'free fluctuations' of the antenna are recorded according to Albert et al. 2006, with a laser Doppler vibrometer, analyzed by fast Fourier transformation, and two parameters are calculated to characterize the spontaneous fluctuations (Albert 2006). These parameters include: the antennal best frequency and power spectral density.

The power spectral density (PSD) is a measure of fluctuation power across frequencies. In the case of the antenna's free fluctuations, this power represents thermal noise and active contributions due

to the motility of Johnston's organ neurons. To assess the fluctuation power, I integrated the power spectral density for frequencies between 100 and 1500 Hz (Effertz 2011).

The resonance or 'best' frequency was taken as the frequency at which the velocity spectra of the free fluctuations displayed a maximum. It is determined by fitting the fast Fourier transformed velocity time trace of free fluctuations with a harmonic oscillator (Göpfert et al. 2005).

The antennal best frequency of wild-type *Canton S* flies is circa 250 Hz, and its power spectral density circa 1500 nm^2. In this study, the best frequency of flies with altered Johnston's organ function ranges between 119 Hz and 689 Hz, whereas the power spectral density varies between 25 nm^2 (loss of amplification) and 9134 nm^2 (excess amplification).

Sound responses of the *Drosophila* antenna

Johnston's organ mechanosensory neurons provide feedback amplification by generating motions. Mechanical amplification by Johnston's organ neurons was assessed by plotting the phase-locked displacement of the antenna, against the stimulus sound particle velocity. In wild-type flies, the displacement characteristically scales linear for large and small particle velocities, but assumes a nonlinear scaling in-between. This compressive nonlinearity arises from the motility of Johnston's organ neurons, and enhances the antenna's displacement response to faint sounds. The gain of this active nonlinear amplification was determined as the ratio between antennal displacements observed in the upper and lower linear regimes (Göpfert and Robert 2002; Albert et al. 2006; Göpfert et al. 2006; Albert et al. 2007a; Nadrowski et al. 2008; Effertz et al. 2011).

The mechanical amplification is probed by stimulating flies with pure tones matching the best frequency of each individual sound receiver. Antennal responses were probed to sound of 16 different intensities with sound particle velocity ranging between ca 0.1 and 10 mm/s. The typical amplification gain for wild-type *Canton S* flies is circa 10 fold. In the mutants examined in this study, gains ranged between 1 and 37 fold.

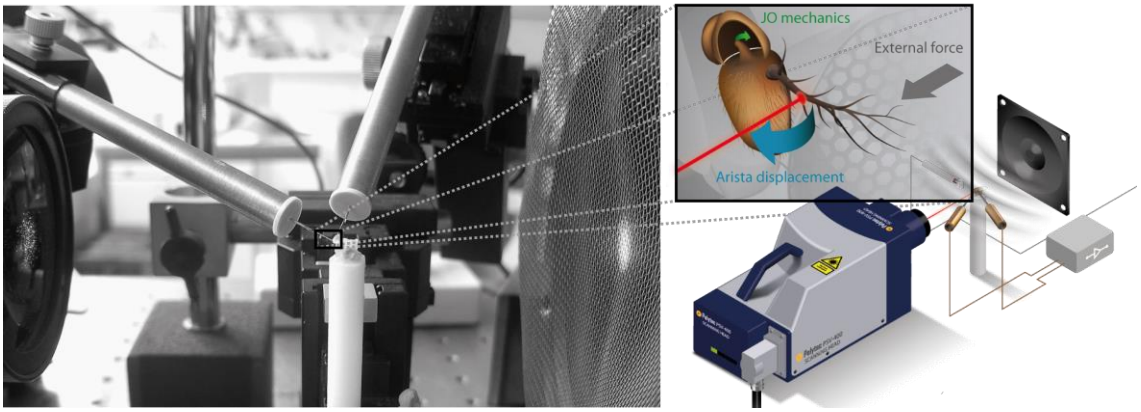

Figure 3: Setup to probe antennal sound response characteristics.

Left: Photography of the recording setup with *Drosophila* mounted on top of a teflon rod (center).
Right: Scheme of the recording setup with laser Doppler vibrometer (below), extracellular recording electrodes (bronze/brown), loudspeaker (black) and a close up of the antenna (Scheme by Christian Spalthoff).

The phase-locked response of the antennal nerve was recorded extracellularly with tungsten wires in form of a compound action potential (CAP). Therefore a recording electrode was inserted between the first antennal segment and the head, and the indifferent electrode was put into the thorax.

To quantify neural sensitivity, three parameters were calculated: the 'maximum CAP response' due to pure tones, a 'hearing threshold', and a 'displacement threshold' (Piepenbrock 2009; Effertz 2011; Effertz et al. 2011):

'maximum compound action potential'

The maximum compound action potential (max CAP) reaches amplitudes of 40 µV for *Canton S* flies. It is the maximum, phase-locked, antennal nerve response (Effertz et al. 2011).

'hearing threshold'

The stimulus sound particle velocity that corresponds to 10 % of the maximum compound action potential response, determined from a Hill-fit.

'displacement threshold'

The antennal displacement that corresponds to 10 % of the maximum compound action potential response, determined from a Hill-fit.

To characterize auditory phenotypes of mutant flies, I defined four categories based on the average mechanical amplification gain. This ranking provides a conservative judgment, of auditory dysfunction (Senthilan and Piepenbrock et al. 2012):

'normal'

Mechanical amplification gains between 5 and 15 fold are considered 'normal'. These flies show typically a 'hearing threshold' of circa 50 µm/s.

'severely impaired'

Johnston's organ function is 'severely impaired', when the antennal displacement response is linearized, documenting the loss of mechanical amplification (< 1.5 fold). The antennal nerve response (CAP) is lost, or only evoked by loud sounds. The corresponding 'hearing threshold', is above 200 µm/s.

'moderately impaired'

Mechanical amplifications gains between 1.5 – 5 fold are ranked as 'moderately impaired' . The 'hearing threshold' is between 50 – 200 µm/s.

'hypersensitive'

Antennal ears are 'hypersensitive' when faint sounds induce larger antennal displacements than in control flies. The antennae, continuously oscillated spontaneously in the absence of sound, and the mechanical amplification gain is above 15. The corresponding 'hearing threshold' is ≤ 50 mm/s.

Correlates of mechano-electrical transducer gating

Mechano-electrical transduction is mediated by transduction channels. The nonlinear gating compliance reflects force activation of these channels. Due to the gating of transduction channels, gating springs that convey force onto these channels relax. This relaxation can be recorded as a stiffness drop, of the *Drosophila* antenna, in response to force steps (Albert et al. 2007b).

This method to record correlates of mechano-electrical transducer gating and is published in: T. Effertz, B. Nadrowski, D. Piepenbrock, J. Albert and M. Göpfert 2012 (Online Methods).

Recording correlates of transducer gating

The nonlinear gating compliance is probed by rapidly deflecting the antenna with force steps. Recording the corresponding antennal displacement reveals an initial overshoot, which is due to a reduced antennal stiffness. This reduction in stiffness reflects the simultaneous gating of transduction channels in the flies Johnston's organ (Albert et al. 2007b; Nadrowski et al. 2008).

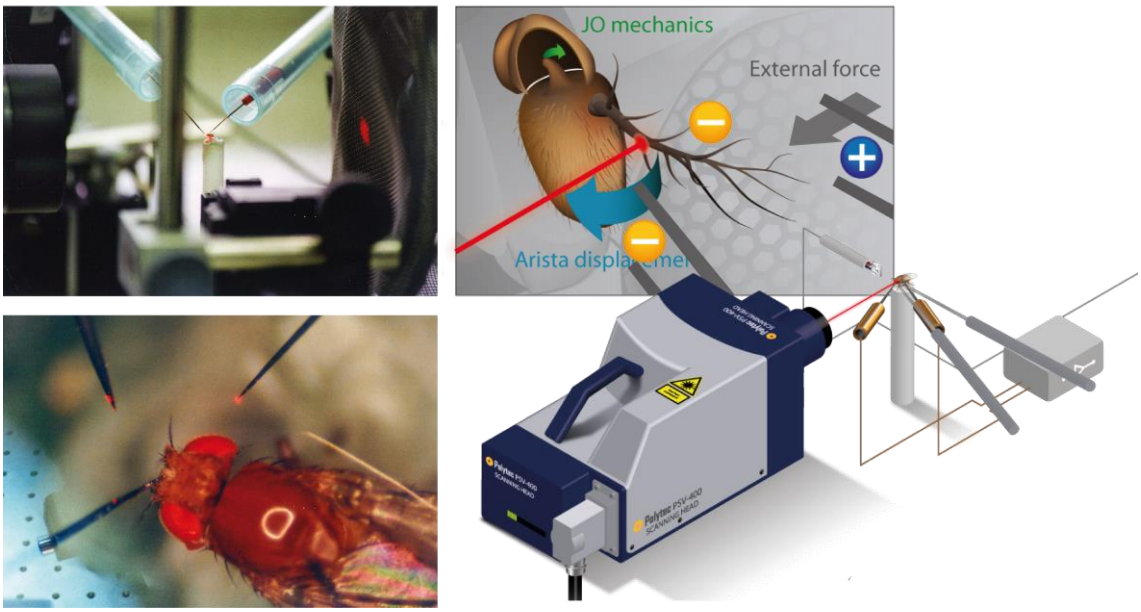

Figure 4: Setup to probe correlates of antennal transducer gating

Photo above left: Side view. Left: scanning laser Doppler vibrometer, center: fly with electrostatic probes, right: speaker (Photography by Sophia-Elise Saitz).
Photo below left: Close up. Lower left: extracellular recording electrode, top: electrostatic probes, lower right: indifferent electrode (Photography by Sophia-Elise Saitz).
Scheme right: Scheme of the recording setup, with laser Doppler vibrometer (below), extracellular recording electrodes (bronze/brown), electrostatic probes (grey) and a close up of the antenna (Scheme by Christian Spalthoff).

The *Drosophila* antenna was deflected in a range of - 10 to + 10 µm using electrostatic force, with a resolution of 28 steps. To deflect the antenna, the fly was charged to circa 100 V against ground with a tungsten electrode, and antennal displacements were elicited with bipolar tungsten stereotrodes (Micro Probe, Inc. WE3ST31.0A5 and WE3ST31.0A10). Antennal displacement

responses were sampled by a Polytec PSV-400 scanning laser Doppler vibrometer at a rate of 100 kHz (Albert et al. 2007b; Effertz et al. 2012).

Time traces were analyzed according to Effertz et al. 2012 (Methods, Data analysis). This includes the calculation of average sound receiver displacements and outlier rejection using a Grubbs test.

The dynamic slope stiffness of the receiver (slope stiffness according to (Nadrowski et al. 2008)), at the initial displacement peak is calculated as (m = 5 ng):

$$K_{peak} = \frac{\partial \left(m * (acceleration_{onset} - acceleration_{peak})\right)}{\partial\, displacement_{peak}}$$

The steady state displacement, which the receivers assumed during prolonged forcing, was deduced from an exponential fit, and the corresponding steady state slope stiffness was calculated as (m = 5 ng):

$$K_{steady} = \frac{\partial\, (m * acceleration_{onset})}{\partial\, displacement_{steady}}$$

The mass, of each individual antennal receiver, was adjusted so that its steady state stiffness matched the average value obtained for the respective strain. This was done to compensate for inter-individual variability of the apparent mass of individual antennal receivers (Albert et al. 2007b; Effertz et al. 2012).

Modeling mechano-electrical transducer gating

In *Drosophila*, the direct mechanical gating of ion channels in Johnston's organ introduces a nonlinear gating compliance, in the mechanics of the antennal receiver. This gating compliance conforms to the gating spring model of transduction in hair cells, which assumes a parallel arrangement of a linear spring and gating springs that convey the stimuli to the ion channels (Howard and Hudspeth 1987; Howard and Hudspeth 1988). These gating springs will relax when the channels open, introducing a nonlinear gating compliance in the mechanics of the receiver (Albert et al. 2007a; Albert et al. 2007b). By analyzing the nonlinear gating compliance in *Drosophila* mutants, I tested for genetic alterations in the mechanical gating of ion channels in Johnston's organ neurons.

This transduction apparatus is described by a symmetric gating spring model. This gating spring model consists of two opposing transducer populations, which are connected to the sound receiver via gating spring (K_{gs}), and a parallel stiffness (K_{lin}).

The stiffness of the receiver depends on the displacement of the sound receiver. Where K_{inf} is the stiffness of the receiver during prolonged forcing (asymptotic stiffness) and the negative term reflects the stiffness drop due to transducer gating.

$$K(x) = K_{inf} - \left(\frac{Nz^2}{k_B T}\right) * P_0(1 - P_0)$$

Equation 1: Gating spring model with one types of channels (2-state gating spring model)

This gating spring model consists of one type of channels. Parameters: N = number of channels, z = single channel gating force, P_O = open probability and K_{inf} = maximum antennal stiffness.

We previously demonstrated that the Johnston's organ bears more than one type of transducers (Effertz et al. 2012). We suggest one sensitive ($_s$) and one insensitive ($_i$) type of transducer. Therefore he introduced a second transducer in the gating spring equation:

$$K(x) = K_{inf} - \left(\frac{N_s z_s^2}{k_B T}\right) * P_{0\_s}(1 - P_{0\_s}) - \left(\frac{N_i z_i^2}{k_B T}\right) * P_{0\_i}(1 - P_{0\_i})$$

Equation 2: Gating spring model with two independent types of channels (4-state gating spring model)

This gating spring model consists of two types of channels, first one is sensitive ($_s$) and second insensitive ($_i$). Parameters: N = number of channels, z = single channel gating force, P_O = open probability and K_{inf} = maximum antennal stiffness.
The following Scheme illustrates the model.

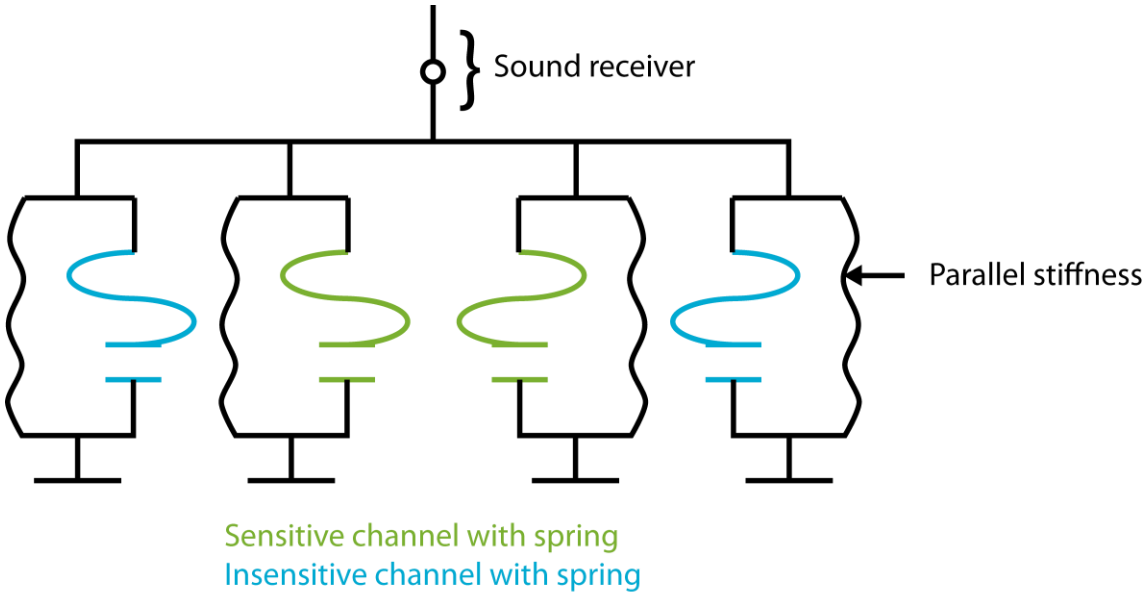

Figure 5: Scheme of the gating spring model

The gating spring model consists of sensitive and insensitive transducers and a linear parallel stiffness (Figure modified from B. Nadrowski, unpublished).

The pooled gating compliance datasets of each mutant fly strain were fitted with both models, using the Matlab R2010b curve fitting toolbox 3.0 (Nonlinear least squares algorithm, trust region).

Model selection with the Akaike information criterion

For model selection the Akaike information criterion with correction for finite sample size (AICc), which is a measure of goodness for fitting results (Burnham and Anderson 2002), was calculated (Effertz et al. 2012).

$$AICc = AIC + \frac{2k(k+1)}{n-k-1} \quad with\ AIC = n\ln\left(\frac{Rss}{n}\right) + 2k$$

n is the number of data points circa 135 for 5 flies per genotype and k the number of free parameters. The model with one channel type has 3 free parameters (N, z, and K_{inf}) whereas the model with two different channels consists of 5 free parameters (N_s, z_s, N_i, z_i and K_{inf}).

To decide if the data is better estimated by the model with one or the model with two channel types following calculated Akaike weights provide a measure of probability between 0 and 1 (low and high probability)(Effertz et al. 2012).

$$w_i = \frac{\exp(-\Delta_i/2)}{\sum_{r=1}^{2}\exp(-\Delta_i/2)}$$

1 Screening for functional contributions of *Drosophila* auditory organ genes

1.1 Introduction

1.1.1 Motivation: Identifying *Drosophila* hearing genes

Identifying new genes, and especially their function, has been one major aspect of biological research during the last decades. Sequencing the genome of humans in 2003 (Gregory et al. 2006) and many model systems like *Drosophila melanogaster* (Adams et al. 2000) has been the first step. But the following quotation of the National Human Genome Research Institute illustrates the current task:

> *"Having the essentially complete sequence of the human genome is similar to having all the pages of a manual needed to make the human body. The challenge to researchers and scientists now is to determine how to read the contents of all these pages and then understand how the parts work together and to discover the genetic basis for health and the pathology of human disease."*
>
> *(The Human Genome Project Completion, National Human Genome Research Institute)*[2]

[2] The Human Genome Project Completion: Frequently Asked Questions, Subtopic: "What will the next 50 years of medical science look like?" Website of the National Human Genome Research Institute http://www.genome.gov/11006943, Last Updated: October 30, 2010
See appendix Figure 45

During the last 20 years, hearing genes of *Drosophila* have been mostly discovered from forward genetic screens. Forward genetics follows the procedure, of mutating the genome randomly, and probing mutant flies for altered phenotypes.

Most genes that affect mechanotransduction and hearing have been discovered by two behavioral screens. Maurice Kernan and colleagues probed the touch response of mutant *Drosophila* larvae. They discovered mutations that affect stereotypical withdraw response, due to stroke with an eyelash (Kernan et al. 1994). The second screen was done by Daniel F. Eberl and colleagues. They examined male behavior to court each other, in response to the *Drosophila* pulse song (Eberl et al. 1997). In 2000, Daniel F. Eberl and colleagues showed that all these mutant fly strains display a corrupted sound-evoked antennal nerve response (Eberl et al. 2000).

Prior knowledge to my study has been that 24 genes are associated with hearing in *Drosophila* (Senthilan et al. 2012). They are listed in the Gene Ontology database and annotated with the term 'sensory perception of sound' (GO: 0007605). The Gene Ontology database (Ashburner et al. 2000) is a project that aims to standardize information on genes.

In collaboration with Senthilan Pingkalai, I approached this issue by reverse genetics. First step has been the identification of the transcriptom of the *Drosophila* ear. The second step included the detection of those genes that are essential for hearing. Identifying genes that are transcribed in the fly's ear was performed by expression profiling. Corresponding results have been confirmed by quantitative real-time polymerase chain reaction (Senthilan et al. 2012).

The aim of my study is to find those *Drosophila* genes that encode information inevitable for hearing via screening of mutants.

1.1.2 Objectives and approach: Screening for altered *Drosophila* Johnston's organ function

Previously to my project 24 genes had been associated with hearing in *Drosophila* (Senthilan et al. 2012). These genes are annotated with the Gene Ontology (Ashburner et al. 2000) term "sensory perception of sound" (Gene Ontology term number: 0007605). This term is defined as:

> *"…the series of events required for an organism to receive an auditory stimulus, convert it to a molecular signal, and recognize and characterize the signal. Sonic stimuli are detected in the form of vibrations and are processed to form a sound." (The Gene Ontology, 2013)*[3]

I aim to identify hearing genes with a forward genetic screen. Preparatory work was conducted by Pingkalai Senthilan and revealed an expression profiling list of 274 genes: the transcriptome of the fly's ear. 201 genes in this list are annotated in the Gene Ontology Database. They encode ion channels, molecular motors or proteins that respond to abiotic stimuli or light.

[3] Gene Ontology terms and annotations, ID GO:0007605, name: sensory perception of sound, ontology: biological process, http://www.ebi.ac.uk/QuickGO/GTerm?id=GO:0007605#info=1, information from 05.08.2013 (Ashburner et al. 2000)

Identifying the *Drosophila* ear transcriptome, does not identify or characterize functional contributions of these genes in hearing. Identifying genes that are required for hearing was done, by probing the antennal response characteristic of corresponding mutant fly strains. Mutant auditory phenotypes are ranked, base on auditory categories (for details see: 'Experimental Approach – Sound response characteristic of the *Drosophila* antenna').

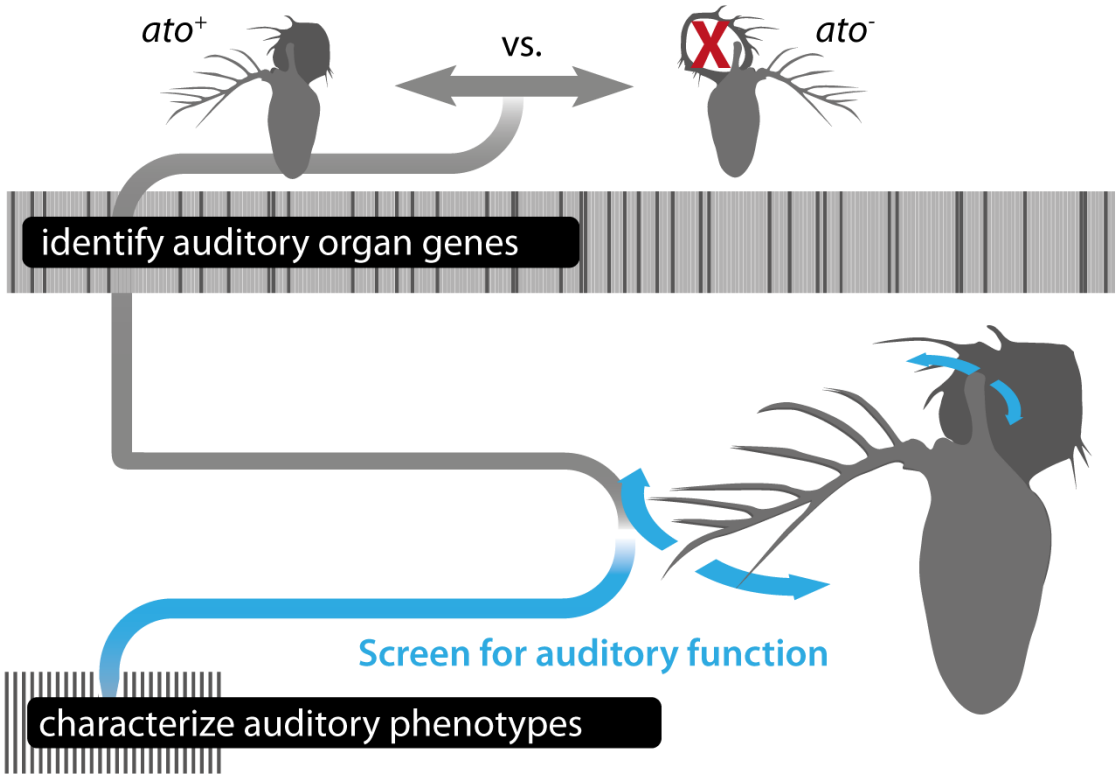

Figure 6: Scheme of my approach to screen for hearing genes

Comparing the transcriptomes, of the second antennal segment, of flies that lack the Johnston's organ (*atonal* mutants) and controls, identified candidate hearing genes. This atonal based screen identified 274 genes that are expressed in the Johnston's organ (Senthilan 2010). Subsequently, 92 mutant fly strains have been probed for auditory organ function, by characterizing auditory phenotypes (Senthilan et al. 2012). Figure C. Spalthoff.

The transcriptome of the *Drosophila*, Johnston's organ, comprises numerous genes that encode ion channels, molecular motors, and surprisingly genes that are known to be involved in response to light. Due to strong differences of photo-electrical and mechano-electrical transduction, this is an astonishingly finding. This is precisely the reason, why I summarize all results on genes that are involved in photo-electrical transduction, and their impact on auditory organ transduction, in a separate chapter, chapter 2.

1.2 Results

Based on the transcriptome of the *Drosophila* ear (Senthilan et al. 2012), 92 different mutant fly strains have been tested. Genes and mutations that were examined for Johnston's organ function are listed in Table 1 and Table 2. Here I describe auditory phenotypes of 64 different mutant fly strains to screen for hearing genes, and I focus on genes that are associated with sensory perception of light in chapter 2.

Mutation	Gene name	Annotation symbol	
Ank2[f02001],CG32373[f02001]	*Ankyrin 2*	*CG32373, CG42734, CG44195*	1
Bili[MB07242]	*Band4.1 inhibitor LRP interactor*	*CG11848*	
Bmcp[BG02446]	*Bmcp*	*CG7314*	1
bw[1]	*brown*	*CG17632*	1
Cad99C[MB08891]	*Cadherin 99C*	*CG31009*	
CG10096[e00276], CG10097[e00276]		*CG10096, CG10097*	1
CG10283[B241]		*CG10283*	2
CG10633[MB05283]	*Ionotropic receptor 64a*	*CG10633*	1
CG11253[EY10866]		*CG11253*	1
CG11388[e03063]		*CG11388*	3
CG13455[MB1092]		*CG13455*	2
CG13636[MB03846]	*sosie*	*CG13636*	1
CG14127[MB00306]		*CG14127*	2
CG14636[MB03866]		*CG14636*	1
CG14693[f03110]		*CG14693*	1
CG14921[C247]		*CG14921*	1
CG17765[C295]			2
CG2025[MB00729]		*CG2025*	
CG30101[f05583]		*CG30101*	1
CG30203[MB02464]		*CG30203*	2
CG31386[EY04626]		*CG31386*	2
CG3280[f01875]		*CG3280*	2
CG3339[MI00332]		*CG3339*	2
CG4091[EY06821]		*CG4091*	4
CG4329[MB01614]		*CG4329*	1
CG4629[MI02585]		*CG4629*	2
CG6053[MB06262]		*CG6053*	5
CG6499[EY02782]		*CG6499*	1
CG7220[MB06775]		*CG7220*	3
CG7730[G5055]		*CG7730*	2
CG8086[f03214]		*CG8086*	1
CG8419[MB06410]		*CG8419*	
CG9313[PADEF334P]		*CG9313*	1
CG9492[KG02504]		*CG9492*	1
d[1]	*dachs*	*CG42840*	4
Dhc36c[MB01026]	*Dynein heavy chain at 36C*	*CG5526*	1
Dhc93AB[MB05444]	*Dynein heavy chain at 93AB*	*CG3723*	1
dtr[MB11825]	*defective transmitter release*	*CG31623*	2
futsch[k68]	*futsch[k68]*	*CG34387*	5
gol[MB03006]	*goliath*	*CG2679*	
Ir75a(MB00253)	*Ionotropic receptor 75a*	*CG14585*	4
Ir75d[MB04616]	*Ionotropic receptor 75d*	*CG14076*	
Ir84a[MI00501]	*Ionotropic receptor 84a*	*CG10101*	2
Ir8a[1]	*Ionotropic receptor 8a*	*CG32704*	2
Ir94b CG31424[MB02190]	*Ionotropic receptor 94b*	*CG31424*	1
kek4[MB11415]	*kekkon4*	*CG9431*	5
Klp68D[KG03849]	*Kinesin-like protein at 68D*	*CG7293*	1
Lin29[MB00729]		*CG2052*	
Naam[KG10548]	*Nicotinamide amidase*	*CG31216*	1
nAcRα-96Aa[EY09706]	*nicotinic Acetylcholine Receptor alpha 96Aa*	*CG5610*	
Nlg2	*Neuroligin 2*	*CG13772*	
Osi2[MI01475]	*Osiris 2*	*CG1148*	2
Pask[MB02780]	*PAS kinase*	*CG3105*	

PIP5K59B[MB02388]	*PIP5K59B*	*CG3682*	[2]
sei[HP21840]	*seizure*	*CG3182*	[5]
shg[2]	*shotgun*	*CG3722*	
Sulf1[MB11661]	*Sulfated*	*CG6725*	
w[1118]	*white*		[1]
wtrw[E754K]	*water witch*	*CG31284*	
y[1]	*yellow*		[1]
y[1]w[1]	*yellow, white*		[1]
y[1]w[1118]	*yellow, white*		[1]
y[1]w[67c23]	*yellow, white*		[1]
yuri[PL00114]	*yuri gagarin*	*CG31732*	[5]

Table 1: List of genes and respective mutations that were screened for Johnston's organ function

I chose *Drosophila* mutant fly strains based on the microarray screen of Pingkalai Senthilan (Senthilan et al. 2012). Johnston's organ function have been published in ([1]) my Diploma thesis (Piepenbrock 2009) [1], ([2]) Bachelor thesis of Sandra Meyer-Jürgens (Meyer-Jürgens 2012), ([3]) Bachelor thesis of Julia Goldamm (Golldamm 2010), ([4]) Bachelor thesis of Swantje Grätsch (Grätsch 2010) and ([5]) Bachelor thesis of Joscha Schmitz (Schmitz 2010). In addition to this 64 mutant fly strains, genes that are known to be involved in vision are shown in Table 2: .

To screen for functional contributions of genes in hearing, I first, probed the best frequency of *Drosophila* antennae and second, stimulated flies with pure tones matching the best frequency of the sound receiver.

1.2.1 Free fluctuation screening

Activity of sensory neurons tunes the antenna to a frequency matching the frequency of the *Drosophila* courtship song (Riabinina et al. 2011). This active tuning increases the sensitivity of the *Drosophila* ear to a small frequency range, the 'best frequency'. A deviation from the typical best frequency provides information on the active feedback amplification of Johnston's organ neurons.

The antennal sound receivers of *Canton S* flies, which are used as wild type controls, have an average best frequency of 253 +/- 20 Hz (mean ± 1 S.D., N = 5). In mutant flies, best frequencies where obtained that deviate from wild-types. Results are plotted in figure 2, top panel: Sound receiver best frequencies (Hz) of mutant flies. Mutations of the following genes result in significantly higher best frequencies, documenting deficits in active antennal tuning: *Ank2, CG10283, CG11253, CG11388, CG13636, CG14921, CG30101, CG30203, CG4329, CG6053, CG6499, CG7730, CG9313, CG9492, dachs, Dhc93AB, Ir75a, Ir84a, Klp68D, Naam, CG17765, yw*. Mutations in the genes: *bw, CG8419, dtr, futsch, Ir75d, Pask, PIP5K59B, Sulf1*, and *white* result in significantly lower best frequencies, documenting amplified active antennal tuning.

The power spectral density (PSD) is a measure of fluctuation power. Results are shown in figure 2, lower panel: Mechanical fluctuation power (nm^2) of mutant flies. When compared to *Canton S* flies (1873 ± 789 nm^2) mutations in *Ank2, Bmcp, CG10283, CG11253, CG11388, CG13636, CG14921, CG2025, CG30101, CG30203, CG31386, CG4091, CG4329, CG6053, CG7730, CG8086, CG9313, CG9492, Dhc36c, Dhc93AB, Ir75a, Ir84a, Ir8a, kek4, Klp68D, Lin29, Naam, Osi2, sei, wtrw* and *yw* result in a significant lower power spectral density. When comparing both parameters, mutant alterations in the fluctuation power were often associated with best frequency shifts.

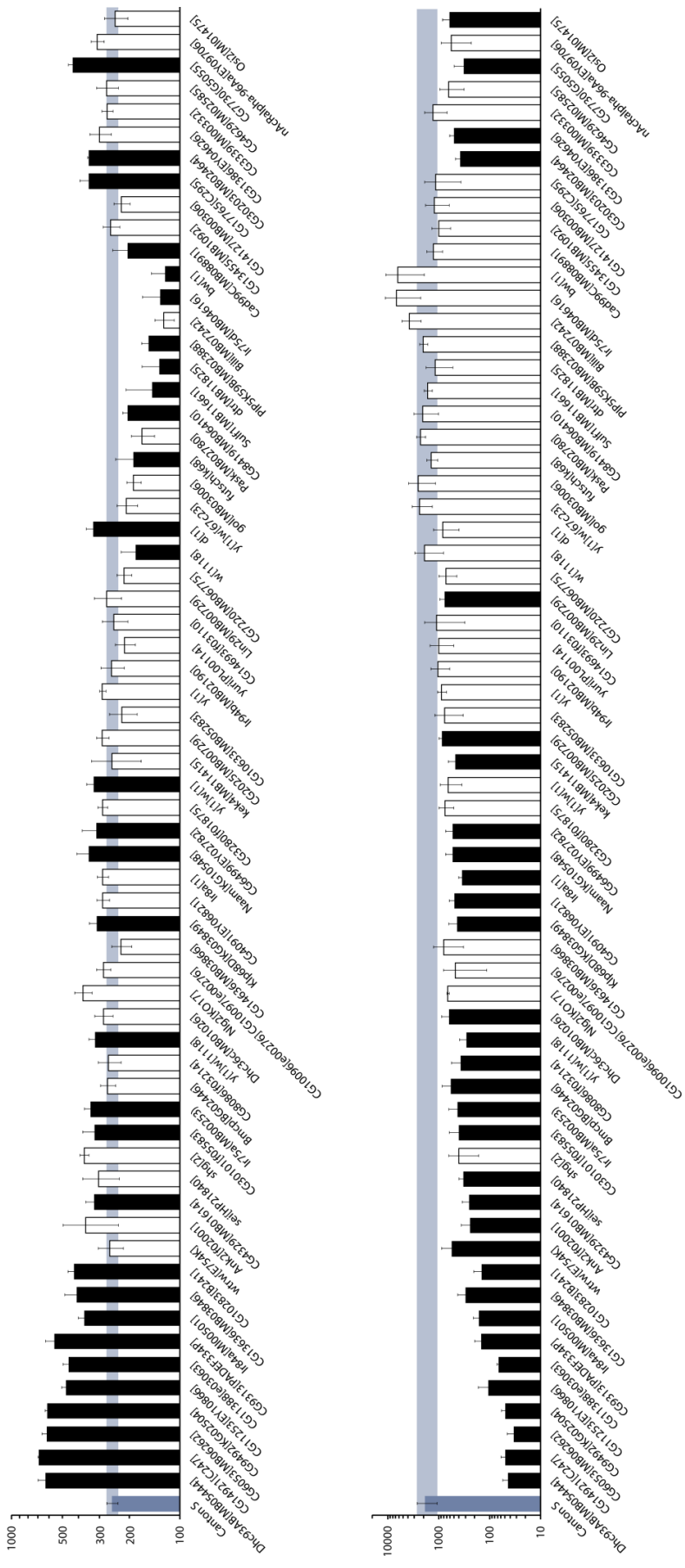

Figure 7: Screen for *Drosophila* hearing genes: Results of antenna free fluctuation recordings.

Top panel: Sound receiver best frequencies (Hz) of mutant flies.
Lower panel: Mechanical fluctuation power (nm^2) of mutant flies.
Data are presented as mean values ± 1 standard deviation. N ≥ 5 flies per strain were probed except *for nAcRa-96Aa, Nlg2, Pask and shg*, where N = 3. The blue bar highlights the standard deviation obtained for *Canton S* controls. Black bars signal significant deviates from controls and empty bars signal the absence of a significant difference (two-tailed Mann-Whitney U test, $p < 0.05$, corrected for multiple comparisons with Benjamini and Yekutieli procedure for control of the false discovery rate).

1.2.2 Characterizing Johnston's organ function

To characterize mutant alterations in detail, I probed the nonlinear compression of the antennal amplifier and the 'hearing threshold'. As shown in figure 3 (top panel), mechanical sensitivity gains occur in the range of 1 – 32 for mutant flies and wild-type *Canton S flies have a gain of 10 ± 2*. Mutant phenotypes are ranked, based on the average amplification gain (for details see: 'Experimental Approach – Sound response characteristic of the *Drosophila* antenna'):

Flies in the category 'severely impaired' (gain < 1.5) are *Dhc93AB*, *CG14921*, *CG6053* and *CG9492* mutants.

Mutations in the following genes 'moderately impair hearing" (gain > 1.5 < 5)': *CG11253*, *CG11388*, *CG9313*, *Ir84a*, *CG13636*, *CG10283*, *wtrw*, *Ank2*, *CG4329*, *sei*, *shg*, *CG30101*, *Ir75a*, *Bmcp*, *CG8086*, *yw*, Dhc36c, Nlg2, *CG10096/CG10097* and *CG14636*.

Mutation of *Klp68D*, *CG4091*, *Ir8a*, *Naam*, *CG6499*, *CG3280*, *kek4*, *CG2025*, *CG10633*, *y* and *Ir94b* results in a significantly reduced gain, but they fit in the category of normal hearing flies (gain >5 and >15).

Hyperamplification (gain > 15) was observed in flies carrying mutations in *bw*, *Ir75d*, *Bili*, and *PIP5k59B*.

Canton S flies have a sound particle velocity threshold of 49 ± 15 µm/s. Mutations with significantly higher thresholds affect the genes *CG4329* 133 ± 23 µm/s, *wtrw* 238 ± 212 µm/s, *CG10283* 124 ± 52 µm/s, *CG13636* 124 ± 52 µm/s, *Ir84a* 215 ± 62 µm/s, *CG9313* 132 ± 41 µm/s, *CG11388* 190 ± 42 µm/s and *CG11253* 336 ± 68 µm/s. No CAPs have been detected for *CG9492*, *CG6053*, *CG14921* and *Dhc93ab*. The mutation in *bw* results in a lower threshold of 23 ± 8 µm/s.

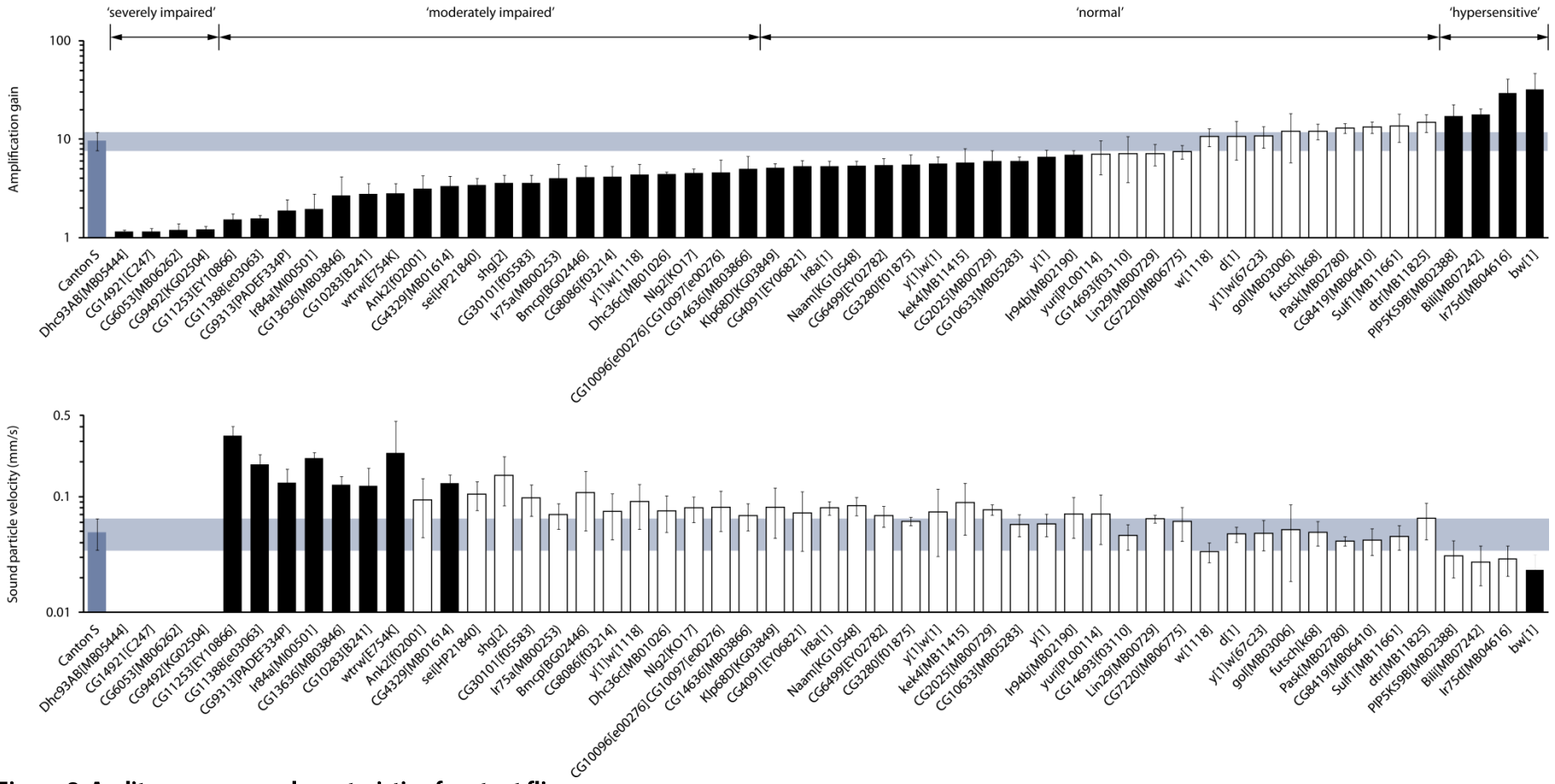

Figure 8: Auditory response characteristic of mutant flies.

Upper panel: Thresholds of CAPs with respect to the sound particle velocity. **Lower panel:** Mechanical amplification gains.

Data are presented as mean values ± 1 standard deviation. N ≥ 5 flies per strain were probed except *for Bili, Nlg2, Pask and shg*, where N = 3 and *dtr*, where N = 2. The blue bar highlights the standard deviation obtained for *Canton S* controls. Black bars signal significant deviates from controls and empty bars signal the absence of a significant difference (two-tailed Mann-Whitney U test, $p < 0.05$, corrected for multiple comparisons with Benjamini and Yekutieli procedure for control of the false discovery rate). Based on the amplification gains, mutations were categorized as follows: 'severely impaired' gain < 1.5, 'moderately impaired' gain 1.5 – 5, 'normal' gain 5 – 15 and 'hypersensitive' gain > 15.

The power spectral density (PSD) of the antenna is often associated with best frequency shifts. Figure 9 A shows a negative correlation of best frequency and PSD. When Johnston's organ neurons provide less energy to move the antenna, it becomes stiffer and it vibrates with a higher frequency, which is circa 700 Hz for dead animals (Albert 2006). High fluctuation power provides energy for amplification as shown in Figure 9 B, which is supported by Figure 9 C showing that lower antennal best frequencies correlate with a higher amplification. The antennal sensitivity, as provided by the 'hearing threshold' (y axis subplot D, for details see: 'experimental approach') depends on the amplification gain. No dependency of the 'displacement threshold' (for details see: 'experimental approach') and amplification gain could be observed (E), and no dependency of amplification gain and maximum compound action potential was discovered (F).

The dependency of amplification gain and power spectral density can be used in the future to quickly screen for mutant alterations. This is of interest when one keeps in mind that recording antennal sound response takes 10x the time of a best frequency and power spectral density recording.

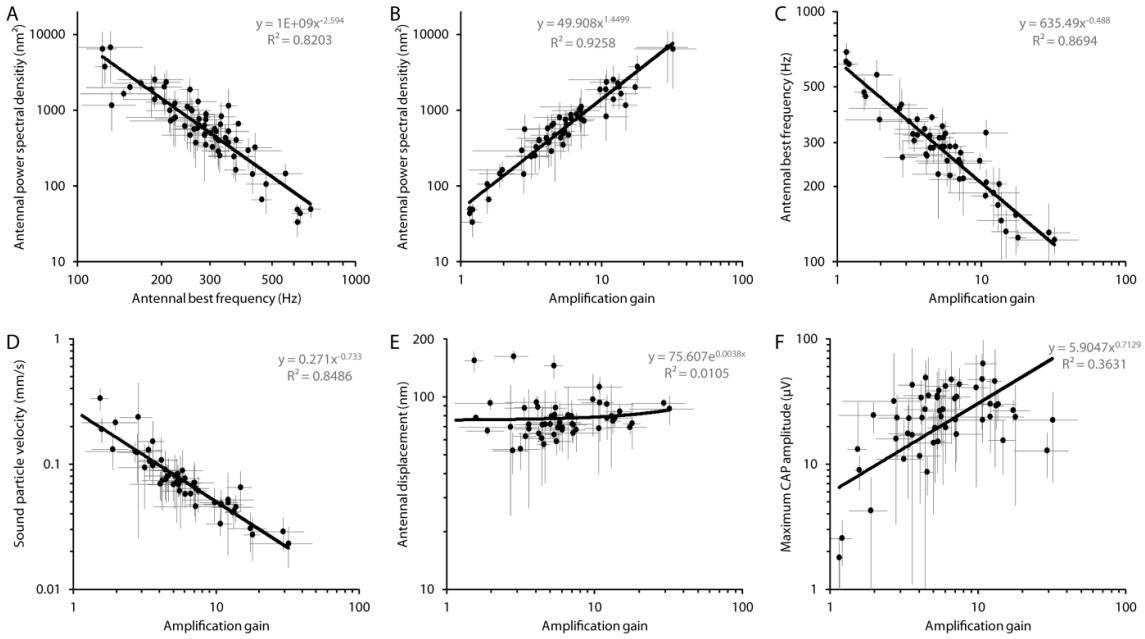

Figure 9: Correlation of recorded parameters

Data are presented as mean values ± 1 standard deviation. N > 3 flies per strain were probed. Nonlinear correlation is shown via power function except for (E) where exponential function is used due to better R^2. A negative correlation of best frequency and system power can be observed in (A). When Johnston's organ neurons provide less energy to move the antenna it becomes stiffer. Subplots (B) and (C) show a correlation between spontaneous antennal vibrations and the sound induced amplification gain. Thus recordings of spontaneous antennal vibrations can be used to quickly screen for mutant phenotypes. Subplot (D) shows the dependency of antennal thresholds on the amplification gain. Whereas subplot (F) shows a weak correlation of amplification gain and maximum compound action potential, no correlation could be observed between amplification gain and 'displacement thresholds'. But, as shown in chapter 2, flies with a strong shift in displacements thresholds have no amplification gain at all. Therefore, recordings of spontaneous antennal vibrations are sufficient as a measure for Johnston's organ function.

This functional screen for 'hearing genes' identified 32 mutations out of 64 mutant fly strains that significantly alter the power spectral density, and 31 that significantly alter the antennal best frequency. Probing the antennal response due to pure tones revealed that 40 mutations significantly alter amplification. Eight mutations significantly increase and one significantly decreases the 'hearing threshold'.

Based on auditory categorize: four mutant fly strains are severely impaired, 20 moderately, 25 do not affect hearing, and four mutations result in hypersensitivity, 'ringing ears'.

Most surprisingly I found additionally a huge number of genes that encode proteins of the phototransduction cascade. Due to this very unexpected finding, I dedicate this type of protein a separate chapter.

1.3 Discussion

My aim was to identify genes that encode proteins which are required for hearing, 'hearing genes'. This I approached by screening for altered hearing phenotypes of mutant fly strains. Sixty-four different mutant fly strains have been probed for alterations in antennal best frequency and power spectral density. Mutations in thirty-one genes were shown to significantly alter the antennal best frequency and mutations in thirty-two genes significantly alter fluctuation power. Next, probing the antennal response to pure tones stimulation of fifty-three mutant fly strains revealed forty mutant fly strains with significant alterations in their mechanical amplification gain, and nine fly strains with altered 'hearing thresholds'.

Four mutations impair the function of the Johnston's organ severely, twenty moderately, twenty-five not and four mutations result in hyperamplification. Genes of the *Drosophila* visual system are shown and discussed in a separate chapter (chapter 2) due to their unexpected appearance.

This screen for 'hearing genes' identified different types of proteins being involved in *Drosophila* hearing. Mutations of molecular motors, like dyneins, impair the function of the *Drosophila* ear. Decreased amplification gain could be observed for mutant flies of *Dhc36c*, and decreased gain and a higher 'hearing threshold' for mutant flies of *CG9313*. In addition, mutations of *CG6053*, *CG9492* and *Dhc93AB* lead to complete absence of any sound evoked compound action potential. Mutations of the kinesin motor protein *Klp68D* lead to a decreased amplification gain, whereas the mutation in the myosin *dachs* shows only a reduced fluctuation power. These findings highlight the importance of dyneins in antennal amplification and suggest that they play a role in positive feedback amplification of the *Drosophila* antenna.

Mutations affecting ion channels, that are known to be involved in response to abiotic stimuli like ionotropic receptors, lead to a decreased amplification gain like *Ir94b*, *Ir8a*, *Ir75a*, and additionally an up shifted 'hearing threshold' for *Ir84a*. In contrast, the mutation of *Ir75d* leads to an increased amplification gain. Mutations of ion channels of the transient receptor family (TRP-channels) like *water witch* (*wtrw*) decrease the amplification gain and shift the 'hearing threshold'. The *trp* and *trp-like* channel affect hearing as well, results are shown in chapter 2. Mutations affecting the glutamate-gated ion channel *CG10633* decrease the amplification gain. In addition the amplification gain of seizure (*sei*) mutants is decreased. It encodes a voltage-gated cation channel.

Mutations affecting structural cytoskeleton constituents like *Ank2* (Pielage et al. 2008) decrease the amplification gain with. A mutation in *futsch*, that is known to be involved in axogenesis (Hummel et al. 2000), axon cargo transport (Bettencourt Da Cruz et al. 2005) and microtubule cytoskeleton organization (Roos et al. 2000) lead to the opposite phenotype with a decreased best frequency.

To further analyze these identified 'hearing genes', corresponding proteins have to be localized and their contribution on transducer gating and adaptation processes should be probed. Dynein motor proteins could contribute to adaptation processes, and they could contribute to amplification. The transcriptome of the *Drosophila* Johnston's organ comprise many more genes, which have not been

probed in my screen. Due to the huge success rate of this screen it is very likely that many more genes wait to be discovered. In addition, the transcriptome of the Johnston's organ comprises interestingly many genes that are known to be involved in sensory perception of light (Senthilan et al. 2012). I discuss the impact of corresponding mutant flies on auditory transduction in the next chapter.

Parts of this screen for functional contributions of *Drosophila* auditory organ genes are published in: "*Drosophila* Auditory Organ Genes and Genetic Hearing Defects, P. Senthilan and D. Piepenbrock et al., Cell, 2012"

2 Genes of the *Drosophila* visual system and their impact on auditory transduction

2.1 Introduction

2.1.1 Motivation: Investigating sensory perception of light and sound

Surprisingly, the transcriptome of the *Drosophila* ear contains a huge number of genes that are known to be involved in sensory perception of light (Senthilan and Piepenbrock et al. 2012). My aim is to identify those genes that functionally contribute to *Drosophila* hearing and to evaluate their function in the Johnston's organ.

Sensory perception is the process of receiving, transducing, encoding and processing external stimuli (Munkong and Juang 2008). Various sensory organs serve the sensation of different modalities. The intensity of light depends on photon numbers, and light wavelength determines the perceived color. In addition, polarized light is used by many invertebrates like *Drosophila* for orientation (Hardie 2012a). Hearing, as a specialized form of mechanosensation, detects wavelength and intensity of sound pressure or sound particle velocity (Göpfert and Robert 2001).

Drosophila eyes and antennal ears look very different. This is simply due to the fact that these sensory organs sense different modalities. The largest eyes of *Drosophila* are its compound eyes, consisting of up to 1000 functional units, the ommatidia. Each ommatidium consists of circa 20 different cells, eight of which are photoreceptors. These photoreceptor cells use specialized microvilli, the rhabdomeres, for phototransduction. The microvilli offer an enormous membrane surface that is densely packed with the photosensing pigment rhodopsin (Katz & Minke, 2009;

Tian, Hu, Tong, & Han, 2012). Rhodopsin activates phospholipase C (PLC) via G–proteins, and PLC hydrolyzes the membrane lipid phosphatidylinositol 4,5-bisphosphate (PIP_2). This hydrolyzation leads to a contraction of the microvilli that seem to activate TRP and TRP-like channels (Hardie & Franz, 2012).

In contrast, the *Drosophila* ear detects gravity, wind and sound particle velocity. The particle velocity is detected by the sound receiving structure that consists of the feathery arista and the third antennal segment, the funiculus (Göpfert and Robert 2002). The sound receiver rotates along the longitudinal axis of the funiculus in response to sound (Caldwell and Eberl 2002). The sound receiving structure is connected via a cuticular hook to an antennal chordotonal organ, the Johnston's organ. The Johnston's organ consists of circa 200 multicellular stretch-receptor units, the scolopidia. Each scolopidium contains two to three sensory neurons that transduce stimulus-induced antennal movements into electrical currents and encode them in action potentials (Göpfert and Robert 2001; Göpfert and Robert 2002; Kamikouchi et al. 2009). In contrast to the second messenger cascade of photo–electrical transduction, mechano–electrical transduction in the fly ear is much faster, operating at microseconds instead of milliseconds. This speed suggests that antennal vibrations directly gate transduction channels in Johnston's organ neurons, without intermittent second messenger cascades.

Due to these observations, it seems obvious that both transduction mechanisms work in different ways. Nevertheless, I show evidence suggesting multiple roles for at least parts of the phototransduction machinery.

2.1.2 Objectives and approaches

To identify functional contributions of genes that are associated with sensory perception of light, I screened for genes that are involved in photoelectrical transduction, chromophore forming, and recycling pathway, and eye morphogenesis.

In the second part of this chapter, I will evaluate the function of rhodopsin in the *Drosophila* Johnston's organ. I approach this question on multiple levels:

- By comparing a *rhodopsin 6* mutant fly with a genetic rescue, I probed the specificity of the mutant phenotype.
- Several *rhodopsin* genes can be found in *Drosophila*. To test which ones of them are involved in hearing, and if they have a redundant function, is probed by rhodopsin single and double mutations.
- Rhodopsin transcription in Johnston's organ was shown with a microarray screen, qPCR and insitu hybridization (Senthilan et al. 2012). To locate rhodopsins expression, I used immunohistochemistry.
- Since rhodopsin is a membrane-bound protein, I tested Johnston's organ for ultrastructural defects with transmission electron micrography.
- To probe if rhodopsins are directly involved in the event of transducer gating, I recorded correlates of transducer gating.
- Physiological experiments will focus on potential roles on temperature-control and the light-dependence of Johnston's organ function.

2.2 Results

To identify functional contributions of genes that are associated with sensory perception of light and evaluating the function of rhodopsin in the *Drosophila* Johnston's organ, I probed the Johnston's organ function of corresponding mutant flies. In addition, we locate rhodopsin expression via immunohistochemistry, test the Johnston's organ for ultrastructural defects, focus on potential roles of rhodopsin on temperature-control and light-dependency, and provide recordings of transducer gating for rhodopsin mutant flies.

2.2.1 Functional screen for genes of the visual system

Key components of the fly's phototransduction cascade like *inaD* and *rhodopsin 6* had been discovered in the transcriptome of the *Drosophila* ear. Interestingly, auditory phenotypes of corresponding mutant flies revealed very strong phenotypes. Due to this unexpected finding, I screened for functional contributions, of additional genes that are associated with the visual sense. I chose genes that are associated with the Gene Ontology terms 'sensory perception of light', 'phototransduction' and 'Rhodopsin biosynthetic process' and probed the Johnston's organ function of corresponding mutant fly strains.

Mutation	Gene name	Annotation symbol	Affiliation with phototransduction, reference	Comment
Arr2[5]	Arrestin 2	CG5962	(Yamada et al. 1990; Tian et al. 2011)	
CalX[A]	Na/Ca-exchange protein	CG5685	(Wang et al. 2005; Tian et al. 2011)	free fluctuation recordings provided by Sandra Meyer-Jürgens
Cam[5]/Cam[n339]	Calmodulin	CG8472	(Tian et al. 2011) (Tian et al. 2011)	
cry[01]	Cryptochrome	CG3772	(Tian et al. 2011)	
eya[2]	eyes absent	CG9554	(Jemc and Rebay 2007)	[4]
Gγ30A[MB02355]	G protein γ30A	CG3694	(Tian et al. 2011)	free fluctuation recordings provided by Sandra Meyer-Jürgens
gl[3]	glass	CG7672	(Renfranz and Benzer 1989)	
inaC[e00783]	inactivation no afterpotential C	CG6518	(Tian et al. 2011)	[2]
inaD[1]	inactivation no afterpotential D	CG3504	(Tian et al. 2011)	
ninaA[1]	neither inactivation nor afterpotential A	CG3966	(Tian et al. 2011)	[3]
ninaB[1]	neither inactivation nor afterpotential B	CG9347	(Tian et al. 2011)	
ninaC[5]	neither inactivation nor afterpotential C	CG5125	(Tian et al. 2011)	[4]
ninaC[MB02664]	neither inactivation nor afterpotential C	CG5125	(Tian et al. 2011)	[1]

ninaE[117a]	neither inactivation nor afterpotential E/rhodopsin1	CG4550	(Tian et al. 2011)	
ninaE[17],Rh6[1]	double mutant fly strain	CG4550, CG5192		
norpA[41]	no receptor potential A	CG3620	(Tian et al. 2011)	
norpA[7]	no receptor potential A	CG3620	(Tian et al. 2011)	[1]
pinta[1]	prolonged depolarization afterpotential (PDA) is not apparent	CG13848	(Tian et al. 2011)	
rdgA[1]	retinal degeneration A	CG42667	(Tian et al. 2011)	
Rh5[2]	rhodopsin 5	CG5279	(Montell 2012)	
Rh5[2],Rh6[1]	double mutant fly strain	CG5279, CG5192		
Rh6[1]	rhodopsin 6	CG5192	(Montell 2012)	
Rh6[1],Rh6[+]	rhodopsin 6 rescue			
rh7[0]	rhodopsin 7	CG5638	(Montell 2012)	
santa-maria[1]	scavenger receptor acting in neural tissue and majority of rhodopsin is absent	CG12789	(Tian et al. 2011)	
stops[1]	slow termination of phototransduction	CG31006	(Wang et al. 2008)	
TRP[1]	transient receptor potential	CG7875	(Tian et al. 2011)	[6]
trpl[302]	trp-like	CG18345	(Tian et al. 2011)	

Table 2: List of *Drosophila* mutants affecting genes of the visual system

This List includes genes that are involved in phototransduction and more general aspects of vision like *eyes absent* (*eya*) that is involved in sensory organ development. Mutant fly strains have been probed for Johnston's organ function. Johnston's organ function have been published in my ([1]) Diploma thesis (Piepenbrock 2009), ([2]) Bachelor thesis of Sandra Meyer-Jürgens (Meyer-Jürgens 2012), ([3]) Bachelor thesis of Julia Goldamm (Golldamm 2010), ([4]) Bachelor thesis of Swantje Grätsch (Grätsch 2010) and ([6]) PhD thesis of Thomas Effertz (Effertz 2011).

If more than one or two genes, maybe the whole phototransduction cascade, are involved in Johnston's organ function, I would expect that these mutations should lead to auditory phenotypes.

To probe the auditory organ function of mutant fly strains I determined their 1) antennal best frequency, 2) sensitivity gain and 3) antennal compound action potential response due to sound stimulation. Genes and mutations that were examined are listed in Table 2.

2.2.1.1 Determining the antennal best frequency and Johnston's organ fluctuation power

Activity of sensory neurons is probed by recording antennal free fluctuations. These recordings provide information about the best frequency as well as the power spectral density. Power spectra of the antenna's free fluctuations of mutant flies are shown in Figure 10. Data are shown as power spectra calculated by fast Fourier transformation of sound receiver displacement time traces.

Power spectra of mutant fly strains *CalX[A]* and *cry[01]* are similar to wild-types like *Canton S* (Piepenbrock 2009). The antennae, of the fly strains with mutations in *inaD* and *santa-maria*, oscillate with a lower amplitude and higher frequency, documenting deficits in active antennal tuning. In comparison, the mutant fly strain *Cam[5]/Cam[n339]* shows very strong oscillations, 'ringing ears'.

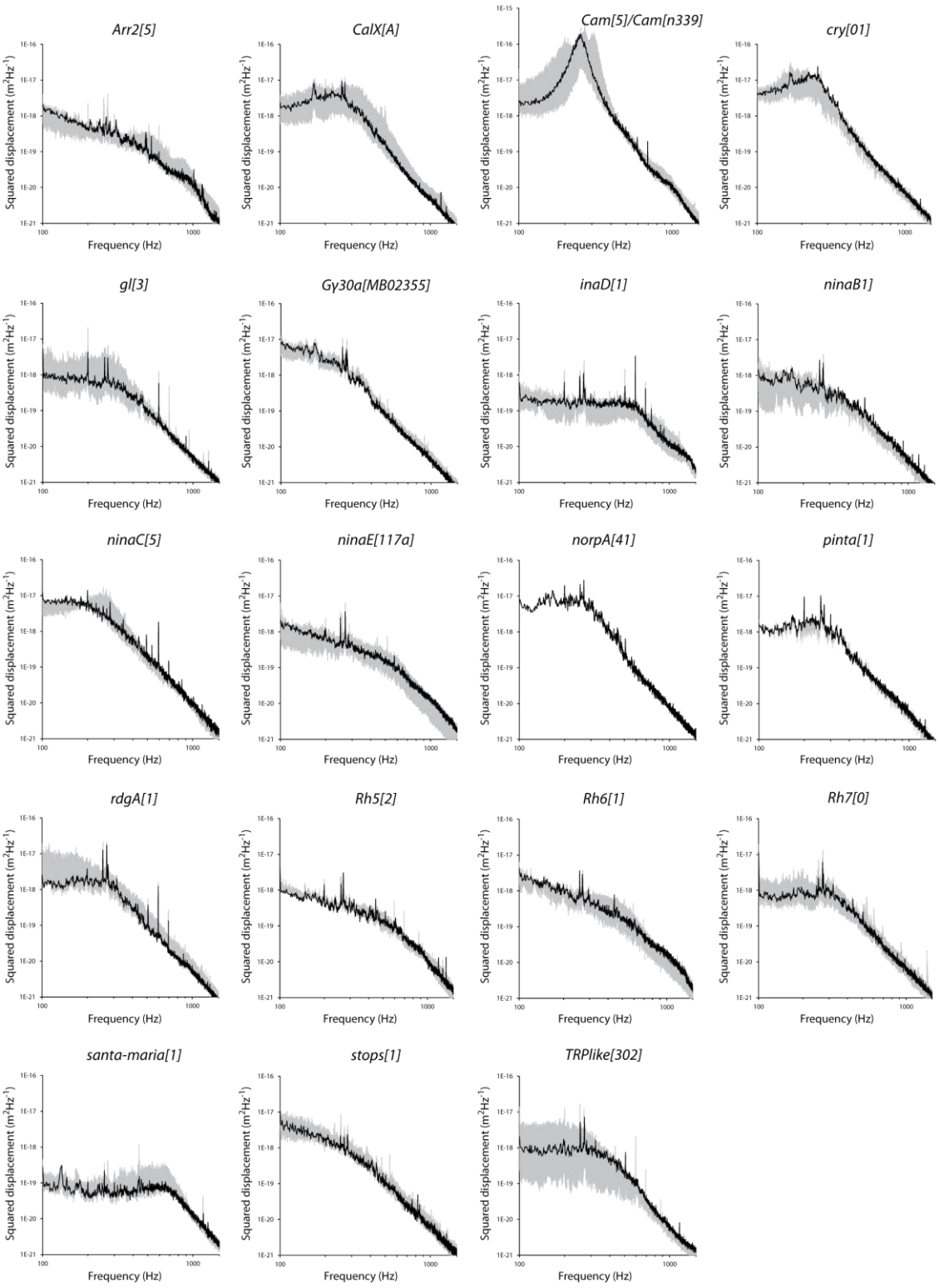

Figure 10: Free fluctuation recordings of *Drosophila* phototransduction mutants.

Black traces: fluctuations obtained from one fly. Grey ghost traces: fluctuations obtained from other animals of the same strain, shown as the range of individual recordings, N = 5 flies/strain, except for *norpA*, where N equals 1. Data for *Ggamma30* and *CalX* was provided by S. Meyer-Jürgens and is included here because I studied antennal sound responses in the respective mutants.

Many mutant fly strains revealed alterations in their power spectra. To quantify these phenotypes, I now determine the best frequency and power spectral density of these spontaneous oscillating antennae.

Antennal best frequency

Determining the best frequency of spontaneous antennal fluctuations revealed significant increases as well as decreases due to mutations.

The best frequency was determined by fitting the fast Fourier transformed velocity time trace of free fluctuations with a harmonic oscillator. The antennal sound receivers of *Canton S* flies, which are used as wild type controls have an average best frequency of 253 +/- 20 Hz (mean ± 1 S.D., N = 5). In mutant flies, best frequencies were: *inaD[1]:* 592 ± 41 Hz, *Arr2[5]:* 454 ± 42 Hz, *santa-maria[1]:* 667 ± 66 Hz, *Rh5[2]* 459 ± 62 Hz, *Rh6[1]* 454 ± 8 Hz, *trp[1]* 394 ± 66, *ninaE[117]* 425 ± 37 and *trpl[302*] 345 ± 72 Hz. All these figures are significantly higher than in wild-type controls, documenting deficits in active antennal tuning.

A systematic comparison of the best frequencies of wild-type and mutant antennae is shown in Figure 11. To facilitate comparisons, I included data from my diploma thesis (Piepenbrock 2009) and data gathered by T. Effertz (*trp*), from the Bachelor theses of S. Grätsch (*eya*), J. Goldamm (*ninaA*) and S. Meyer-Jürgens (*CalX*, *Gγ30a*, *inaC*).

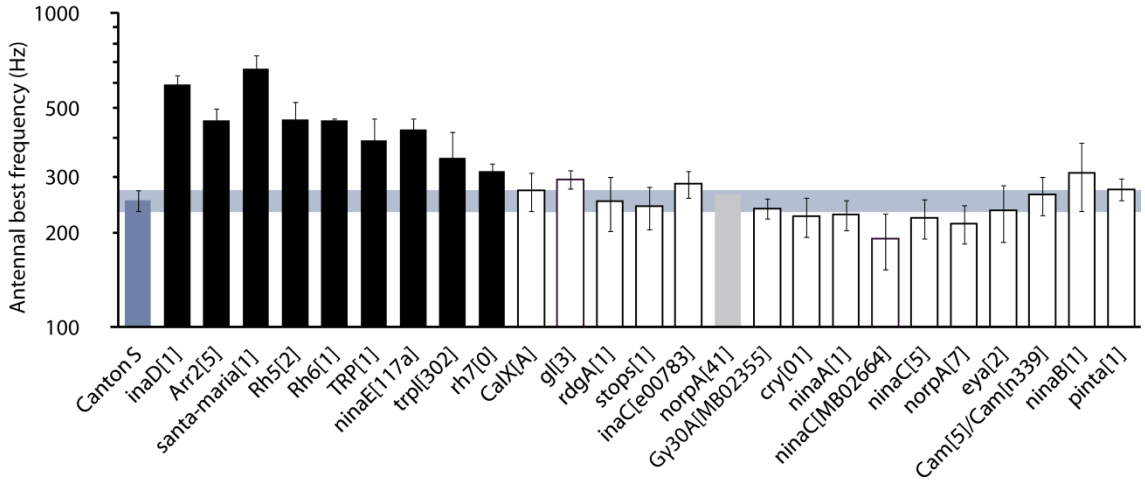

Figure 11. Sound receiver best frequencies (Hz) of *Drosophila* phototransduction mutants.

Data are presented as mean values ± 1 standard deviation. N ≥ 5 flies per strain were probed except for *norpA* (highlighted in grey), where N = 1. The blue bar highlights the standard deviation obtained for *Canton S* controls. Black bars signal significant deviates from controls and empty bars signal the absence of a significant difference (two-tailed Mann-Whitney U test, $p < 0.05$, corrected for multiple comparisons with Benjamini and Yekutieli procedure for control of the false discovery rate).

These alterations described the frequency changes of spontaneous fluctuations due to mutations. To quantify the amplitude of these oscillations, I determined the power spectral density.

Johnston's organ fluctuation power

Determining the power spectral density of spontaneous antennal fluctuations revealed significant increases as well as decreases due to mutations. The power spectral density (PSD) is a measure of fluctuation power, distributed over a frequency range. To assess the fluctuation power, I integrated the power spectral density for frequencies between 100 and 1500 Hz.

When compared to *Canton S* flies (1873 ± 789 nm²), mutations in *inaD* (100 ± 28 nm²), *Arr2* (187 ± 23 nm²), *santa-maria* (78 ± 33 nm²), *Rh5* (207 ± 23 nm²), *Rh6* (329 ± 98 nm²), *trp* (255 ± 96 nm²), *ninaE* (234 ± 118 nm²), *trpl* (338 ± 301 nm²), *gl* (409 ± 296 nm²), *stops* (554 ± 179 nm²), *inaC* (463 ± 244 nm²), *Ggamme30a* (740 ± 241 nm²), *ninaB* (163 ± 101 nm²) and *pinta* (392 ± 92 nm²) result in a significant lowered power spectral density, whereas mutations in *Calmodulin* (9134 ± 1904 nm²) lead to significant increased power. No significant alterations in the power spectral density were detected in flies carrying mutations in *CalX*, *rdgA*, *cry*, *ninaA*, *ninaC, norpA* and *eya*.

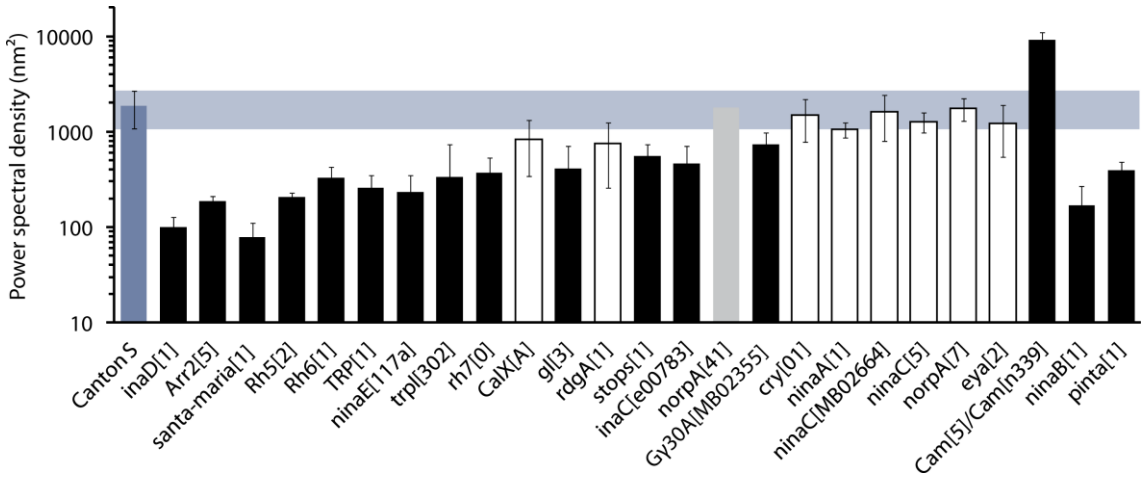

Figure 12: Mechanical fluctuation power (nm²) of the antenna in *Drosophila* phototransduction mutants.

Data are presented as mean values ± 1 standard deviation. N ≥ 5 flies per strain were probed except for *norpA* (highlighted in grey), where N = 1. The blue bar highlights the standard deviation obtained for *Canton S* controls. Black bars signal significant deviates from controls and empty bars signal the absence of a significant difference (two-tailed Mann-Whitney U test, $p < 0.05$, corrected for multiple comparisons with Benjamini and Yekutieli procedure for control of the false discovery rate). To facilitate comparisons, I included data from additional thesis, see Table 2.

Mutant alterations in the power of the fluctuations of the antenna were often associated with best frequency shifts. In 18 of 25 strains, decrease of fluctuation power was accompanied by increase in best frequency. Just 5 strains (*stops, inaC, Ggamma30a, ninaB and pinta*) showed a decrease in fluctuation power but no shift in their best frequency. And *Cam* mutant flies have an increased fluctuation power with no shift in best frequency. Only one single strain (*ninaC[MB02664]*) displays slightly decreased fluctuation power without a shift in best frequency.

These fluctuations arise from active movements of Johnston's organ neurons. They boost the sensitivity of the *Drosophila* antennal ear. To quantify the factor gain of amplification I probed antennal response characteristic due to pure tones.

2.2.1.2 Genes of the *Drosophila* visual system affect the sensitivity of the auditory organs

Quantifying the sensitivity of the *Drosophila* antenna, of mutations affecting genes that are known to be involved in the sensory perception of light, revealed that most mutations significantly negatively impact the Johnston's organ function.

To assess the impact of mutations on active feedback amplification, I measured the nonlinear compression of the antennal amplifier and calculated the amplification gain.

To quantify neural sensitivity, I plotted the compound action potential amplitude (CAP) as a function of sound particle velocity and sound receiver displacement. To compare the CAP between different mutant fly strains the maximum CAP responses, the 'hearing threshold' and the 'displacement threshold' have been plotted (for details see: 'Experimental Approach – Sound response characteristic of the *Drosophila* antenna').

Mechanical feedback amplification is lost in mutations affecting genes of the *Drosophila* visual system

Nonlinear compression of the amplifier is shown by plotting the antennal tip displacement as a function of stimulus sound particle velocity over a range of 10^{-3} – 10^{2} mm s^{-1}. One example of nonlinear compression is the mutation *ninaC[5]*. This mutant fly strain is similar to wild-type *Canton S* flies (Piepenbrock 2009) that have an intact antennal amplifier.

Whereas the fly strains *Cam[5]/Cam[n339]*, *eya[2]* and *stops[1]* show a compressive nonlinearity, mutations in *Arrestin*, *inaD*, and all rhodopsins that have been probed, display a linear relation of sound receiver displacement to sound particle velocity. This linearization of the antennal mechanics signals a loss of Johnston's organ neuron motility and active mechanical amplification.

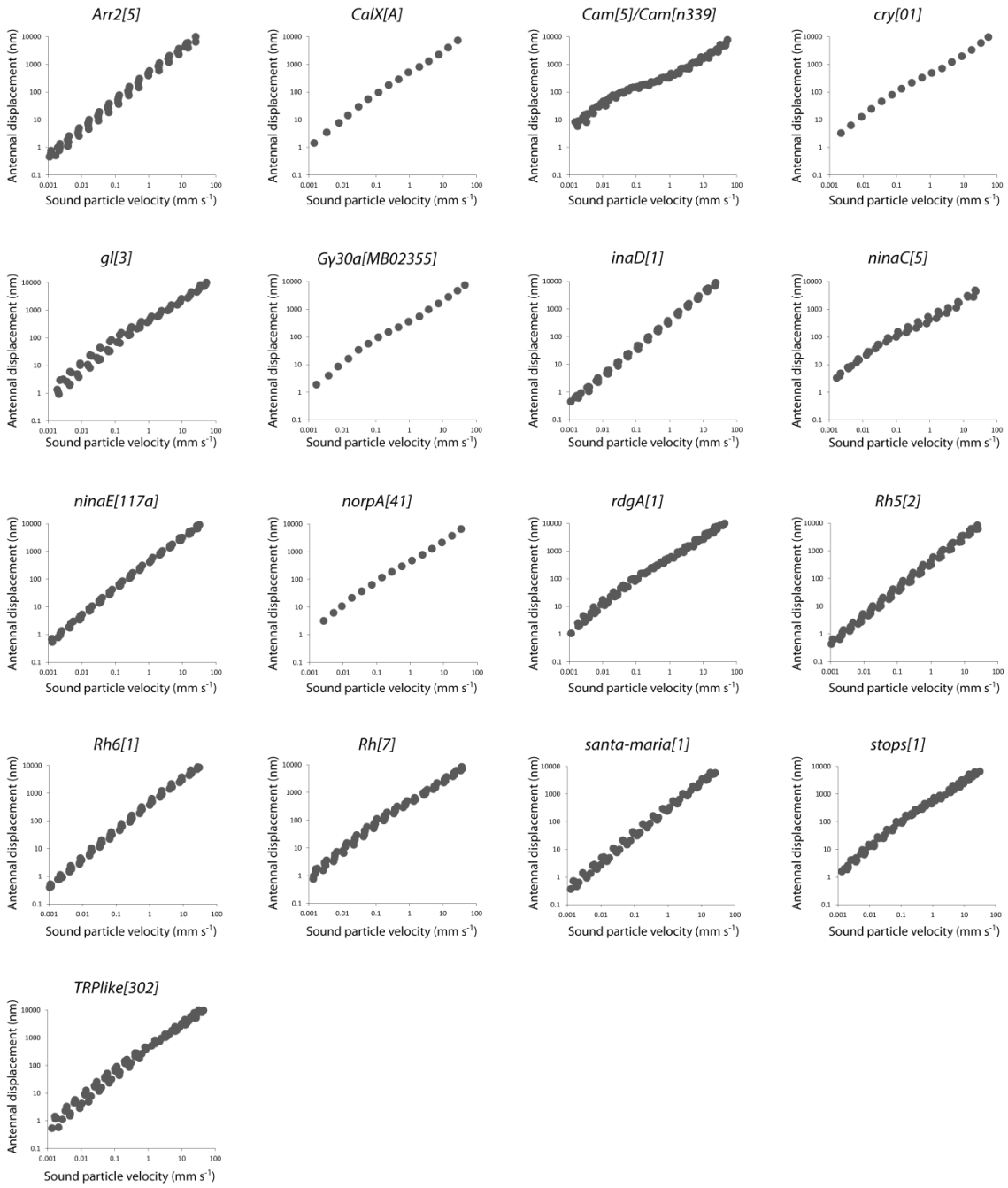

Figure 13: Mechanical response characteristics of *Drosophila* phototransduction mutants.

Johnston's organ neurons provide frequency specific mechanical amplification that can be observed as a nonlinear compression, resulting in a nonlinear relation of sound particle velocity and antennal displacement (e.g. *cry, ninaC, rdgA*). N = 5 flies/strain, except for *CalX*, *cry*, *Gγ30a* and *norpA*, where N equals 1.

Nonlinear compression means that faint sound undergo a larger enhancement than louder ones, providing intensity- and frequency dependent signal amplification. The mechanical sensitivity of the antenna is quantified as the ratio between its displacement amplitude and the corresponding sound particle velocity. By normalizing this sensitivity in the lower linear regime to that in the upper linear regime, it is possible to quantify the mechanical sensitivity gain that is provided by this

active amplification. The mechanical sensitivity gain is thus defined as the difference of the mechanical sensitivity between the lower linear regime and the upper linear regime.

The mutant strains displayed a wide variety of amplification gains. Overall, the lowest observed amplification gain was 1.2 and the highest observed was 37.2 (Figure 14).

Mutations in the following genes lead to 'severely impaired' Johnston's organ function (gain < 1.5): *inaD* (1.2 ± 0.1), *Arr2* (1.3 ± 0.1), *santa-maria* (1.3 ± 0.1), *Rh 5* (1.4 ± 0.2), *Rh 6* (1.4 ± 0.2) mutants.

'Moderately impaired' (1.5 < gain < 5.5) Johnston's organ function display flies with mutations in: *trp* (1.7 ± 0.3), *ninaE* (1.8 ± 0.3), *trpl* (2.6 ± 1.1), *rh7* (4.1 ± 0.7), *gl* (4.6 ± 1.7), *stops* (4.9 ± 1.2).

'Normal hearing' (5 < gain < 15) flies: *inaC* (5.5 ± 0.6). Note that this strain displays a significantly reduced sensitivity gain with respect to wild-type flies.

Flies that are put into the category of 'hyperamplification' (gain > 15): *eya* (15.3 ± 3) and *Cam* (37.2 ± 6.8).

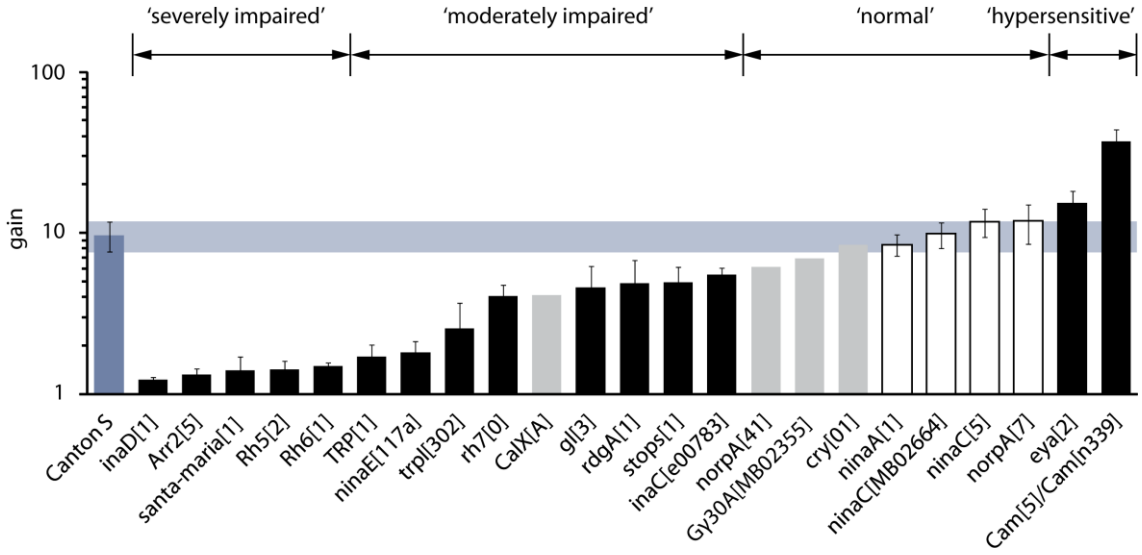

Figure 14: Mechanical amplification gains of *Drosophila* phototransduction mutants.

Data are presented as mean values ± 1 standard deviation. N ≥ 5 flies per strain were probed except for *CalX*, *norpA*, *Gγ30a* and *cry* (highlighted in grey), where N = 1. The blue bar highlights the standard deviation obtained for *Canton S* controls. Black bars signal significant deviates from controls (two-tailed Mann-Whitney U test, $p < 0.05$, corrected for multiple comparisons with Benjamini and Yekutieli procedure for control of the false discovery rate), and empty bars signal the absence of a significant difference. Based on the amplification gains, mutations were categorized as follows: 'severely impaired' gain < 1.5, 'moderately impaired' gain 1.5 – 5, 'normal' gain 5 – 15 and 'hypersensitive' gain > 15. To facilitate comparisons, I included data from additional thesis, see Table 2.

Probing the nonlinear amplification gain revealed thirteen mutations that lead to a significantly decreased and two that lead to a significantly increased gain. Besides providing amplification, the Johnston's organ transduces mechanical sound receiver vibrations to cellular electrochemical signals. This I examine in the next chapter.

Maximum compound action potential responses

Probing the maximum antennal nerve response revealed mutations that decrease the amplitude of the compound action potential (CAP). The nerve response is recorded extracellularly as a CAP. Since the CAP is a summation of single cell action potentials the maximum antennal CAP correlates with the number of neurons that responds to a stimulus.

Probing control flies (*Canton S*) show a strong variability of 41 ± 34 µV. This is mostly due to limitations in the experiment itself: both the distance between the recording electrode and the nerve and the quality of the electrode significantly impacts this reading. Flies with mutations in *inaD* 1.6 ± 1, *Arr2* 5.9 ± 3.2, *santa–maria* 3.6 ± 4.3, *Rh5* 3.3 ± 3.2 and *Cam* 12 ± 4.1 µV have a low maximum CAP ($p = 0.062$).

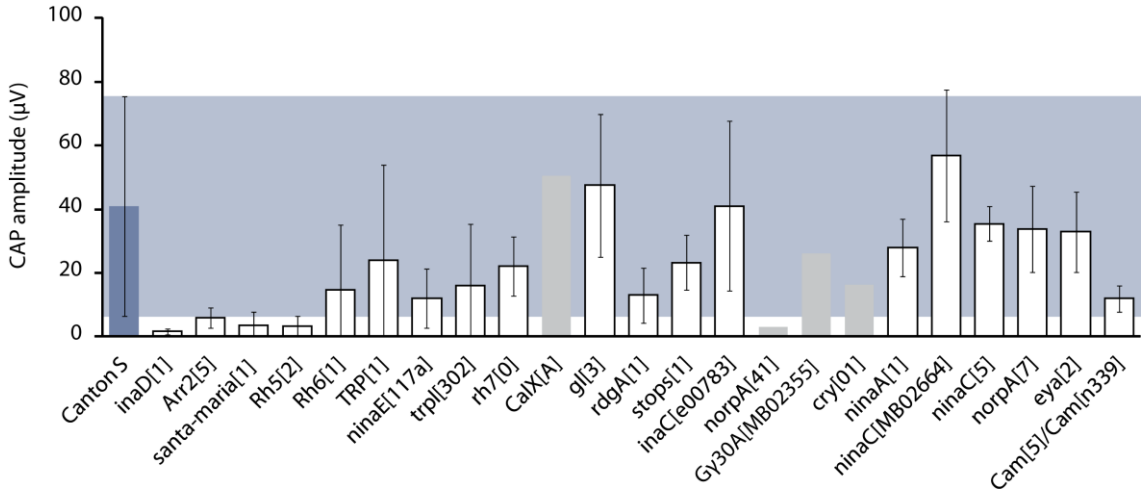

Figure 15: Maximum compound action potential amplitudes of *Drosophila* phototransduction mutants.

Data are presented as mean values ± 1 standard deviation. N ≥ 5 flies per strain were probed except for except for *CalX*, *norpA*, *Gγ30a* and *cry* (highlighted in grey), where N = 1. Blue ghost trace indicates level of standard deviation of *Canton S* flies that are used as wild type controls. Empty bars are not significantly different from *Canton S* (two-tailed Mann-Whitney U test, $p < 0.05$, corrected for multiple comparisons with Benjamini and Yekutieli procedure for control of the false discovery rate). To facilitate comparisons, I included data from additional thesis, see Table 2.

No significant changes ($p < 0.05$) in the maximum CAP response have been discovered, but some mutations lead apparently to a decreased CAP. These findings indicate that mechano-electrical transduction or transmission of electric signals is impaired.

To probe the sensitivity of the Johnston's organ neurons I quantified the 'hearing threshold' and the 'displacement threshold'.

Auditory sensitivity

Thresholds of sound-evoked antennal nerve potentials are shown in Figure 17. Nerve potentials were measured in response to pure tones of different sound particle velocities at the antenna's mechanical best frequency. Normalized potential amplitudes were plotted against the corresponding sound particle velocities and fitted with a Hill equation. Thresholds were defined as the sound particle velocity corresponding to 10% of the maximum amplitude of the nerve potentials.

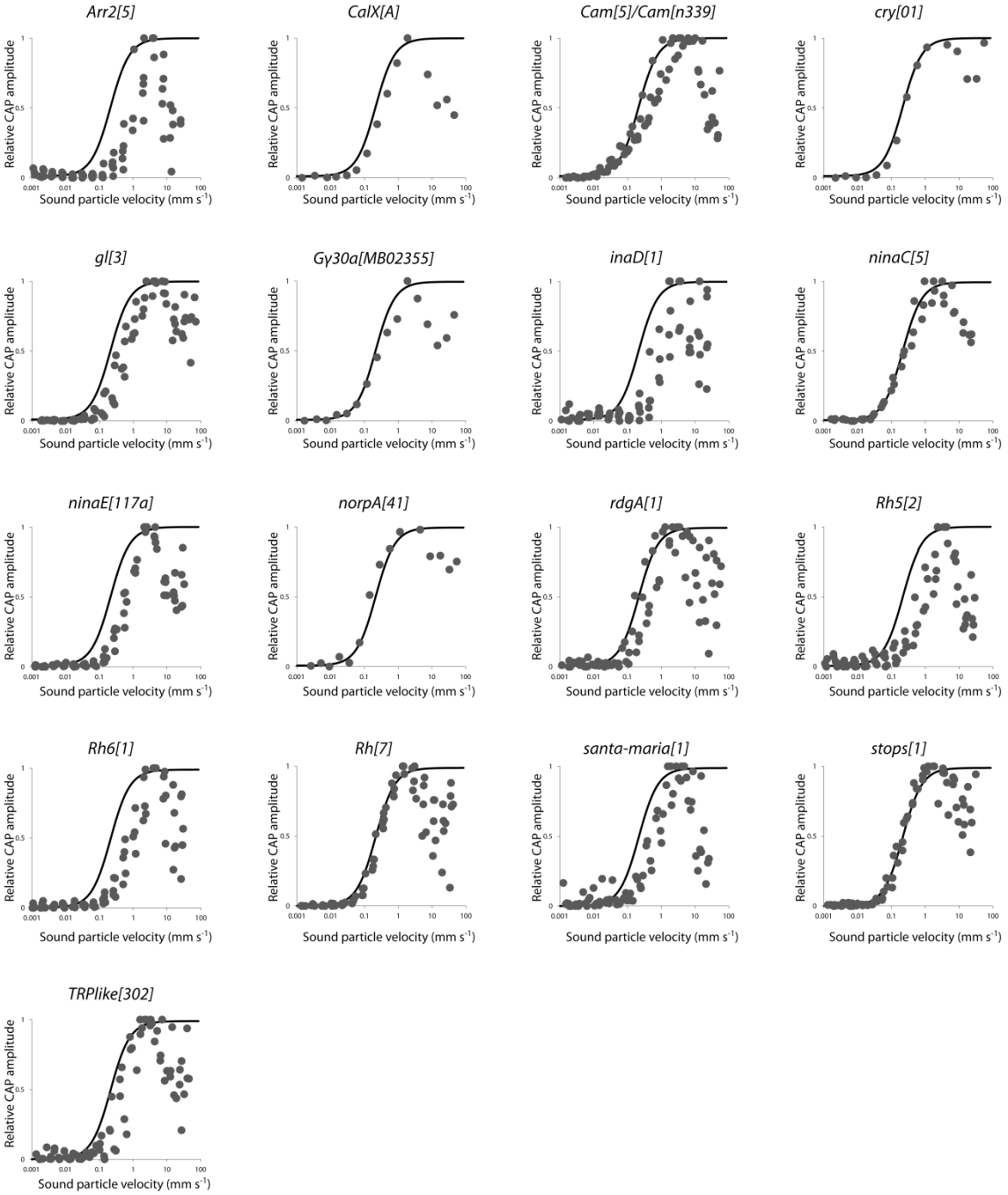

Figure 16: Compound action potential response as function of sound particle velocity.

The compound action potential dynamic range is typically between 50 and 1000 µm/s, sound particle velocity corresponding to 10 % and 90 % increase of the CAP, determined by a Hill-fit (e.g. *Canton S, ninaC[5], stops[1]).* Black slopes are Hill-fits from *Canton S* flies for comparison. N = 5 flies/strain, except for *CalX*, *cry*, *Gγ30a* and *norpA*, where N equals 1.

Canton S wild-type flies have a sound particle velocity threshold *of* 49 ± 15 µm/s (mean ± 1 S.D.). The corresponding values 443 ± 232 for *inaD* mutants, 288 ± 316 for *Arr2* mutants, *santa-maria* 166 ± 53, *Rh5* 231 ± 91, *Rh6* 281 ± 142, *trp* 204 ± 66, *ninaE* 202 ± 71, *trpl* 273 ± 186, *gl* 155 ± 85 and *rdgA* 116 ± 48 µm/s were significantly higher than in *Canton S* flies.

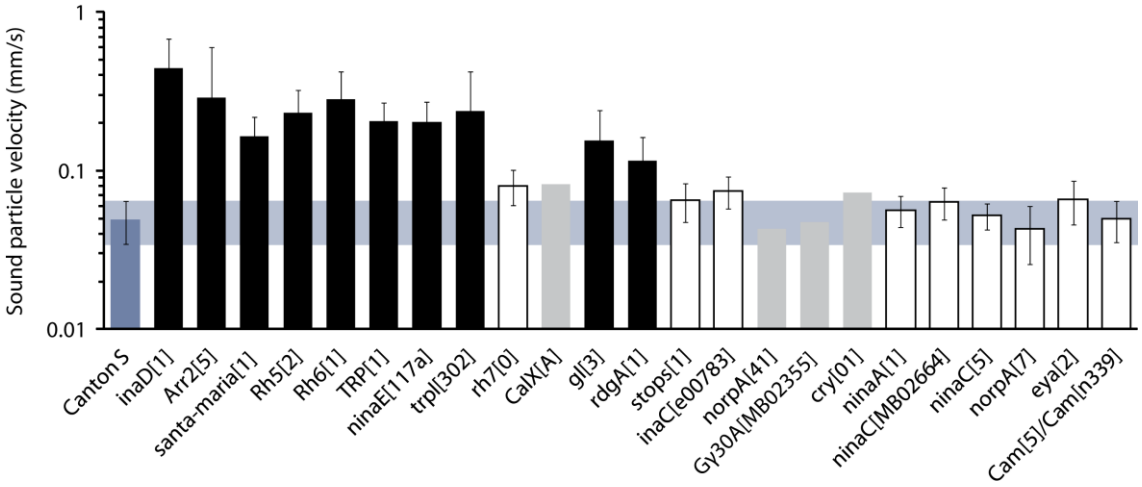

Figure 17: Thresholds of CAPs with respect to the sound particle velocity of *Drosophila* phototransduction mutants.

The threshold for each fly was calculated as the sound particle velocity corresponding to 10 % of the maximum CAP response determined from a Hill-fit. Data are presented as mean values ± 1 standard deviation. N ≥ 5 flies per strain except for *CalX, norpA, Gγ30a and cry* (highlighted in grey), where N = 1 have been probed. Blue bar: standard deviation of *Canton S* flies that are used as wild-type controls. Black bars highlight significant deviations from *Canton S* flies (two-tailed Mann-Whitney U test, $p < 0.05$, corrected for multiple comparisons with Benjamini and Yekutieli procedure for control of the false discovery rate) and empty bars signal the absence of statistical significance. To facilitate comparisons, I included data from additional thesis, see Table 2.

The 'hearing threshold' is a measure of the sensitivity of the Johnston's organ to the stimulus sound particle velocity. Therefore it depends on the amplification provided by JO neurons. These result shows that 10 mutations lead to Johnston's organs that are significantly less sensitive to sound. The compound action potentials are shifted to louder sounds.

Displacement thresholds

To test whether the 'hearing threshold' shifts observed in the mutants solely reflect alterations in the mechanical sensitivity of the antennal receiver due to impairments in amplification, I plotted the nerve potential amplitudes directly against the receiver's displacement, thereby ignoring the mechanical sensitivity of the receiver (Effertz et al. 2011).

The respective 'displacement thresholds' of the potentials were determined from Hill fits using 10% of the maximum amplitude assumed by the fits as the threshold criterion.

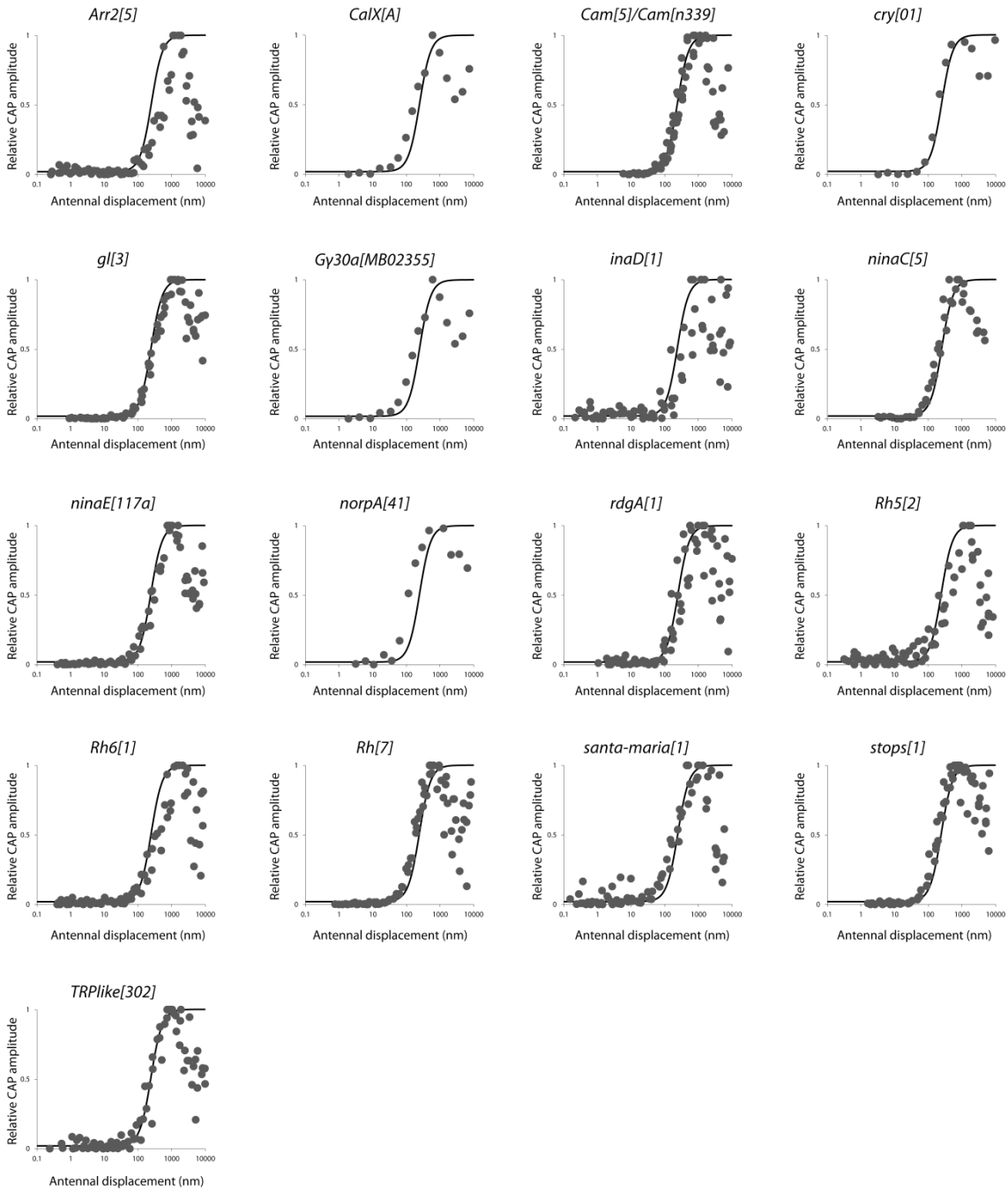

Figure 18: Compound action potential response as function of antennal displacement.

The compound action potential dynamic range is typically between 100 and 600 nm e.g. *Canton S*, *gl[3]*, *stops[1]* (antennal displacement corresponding to 10 % and 90 % increase of the CAP, determined by a Hill-fit). Black slopes are Hill-fits from *Canton S* flies for comparison. N = 5 flies/strain, except for *CalX*, *cry*, *Gγ30a* and *norpA*, where N equals 1.

Canton S flies showed a mean 'displacement threshold' of 97 ± 20 nm. Not a single mutant *Drosophila* strains revealed significant alterations (two-tailed Mann-Whitney U test, $p < 0.05$, corrected for multiple comparisons with Benjamini and Yekutieli procedure for control of the false discovery rate). Mutations in *Arr2* (209 ± 94 nm) slightly but not significantly ($p = 0.07$) increased

this threshold, whereas mutations in *santa-maria* (54 ± 6 nm) and *inaC* (65 ± 7 nm) slightly but not significantly (p = 0.07 and 0.1) decreased it.

Judging from these observations, it seems likely that the observed alterations of the amplification gain as well as the 'hearing threshold' are due to changes in the amplification process, and not due to alterations in the displacement sensitivity of the Johnston's organ neurons. In the three mutants *santa-maria*, *inaC*, and *Arr2*, the observed alterations might be due to both factors.

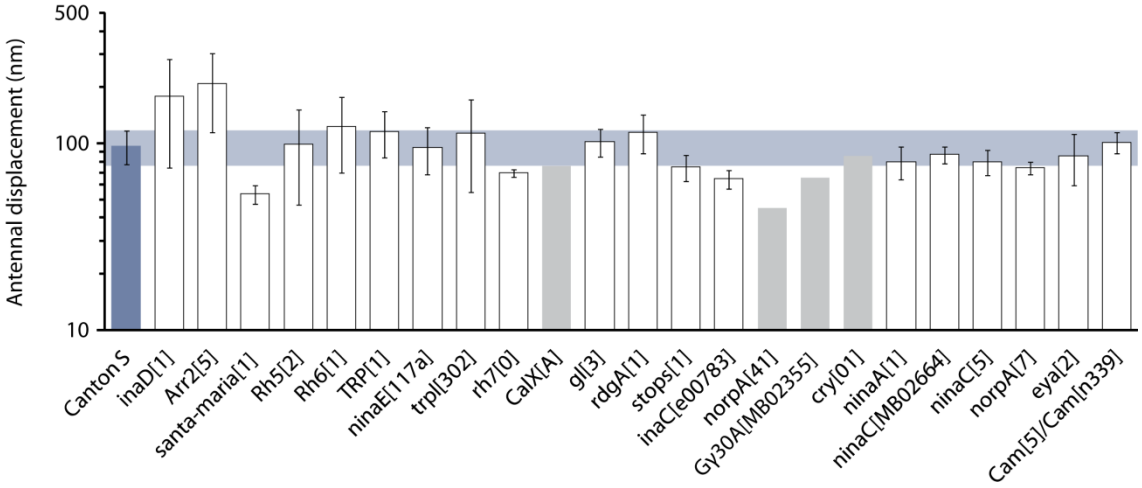

Figure 19: 'Displacement thresholds' of *Drosophila* phototransduction mutants.

The 'displacement threshold' for each fly was calculated as the antennal displacement corresponding to 10 % of the maximum CAP response determined from a Hill-fit. Data are presented as mean values ± 1 standard deviation. N ≥ 5 flies per strain except for *CalX*, *norpA*, *Gγ30a and cry* (highlighted in grey), where N = 1 have been probed. Blue bar: standard deviation of *Canton S* flies that are used as wild-type controls. Black bars highlight significant deviations from *Canton S* flies (two-tailed Mann-Whitney U test, $p < 0.05$, corrected for multiple comparisons with Benjamini and Yekutieli procedure for control of the false discovery rate) and empty bars signal the absence of statistical significance. To facilitate comparisons, I included data from additional thesis, see Table 2.

This screen revealed defects in amplification, sensitivity the Johnston's organ and potentially defects in mechano-electrical transduction. Additionally it revealed that visual rhodopsin which plays a central role as the light detector in photoelectric transduction has a strong impact on Johnston's organ function.

For this reason I focus in the next chapter on rhodopsins by expanding this screen on double mutant flies, a genetic rescue and probe their impact on mechano-electrical transducer gating

.

2.2.2 Characterizing the function of rhodopsin in *Drosophila* hearing

In the previous chapter, I have shown that a large number of mutations affecting genes, that are associated with vision, also affect hearing. Quite unexpectedly, these genes include visual rhodopsins. The protein rhodopsin is known to be the light detector of the visual sense (Lindsley and Zimm 1992; Rister and Desplan 2011). Whereas seven different rhodopsin proteins are known in *Drosophila*, only the rhodopsin genes *Rh3*, *Rh4*, *Rh5* and *Rh6* have been detected in the Johnston's organ of the fly (Senthilan et al. 2012). To learn more about the relationship between rhodopsins and hearing, I studied their expression and functional relevance in Johnston's organ. In addition to *rhodopsin 5* and *rhodopsin 6*, I also functionally analyzed *rhodopsin 1* and *rhodopsin 7*, which had not been detected in Johnston's organ by Senthilan et al. 2012. By comparing a *rhodopsin 6* mutant fly with a genetic rescue I show, that the mutant phenotype observed from *rhodopsin 6* mutants is rhodopsin specific. In addition, I provide evidence that *rhodopsin 5* and *rhodopsins 6* have a partial non redundant function by providing data of double mutant fly strains (*ninaE* and *Rh6* as well as *Rh5* and *Rh6*).

2.2.2.1 Rescue experiment and double mutations

Probing antennal free fluctuations of the following fly strains revealed that the genetic rescue for *rhodopsin 6* (Figure 20, subplot A) has a power spectrum which is different from *rhodopsin 6* mutant flies (Figure 10). This indicates that the genetic *Rh6 rescue* restores the typical auditory phenotype. Furthermore, the power spectra of both double mutant fly strains, *ninaE*, *rhodopsin 6* and *rhodopsin 5*, *rhodopsin 6* show a smaller peak of power than the *Rh6 rescue* (Figure 20, subplot A).

The nonlinear feedback amplification boosts the antennal sensitivity to faint sound. It is probed by stimulating each fly with sinusoidal sound matching the best frequency of the respective antenna. The mechanical response characteristic of *Rh6 rescue* und *Rh5,Rh6* double mutant flies is shown in Figure 20, subplot B). It revealed a nonlinear slope for *Rh6 rescues* and a linear slope for *Rh5,Rh6* double mutant flies. This indicates that the antennal amplifier of *Rh6 rescues* is functional, whereas the one from *Rh5,Rh6* double mutant is defect. Plotting the normalized CAP, as function of sound particle velocity, shows differences between the fly strains. The CAP dynamic range of *Rh6 rescues* look very similar to those of *Canton S* flies (black trace, Hill-fit of *Canton S* flies). The CAP of *Rh5,Rh6* double mutants is shifted to higher sound intensities when compared with *Canton S* flies (Figure 20, subplot C). Plotting the normalized compound action potential amplitude as function of arista displacement (Figure 20, subplot D) revealed not alterations of *Rh6 rescues* and *Canton S* (black trace, Hill-fit of *Canton S* flies) but a shift for *Rh5,Rh6* double mutant flies when compared with *Canton S*.

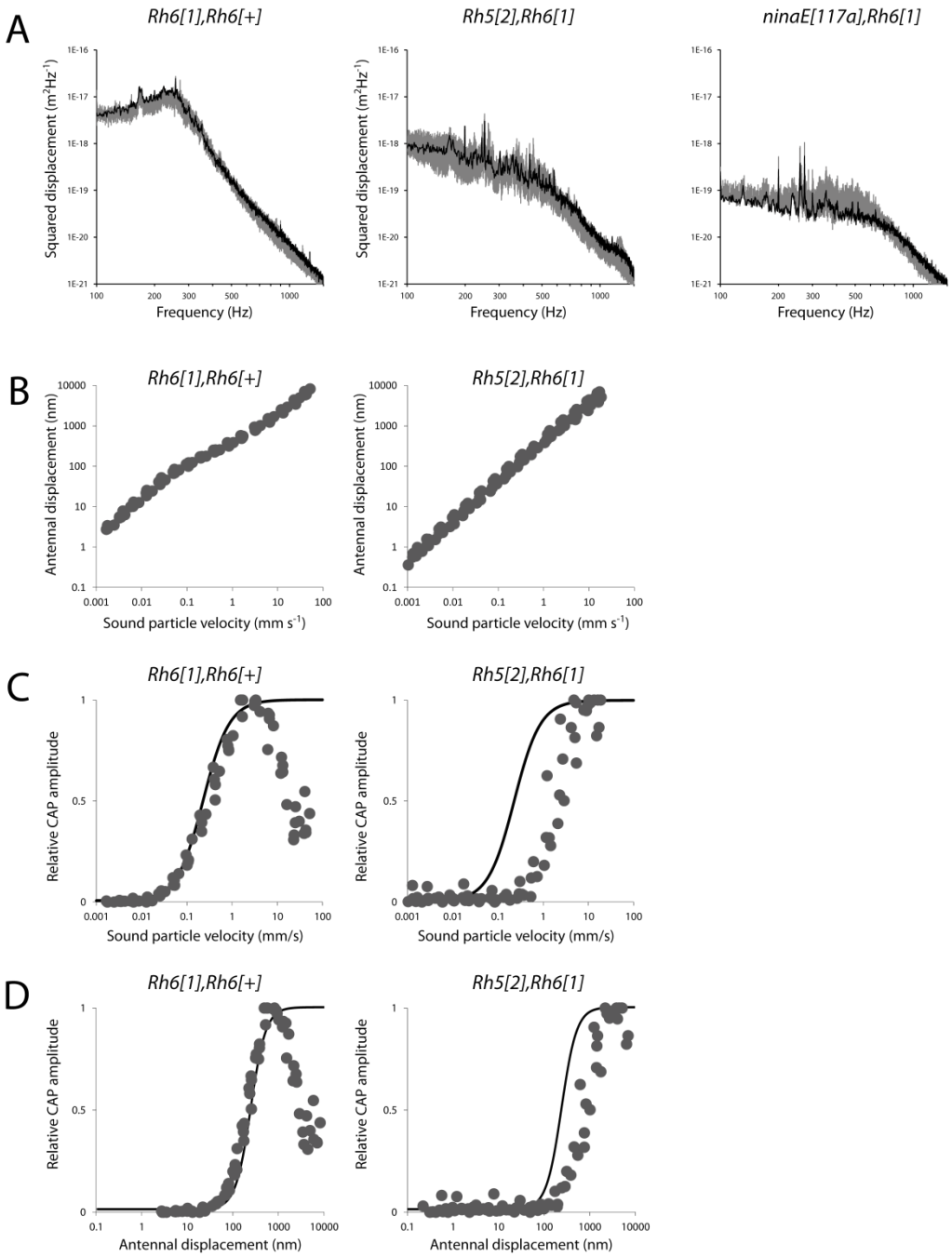

Figure 20: Rhodopsin rescue and double mutant flies.

A) Free fluctuation recordings. Data are plotted as power spectra (x-axis: frequency, y-axis: squared displacement). Grey ghost traces show the range of individual recordings, N = 5 flies. One exemplary recording in each dataset is highlighted in black.
B) Mechanical response characteristics. Each dataset includes N = 5 flies.
C) Compound action potential response as function of sound particle. Each dataset includes N = 5 flies. Black trace is the Hill-fit of *Canton S* flies.
D) Compound action potential response as function of arista displacement. Each dataset includes N = 5 flies. Black trace is the Hill-fit of *Canton S* flies.

These observations are quantified by calculating the best frequency, fluctuation power, amplification gain, maximum CAP amplitude, 'hearing threshold' and 'displacement threshold'.

Mutations in rhodopsin affect active antennal tuning

The best frequencies of *Canton S* flies have a mean value of 253 ± 19 Hz (± 1 S.D.). The genetic *rhodopsin 6* rescue 253 ± 8 Hz is not significantly different from *Canton S* flies but significantly different (two-tailed Mann-Whitney U test, p = 0.0079) from *rhodopsin 6* (454 ± 8 Hz) mutant flies. Mutations in *rhodopsin 1* (*ninaE*) 425 ± 37 Hz and *rhodopsin 5* (459 ± 62 Hz), rhodopsin 7 (313 ± 18 Hz) and both double mutant fly strains *ninaE[117a], Rh6[1]* (542 ± 52 Hz) *and Rh5[2], Rh6[1]* (396 ± 49 Hz) significantly increase the best frequency compared to *Canton S*.

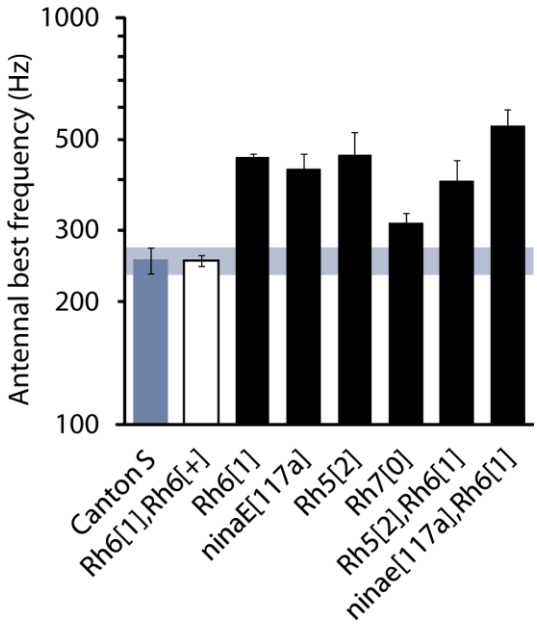

Figure 21: Sound receiver best frequencies of *Drosophila* rhodopsin mutants.

Data are presented as mean values ± 1 standard deviation. N = 5 flies per strain were probed. Blue ghost trace indicates level of standard deviation of *Canton S* flies that are used as wild type controls. Black bars deviate significantly from *Canton S* flies (two-tailed Mann-Whitney U test, $p < 0.05$, corrected for multiple comparisons with Benjamini and Yekutieli procedure for control of the false discovery rate) and empty bars are not significantly different from *Canton S*.

Mutations in rhodopsin impair active amplification

The power spectral density which is a measure of the Johnston's organ system power providing energy for nonlinear amplification is calculated as the in integral between 100 – 1500 Hz of the power spectral density.

Johnston's organ system power of *ninaE[117a]* 234 ± 118 nm², Rh5[2] 207 ± 23 nm², Rh6[1] 329 ± 98 nm² the double mutant fly strain Rh5[2],Rh6[1] 219 ± 97 nm² and *ninaE,Rh6* 41 ± 24 nm are significantly decreased when compared to *Canton S* 1873 ± 789 nm².

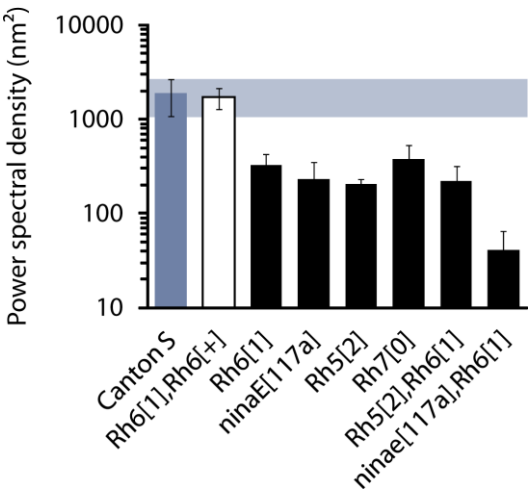

Figure 22: Johnston's organ fluctuation power of *Drosophila* rhodopsin mutants.

Data are presented as mean values ± 1 standard deviation. N ≥ 5 flies per strain were probed. Blue ghost trace indicates level of standard deviation of *Canton S* flies that are used as wild type controls. Black bars deviate significantly from *Canton S* flies (two-tailed Mann-Whitney U test, $p < 0.05$, corrected for multiple comparisons with Benjamini and Yekutieli procedure for control of the false discovery rate) and empty bars are not significantly different from *Canton S*.

To analyze the amplification provided by the Johnston's organ calculated amplification gain. The nonlinear sensitivity gains of *Rh6* rescue flies 10.9 ± 1.4 is not significant different from *Canton S* 9.7 ± 2.1 flies but significantly higher compared to *Rh6* mutant flies 1.5 ± 0.1. Mutations in *ninaE* (1.8 ± 0.3), *Rh5* (1.4 ± 0.2), *Rh6* (1.5 ± 0.1) and the double mutant *Rh5,Rh6* (1.5 ± 0.3) result in a significantly lowered nonlinear sensitivity gain.

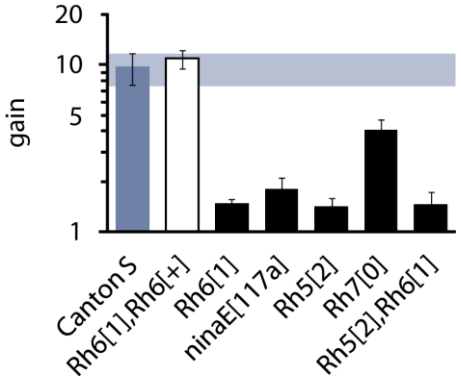

Figure 23: Mechanical amplification gains of *Drosophila* rhodopsin mutants.

Data are presented as mean values ± 1 standard deviation. N ≥ 5 flies per strain were probed. Blue ghost trace indicates level of standard deviation of *Canton S* flies that are used as wild type controls. Black bars deviate significantly from *Canton S* flies (two-tailed Mann-Whitney U test, $p < 0.05$, corrected for multiple comparisons with Benjamini and Yekutieli procedure for control of the false discovery rate) and empty bars are not significantly different from *Canton S*. Based on this amplification gain, mutations are ranked by the following categories: single mutant *Rh5[2]* and *Rh6[1]* as well as double mutant *Rh5[2],Rh6[1]* are 'severely impaired' (gain < 1.5), *ninaE[117a]* and Rh7*[0]*

'moderately impaired' (gain 1.5 – 5) and *Rh6 rescue* (*Rh6[1],Rh6[+]*) 'normal hearing' (gain 5 – 15).

For sound stimulation at best frequency, the maximum compound action potential response for *Canton S* flies is 40.9 ± 34.4 µV. The *rhodopsin 6* rescue (35.7 ± 14.3 µV) and *rhodopsin 6* mutant (14.7 ± 20.5) do not significantly differ from *Canton S*, but mutations in *rhodopsin 1* (12 ± 9.3), *rhodopsin 5* (3.3 ± 3.2) and the double mutant *rhodopsin 5*, *rhodopsin 6* (9.7 ± 9.3) have a significantly reduced maximum compound action potential response.

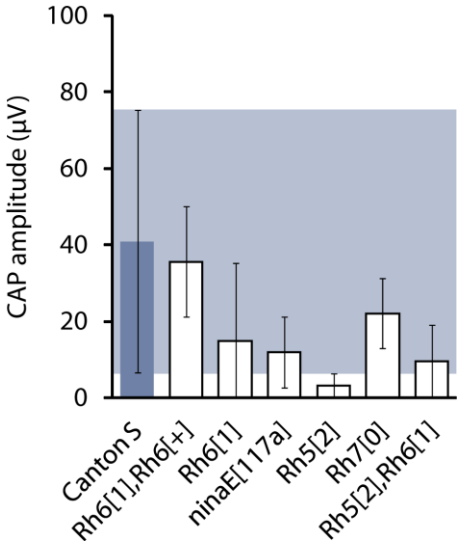

Figure 24: Amplitudes of sound-evoked potentials in *Drosophila* rhodopsin mutants.

Data are presented as mean values ± 1 standard deviation. N ≥ 5 flies per strain were probed. Blue ghost trace indicates level of standard deviation of *Canton S* flies that are used as wild type controls. Black bars deviate significantly from *Canton S* flies (two-tailed Mann-Whitney U test, $p < 0.05$, corrected for multiple comparisons with Benjamini and Yekutieli procedure for control of the false discovery rate) and empty bars are not significantly different from *Canton S*.

To determine the sensitivity of the Johnston's organ to sound I analized the antennal nerve amplitude in response to the stimulus sound particle velocity.

Canton S flies have a 'hearing threshold' of 49 ± 15 µm/s. Mutations, of *Rh6* 281 ± 142 µm/s, *ninaE1* 202 ± 70 µm/s, *Rh5* 231 ± 91 µm/s, *Rh7* 81 ± 20 and *Rh5,Rh6* 650 ± 223 mm/s result in a significantly higher 'hearing threshold', whereas no fly showed a significantly lowered CAP threshold. The *Rh6* rescue is not significantly different from *Canton S* flies.

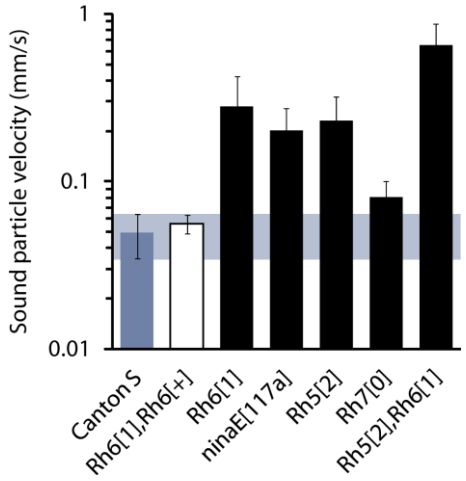

Figure 25: Thresholds of CAPs with respect to the sound particle velocity in *Drosophila* rhodopsin mutants.

Data are presented as mean values ± 1 standard deviation. N ≥ 5 flies per strain were probed. Blue ghost trace indicates the level of the standard deviation obtained for Canton S wild-type controls. Black bars deviate significantly from *Canton S* flies (two-tailed Mann-Whitney U test, $p < 0.05$, corrected for multiple comparisons with Benjamini and Yekutieli procedure for control of the false discovery rate) and empty bars are not significantly different from *Canton S*.

The antennae of *Canton S* flies had to be displaced for 97 ± 20 nm to elicit 10 % of the maximum compound action potential, which is defined here as the 'displacement threshold'. *Rh5,Rh6* double mutations significantly increased the 'displacement threshold' to 295 ± 88 nm, whereas flies with mutations in *Rh7* had a significantly decreased 'displacement threshold' (69 ± 3 nm).

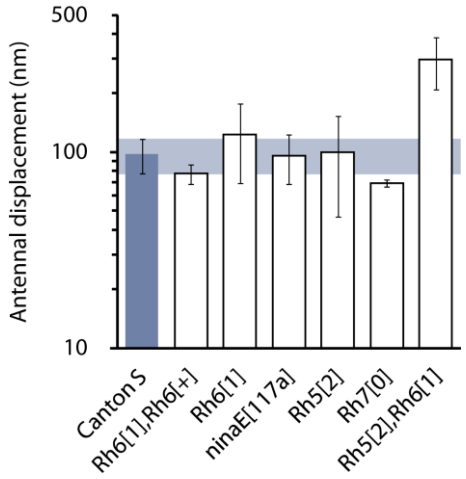

Figure 26: 'Displacement thresholds' in *Drosophila* rhodopsin mutants.

Data are presented as mean values ± 1 standard deviation. N ≥ 5 flies per strain were probed. Blue ghost trace indicates level of standard deviation of *Canton S* flies that are used as wild type controls. Black bars deviate significantly from *Canton S* flies (two-tailed Mann-Whitney U test, $p < 0.05$, corrected for multiple comparisons with Benjamini and Yekutieli procedure for control of the false discovery rate) and empty bars are not significantly different from *Canton S*.

2.2.2.2 Rhodopsin 5 and rhodopsin 6 impact mechano–electrical transduction in the *Drosophila* Johnston's organ

To test, whether the reduced auditory sensitivity in *rhodopsin* mutants reflects, defects in mechanotransduction, I tested for mechanical correlates of channel gating. In *Drosophila*, the direct mechanical gating of ion channels in Johnston's organ introduces a nonlinear gating compliance in the mechanics of the antennal receiver. This gating compliance conforms to the gating spring model of transduction in hair cells, which assumes a parallel arrangement of a linear spring, which represents the linear elasticity of JO and the antennal joint and gating springs that convey the stimuli to the ion channels. These gating springs will relax when the channels open, introducing a nonlinear gating compliance in the mechanics of the receiver (Albert et al. 2007a; Albert et al. 2007b). By analyzing the nonlinear gating compliance in rhodopsin mutants, I tested whether the mechanical gating of ion channels in JO neurons depends on rhodopsins.

The nonlinear gating compliance is plotted in Figure 27. The peak slope stiffness (red dots) reflecting the gating compliance and the steady state slope stiffness, which is the linear stiffness (blue dots) of the *Drosophila* antenna, are plotted against antennal displacements ranging between -10 to + 10 μm.

As shown in the first row of Figure 27, the gating compliance is present in *Canton S, Rh6* rescue, *Rh6* mutant and *Rh5,Rh6* double mutant flies. In *Rh6* and especially *Rh5,Rh6* mutants, however, the nonlinear stiffness drop at small displacements is much less pronounced. Control and rhodopsin mutant flies both show mechanically evoked compound action potential (second row in Figure 18, orange dots), but the in *Rh5,Rh6* the response is broadened, indicating that rhodopsin double mutant flies are less sensitive due to small antennal displacements.

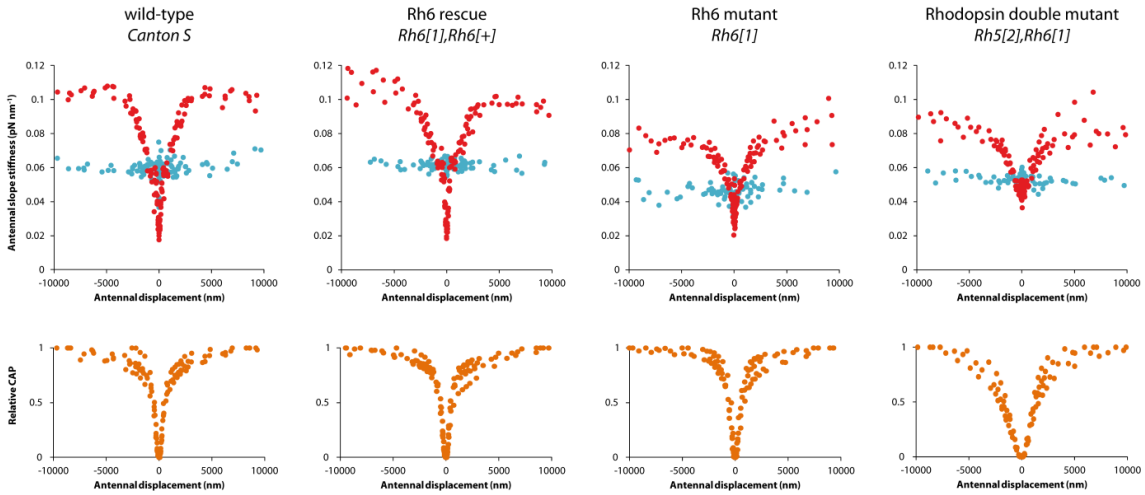

Figure 27: Correlates of mechano–electrical transducer gating of rhodopsin mutant flies.

Each dataset includes N = 5 flies. First row: The plots show peak slope stiffness (red) of the antennal ear as a function of antennal displacement and in blue the steady state slope stiffness. Second row: relative compound action potentials due to peak displacement. First column: *Canton S*, second column *rhodopsin 6* rescue, third column: *rhodopsin 6* mutants and fourth column: double mutants for *Rh5* and *Rh6*.

To quantify these alterations, I fitted the nonlinear gating compliance with a four-state gating spring model that comprises two types of mechanically gated channels. The different types of channels differ in their sensitivities. Previous studies have shown, that the more sensitive channel type is NOMPC-dependent and mediates hearing, whereas the less sensitive channel seems implicated in wind/gravity-sensing and has hitherto not been linked to a channel protein.

According to the four-state gating spring model, the displacement-dependent stiffness of the receiver, K(x) can be written as:

$$K(x) = K_{inf} - \left(\frac{N_s z_s^2}{k_B T}\right) * P_{0\_s}(1 - P_{0\_s}) - \left(\frac{N_i z_i^2}{k_B T}\right) * P_{0\_i}(1 - P_{0\_i})$$

Equation 1: Gating spring model with two independent types of channels

This gating spring model consists of two types of channels, first one is sensitive ($_s$) and second insensitive ($_i$) (Effertz et al. 2012). Parameters: N = number of channels, z = single channel gating force, P_O = open probability and K_{inf} = maximum antennal stiffness.

Since the gating compliance of double mutants (*Rh5,Rh6*) looks less sharp than that of controls, I had to decide, if the model consisting of one channel type or the one with two different channels describes the data best. Because the model with one channel type is used if one of the two transducers is non functional (Effertz et al. 2012).

$$K(x) = K_{inf} - \left(\frac{Nz^2}{k_B T}\right) * P_0(1 - P_0)$$

Equation 2: Gating spring model with one types of channels

This gating spring model consists of one type of channel. Parameters: N = number of channels, z = single channel gating force, P_O = open probability and K_{inf} = maximum antennal stiffness.

This decision is made by fitting the slope stiffness data, of each genotype, with the model containing one channel type and the model with sensitive and insensitive channels. The Akaike information criterion with correction for finite sample size (AICc) is a measure of goodness for fitting results (Burnham and Anderson 2002). Table 3 presents the Akaike weights (w_i), which can assume values between 0 and 1 (low and high probability that the respective model describes the data better) Akaike weights (w_i) revealed that the gating spring model with two transducer types describes the dynamic stiffness of *Canton S*, *Rh6* rescue and *Rh6* mutant flies better than the model with just one type of channel. The latter model, however, sufficed to describe the dynamic stiffness in *Rh5,Rh6* double mutants, indicating that channels of the second type fail to gate.

		AICc		w_i	
		1 channel type	2 channel type	1 channel type	2 channel type
	n	k = 3	k = 5	k = 3	k = 5
Canton S	135	-1375.7	-1534.7	0.00	1.00
Rh6 rescue	135	-1259.4	-1405.1	0.00	1.00
Rh6 mutant	130	-1363.1	-1409.9	0.00	1.00
Rh5,Rh6 double mutant	135	-1577.3	-1574.4	0.79	0.21

Table 3: Comparing one channel with two channel gating spring models with Akaike.

To choose between the gating spring model with 1 channel type (3 model parameters) and the one with 2 channel types (5 model parameters) the Akaike information criterion was calculated. AICc (Akaike information criterion with correction for finite sample size) and wi (Akaike weights) have been calculated based on the number of data points (n) and model parameters (k) following the procedure published in Effertz et al, 2012. Akaike weights that point out which model describes the data best are highlighted in red.

Double mutant fly *Rh5,Rh6* should be fitted via the gating spring model with just one channel type. Figure 28 shows, that fits of the gating spring model for *Canton S* and *Rh6 rescues* look the same whereas *Rh6* mutants have a less pronounced gating compliance and *Rh5,Rh6* double mutants only show a small residual gating compliance.

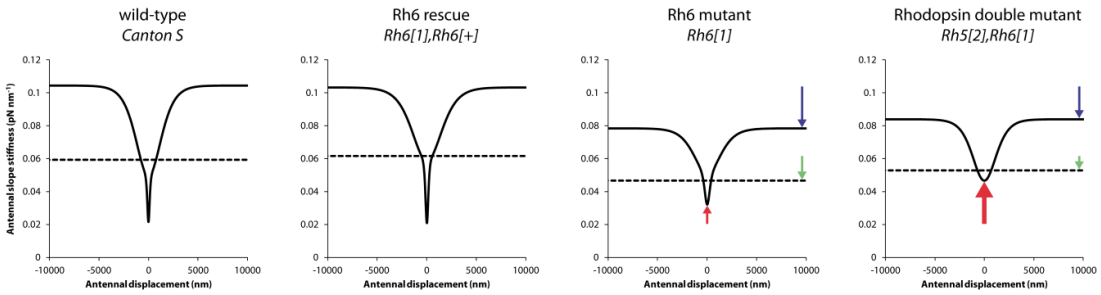

Figure 28: Fits of gating spring models for *Drosophila* rhodopsin mutants.

Canton S, *Rh6 rescue* and *Rh6* mutant flies are analyzed with the gating spring model consisting of sensitive (N_s) and insensitive (N_i) channels. *Rh6* mutant flies have less channels opening to small displacements (highlighted with small red arrow). In addition Rh5,Rh6 double mutant flies are fitted with the model with one channel. This fit reveals that sensitive channels are completely lost in *Rh5,Rh6* double mutant flies, indicated by a large red arrow. Both rhodopsin mutant fly strains have a reduced K_∞, highlighted with blue arrows and reduced parallel stiffness (K_{lin}), green arrow.

Parameter values obtained, by fitting the receiver's dynamic stiffness, with gating spring models, are provided in Table 4. All flies have a shallow gating compliance that is due to gating of insensitive channels (N_i). *Canton S, Rh6 rescues* and Rh6 mutant flies also have insensitive channels. But the single channel gating force (z_s) of sensitive channels is decreased by 47 % (44 fN to 30 fN) in *Rh6* mutants. Due to the loss of a sharp gating compliance and supported by the Akaike information criterion, *Rh5,Rh6* mutants are fitted with the gating spring model with 1 channel type. Therefore, *Rh5,Rh6* mutants have no sensitive but only insensitive channels (judged on the number and gating force of this channels). The single channel gating force of insensitive channels (z_i) stays constant ~ 4.5 fN.

In line with the gating spring model, the antennal stiffness can be understood as the sum of a linear stiffness (K_{lin}) that reflects the linear elasticity of the antennal joint and Johnston's organ, and the stiffness of the gating springs (K_{GS}). By fitting the stiffness data, obtained for each fly strain, the asymptotic stiffness $K_\infty = K_{lin} + K_{GS}$ was deduced. The asymptotic stiffness (K_∞) was reduced in *Rh6* (78 µN/m) and *Rh5,Rh6* mutant flies (84 µN/m) when compared to *Canton S* (105 µN/m) or *Rh6 rescue* (103 µN/m) flies. This decrease in asymptotic stiffness reflects a drop of both K_{lin} and K_{GS}.

The gating spring stiffness (K_{GS}) of *Rh6* and *Rh5,Rh6* mutant flies is reduced (32 and 31 µN/m) compared to *Canton S* (45 µN/m) and *Rh6* rescue (42 µN/m). Since K_{GS} is the combined gating spring stiffness of sensitive and insensitive transducers K_{GS} drops due to a decrease in the count of channels (N_i and N_s) and decrease of z_s.

The linear stiffness (K_{lin}) observed in *Rh6* (47 µN/m) and *Rh5,Rh6* mutants (53 µN) is reduced when compared to *Rh6 rescue* flies (62 µN/m). A decreased linear stiffness can be explained by a reduced number of auditory neurons (Effertz et al. 2012). A decrease of this passive stiffness could be additionally explained by an interrupted connection of some but not all neurons to the antennal joint, an increased joint friction or decrease in stiffness of non transducing cells (Nadrowski et al. 2008).

	N_s			z_s (fN)			N_i			z_i (fN)			K_∞ (µN/m)			K_{lin} (µN/m)			K_{GS} (µN/m)	Number of flies
	Coefficient	95 % confidence bounds		Coefficient	95 % confidence bounds		Coefficient	95 % confidence bounds		Coefficient	95 % confidence bounds		Coefficient	95 % confidence bounds		Coefficient	95 % confidence bounds		K_∞ - K_{lin}	
Canton S	161	104	219	53	45	62	38550	34280	42820	4.8	4.5	5.1	105	103	106	59	58	60	45	5
Rh6 rescue	329	209	448	44	36	51	43610	34780	52440	4.1	3.7	4.5	103	101	105	62	61	62	42	5
Rh6 mutant	314	28	601	30	19	41	19200	13610	24780	5.0	4.1	5.9	78	77	80	47	46	48	32	5
Rh5,Rh6 mutant	-	-	-	-	-	-	23150	19510	26790	5.1	4.8	5.5	84	82	85	53	52	54	31	5

Table 4: Gating spring model parameter values of rhodopsin mutant flies

Data are presented as fit coefficients (with lower and upper confidence bounds), deduced by fitting receiver mechanics with gating spring model consisting of two different channels (*Canton S, Rh6 rescue, Rh6* mutant) and the gating spring model with one type of channel (*Rh5,Rh6* mutant). N = 5 flies where recorded per strain. R^2 for *Canton S* = 0.9842, *Rh6 rescue* = 0.9586, *Rh6* mutant = 0.9373 and *Rh5Rh6* mutant = 0.9522.

Table 5 provides an overview of parameters of: *Rh6* rescues in comparison with *Rh6* single mutant and *Rh5,Rh6* double mutant flies. Most alterations of corresponding parameters are similar between *Rh6* and *Rh5,Rh6* mutant flies. Differences between single and double mutant flies can be observed for the 'hearing threshold', 'displacement threshold' and number of sensitive transducers.

Parameters	***Rh6 rescue***	***Rh6* mutant**	***Rh5,Rh6* mutant**
Best frequency (Hz)	253	↑ 454	↑ 396
Power spectral density (nm^2)	1713	↓ 329	↓ 219
Sensitivity gain	11	↓ 1.5	↓ 1.5
Maximum CAP (µV)	36	↓ 15	↓ 10
'Hearing threshold' (µm/s)	56	↑ 281	↑↑ 650
Threshold of antennal displacement (nm)	77	↑ 123	↑↑ 295
K_{inf} (µN/m)	103	↓ 78	↓ 84
K_{lin} (µN/m)	62	↓ 47	↓ 53
K_{GS} (µN/m)	42	↓ 32	↓ 31
N_s	329	– 314	↓↓ 0
z_s (fN)	44	↓ 30	–
N_i	43610	↓ 19200	↓ 23150
z_i (fN)	4	↑ 5	↑ 5

Table 5: Parameter survey of *Rh6* and *Rh5Rh6* mutant flies

This table summarizes all parameters obtained for *Rh6* and *Rh5,Rh6* mutant flies and compare them with parameters obtained for *Rh6 rescue* flies. Distinct alterations of mutant flies compared with rescues are highlighted with arrows. Double arrows highlight differences between *Rh6* and *Rh5,Rh6* mutant flies. *Rh6* and *Rh5,Rh6* mutant flies show less active feedback amplification due to a decreased power spectral density, amplification gain, shifted 'hearing threshold' and increased best frequency. The idea of a weaker coupling of antennae and transducers is supported by a shifted 'displacement threshold' in addition with no N_s of *Rh5,Rh6* double mutant flies.

In the previous chapter I have shown that rhodopsin mutant flies lack mechanical amplification. To reveal the molecular mode of action, I probed correlates of mechano–electrical transduction. This gating compliance is described by the gating spring model revealing insight into the mode of action.

In *Drosophila Rh6* and *Rh5,Rh6* mutants, the stiffness of elements that are in series with the transducers and that are parallel to the transducers, are altered. Fits of the gating spring model yielded differences between controls and rhodopsin mutants. The count of insensitive transducers is decreased in *Rh6 and Rh5,Rh6* double mutants. *Rh5,Rh6* double mutants have no sensitive transducers at all. In addition, K_{GS} is reduced due to a reduced count of channels. The decrease of the linear stiffness indicates alterations of non transducing components.

To summarize these findings: some transducers get lost and remaining transducers become less sensitive.

2.2.3 Effects of environmental conditions

So far I have shown that genes of the *Drosophila* visual system are required for Johnston's organ function. They are involved in the process of amplification that boosts the ear sensitivity to faint sound. But since the phototransduction cascade and its rhodopsins are known to be a sensor of light or temperature, I probed if they regulate amplification in the Johnston's organ in a light or temperature dependent way.

2.2.3.1 Light dependent recordings

The presence of rhodopsin and other phototransduction proteins in the *Drosophila* ear provokes the question if auditory transduction is light dependent. To address this question, I have grown flies for one generation under 24h/day in light and 24h/day in complete darkness and controls in 12:12 h light:dark rhythm (8 am – 8 pm light) and probed their auditory response characteristic.

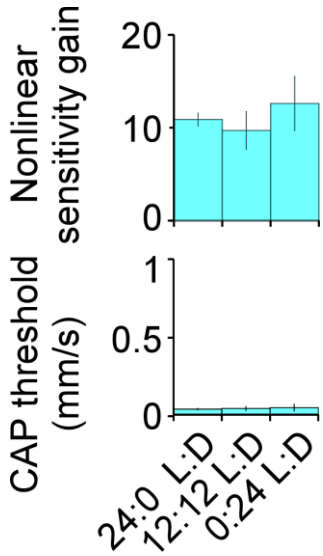

Figure 29: Probing Johnston's organ function for light dependency.

Data are presented as mean values ± 1 standard deviation. N = 5 flies per strain were probed (Senthilan and Piepenbrock et al. 2012). No significant alterations can be observed (two-tailed Mann-Whitney U test, $p < 0.05$).
Upper panel: Nonlinear sensitivity gains.
Lower panel: Sound particle velocity thresholds of compound action potential response ('hearing threshold').

Canton S wild–type flies reared at 24:0, 12:12, and 0:24 hr light:dark conditions all displayed normal Johnston's organ sound responses. With this data I could not show significant differences, indicating rhodopsin are operating in a light independent way in the flies' ear.

2.2.3.2 Chromophore retinal and Johnston's organ function

Another way to test, if the Johnston's organ function depends on light, is: to remove its chromophore. Rhodopsins consist of the protein opsin and the chromophore retinal. *Drosophila* requires 3–OH–11–*cis*–retinal (Montell 2012; Wang et al. 2012). This retinal is metabolized from

its precursor beta-carotene (vitamin A) that is absorbed from the food (Wang et al. 2007). Upon light stimulation 3–OH–11–*cis*–retinal undergoes a conformational change to 3–OH–11–*trans*–retinal which is then released. Trans-retinal is then recycled to *cis*-retinal via an enzymatic metabolic pathway (Montell 2012).

I tested the hypothesis that Johnston's organ function requires retinal by feeding flies with dietary food (vitamin A depleted) and by interrupting the uptake of vitamin A, with a mutation in the gene *santa-maria*.

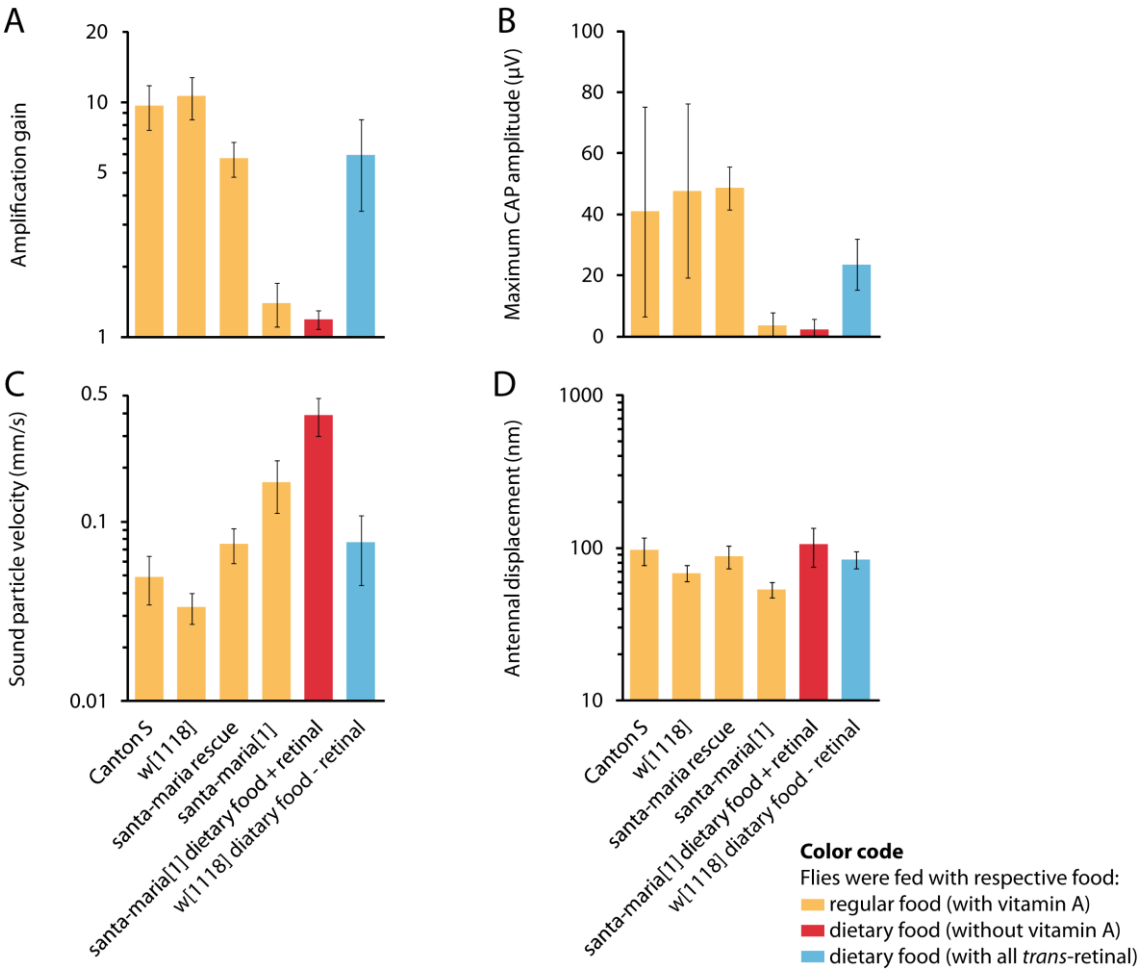

Figure 30: Impact of retinal on Johnston's organ function

Data are presented as mean values ± 1 standard deviation. N = 5 flies per strain were probed (Senthilan and Piepenbrock et al. 2012). Color code: orange = flies where fed with regular food, red = dietary food with all-trans retinal, blue dietary fly food without all-trans retinal (dietary food = vitamin A depleted: for details of regular and dietary fly food see chapter 4.5.1)
A: Mechanical amplification gain
B: Maximum compound action potential
C: 'Hearing threshold'
D: Antennal 'displacement threshold'

Interrupting the beta-carotene uptake, with a mutation in *santa-maria*, does alter the Johnston's organ function significantly. The sensitivity gain is completely abolished. *Santa-maria* encodes a scavenger protein that is required for beta-carotene metabolisms in neural tissue (Wang et al. 2007; Wang and Montell 2007). This mutant phenotype can be restored via a *UAS-santa-maria NP0761-GAL4* driven rescue demonstrating that *santa-maria* is the cause for this phenotype.

To circumvent the interrupted uptake of beta-carotene in *santa-maria* mutants (Shen et al. 2011), flies had been fed with retinal (all *trans*–retinal). But this does not restore the mutant phenotype. Flies feed with dietary food (beta-carotene depletion) with additionally added retinal have even higher sound particle velocity thresholds compared to *santa-maria* mutants raised on regular food. Control recordings show that *w[1118]* mutant flies, (genetic background of *santa-maria*), have an slightly impaired Johnston's organ function when raised on dietary food (vitamin depleted and without retinal) compared to regular food (with vitamin A). This indicates that vitamin A might be required and not *trans*–retinal.

2.2.3.3 Probing the temperature-dependence of Johnston's organ function

Since rhodopsins are known to be involved in thermosensation (Minke and Peters 2011; Shen et al. 2011), it is worth the effort to probe Johnston's organ function, for temperature dependency. It would be conceivable that rhodopsins are involved in a temperature regulation of Johnston's organ function. It is known that mosquitoes shift their antennal best frequency due to changes in temperature, but *Drosophila* does not (Jörg T. Albert, private communication). Is this indicating that Johnston's organ function in *Drosophila* is regulated in dependency of temperature? Removing the potential temperature sensor rhodopsin, in the Johnston's organ, should result in a shift of frequency tuning and Johnston's organ fluctuation power. In return, controls (*Rh6* rescues) should compensate for this temperature dependent shift.

Antenna free fluctuations, a measure of frequency tuning and power supply for amplification, of control flies (*Rh6 rescue*) and *Rh6* mutant flies, have been probed in a temperature range of 0 to 40°C. Therefore flies have been directly mounted on a thermoelectric cooling device.

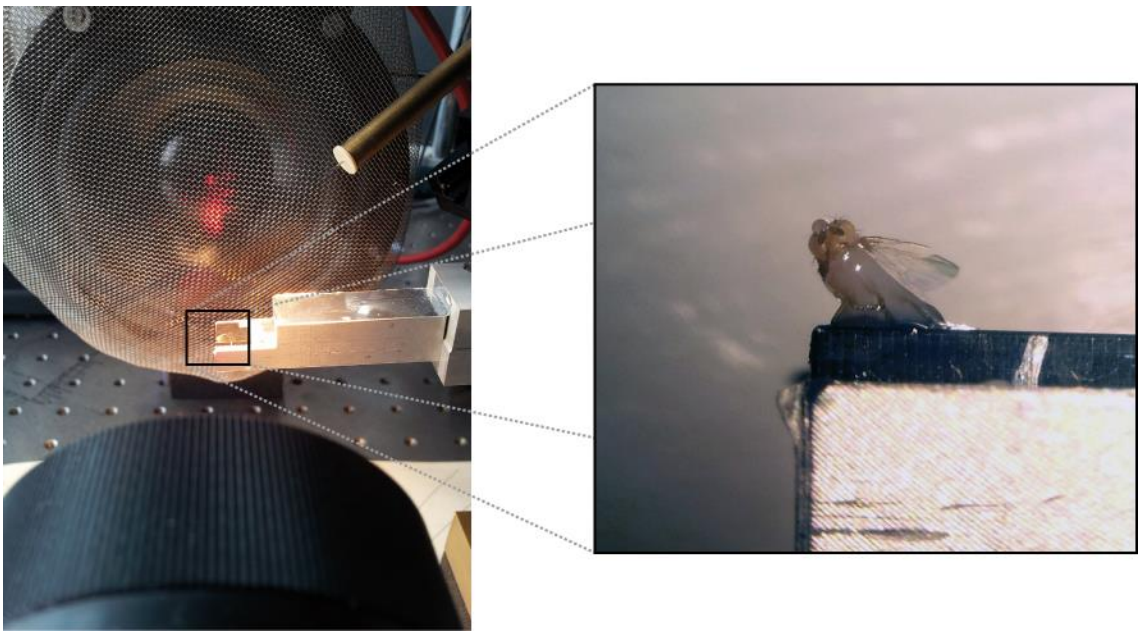

Figure 31: Experimental set-up to probe for temperature dependent Johnston's organ function

Flies have been directly mounted on a thermoelectric cooling device, and adapt for 5 minutes to the respective temperature before antennal free fluctuations have been recorded. Left photography: overview, right photography: close up.

By comparing the best frequency and fluctuation power, in between one fly strain, no significant differences can be observed (two-tailed Mann-Whitney U test, $p < 0.05$). This result confirm the mutant phenotype of *Rh6[1]* flies compared with *Rh6* rescues (see chapter 2.2.2.1).

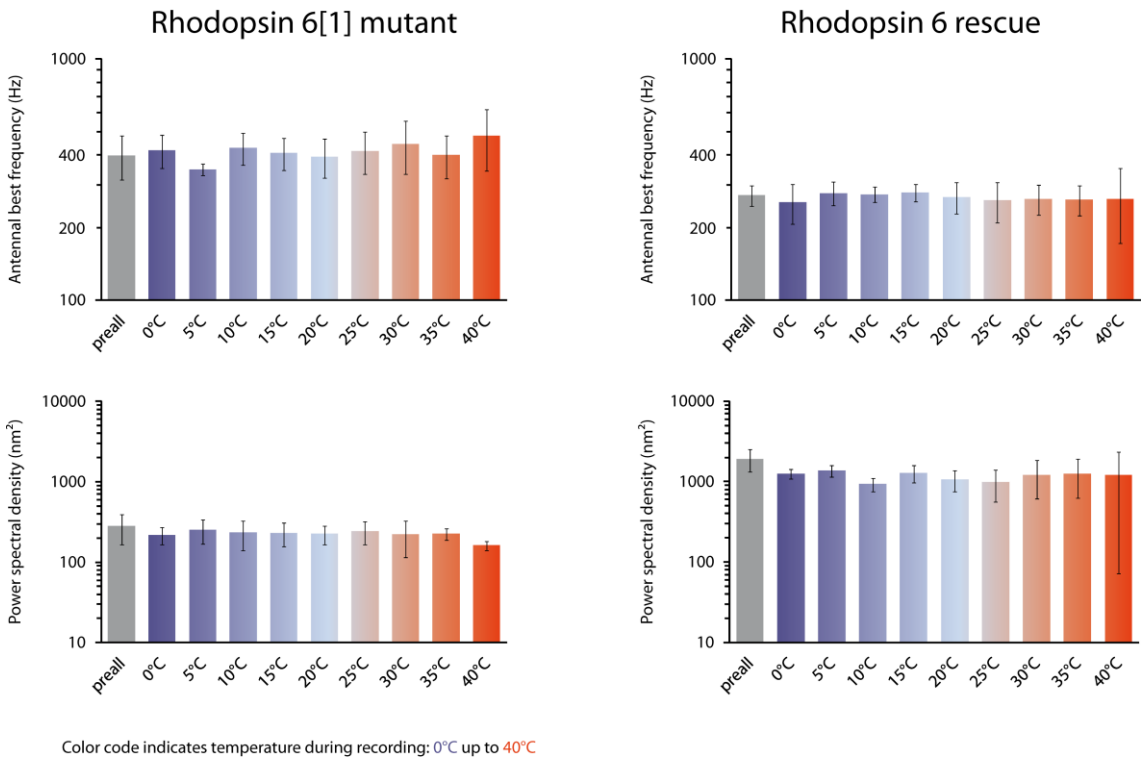

Figure 32: Recordings of antennal free fluctuations during different temperatures.

Data are presented as mean values ± 1 standard deviation. N = 3 flies per strain were probed for each temperature. First row: best frequency (Hz). Second row: power spectral density (nm^2). No significant alterations have been detected (two-tailed Mann-Whitney U test, $p < 0.05$). Recordings have been done in a randomized order.

Temperature dependent recordings could be improved by prolonging the time to adapt flies to a certain temperature. A redundant function of Rhodopsins could hide any mutant phenotype in this experiment. Probing rhodopsin double knockouts should be the next step.

2.2.4 Rhodopsin antibody staining labels the Johnston's organ

It is shown that rhodopsin 5 and 6 are transcribed in the Johnston's organ, probed via mRNA microarray and confirmed via quantitative real-time PCR (Senthilan et al. 2012). To localize rhodopsin proteins in the Johnston's organ, fluorescence labeling was performed. To localize rhodopsin, co-staining with phalloidin that stains actin rich scolopale rods surrounding the sensory cilia and anti-HRP (horseradish peroxidase) staining of sensory neurons is done. Pictures were taken by confocal fluorescence imaging.

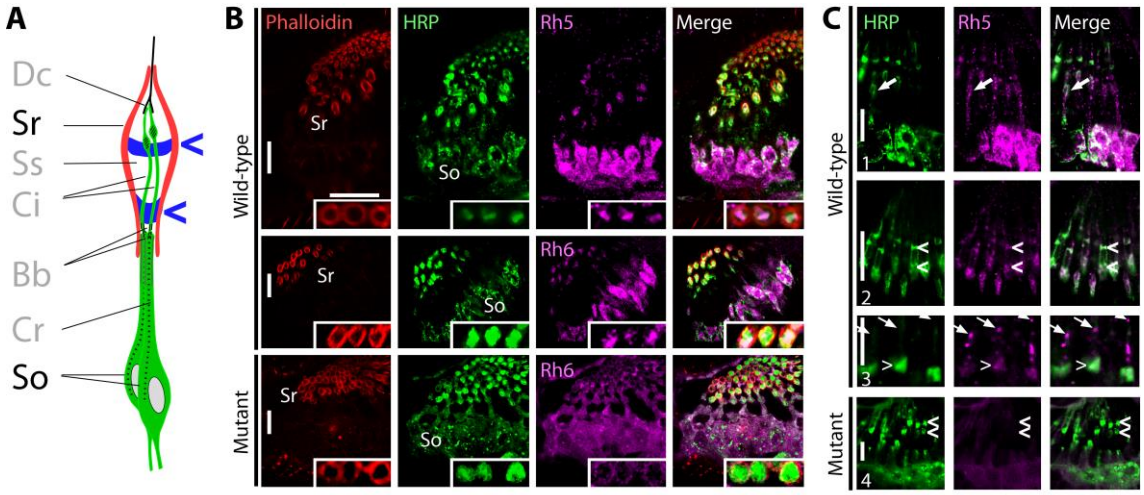

Figure 33: Rhodopsin expression in the Johnston's organ (published in Senthilan and Piepenbrock et al. 2012).

A Scheme of a scolopidium with Dendritic cap (Dc), Scolopale space (Sc), Cilium (Ci), Basal body (Bb), Ciliary rootlet (Cr) and two structures that that are stained in the antibody staining (**B**): Scolopale rootlets (Sr) and Somata (So). Blue arrowheads point towards the bands in the scolopale space that are recognized by anti-HRP.
B "Fluorescence labeling of Johnston's organs in wild type-flies and *Rh5[2],Rh6[1]* double mutants. Phalloidin labels the scolopale rods (Sr) that surround the cilia and anti-HRP labels neuronal membranes. In the wild-type, anti-Rh5 and -Rh6 specifically label Johnston's organ neuron somata and cilia, whereas in the mutants only unspecific labeling is observed. Insets: cross-sections through the scolopales documenting co-localization of anti-HRP and anti-Rh5/anti-Rh6. In the mutants, unspecific anti-RH6 staining superimposes with phalloidin. Scale bars, 10 µm; insets 5 µm." (Senthilan and Piepenbrock et al. 2012)
C "Ciliary localization of Rhodopsins. Row 1: anti-Rh5 staining of inner dendritic segments (arrows). Row 2, arrowheads: anti-Rh5 labeling of the two anti- HRP-positive bands in the scolopale space depicted in (**A**). Row 3: anti-Rh5 labeling extends from the distal bands (arrowhead) into the ciliary tips (arrows). Row 4: Persistence of anti-HRP-positive bands (arrowheads) in *Rh5[2],Rh6[1]* double mutants. Scale bars, 10 µm (rows 1, 2, and 4) and 5 µm (row 3)." (Senthilan and Piepenbrock et al. 2012)
Samples were prepared and stained by Stephanie Pauls, images were taken with support of Martin C. Göpfert.

Antibodies against the respective rhodopsins label the somata of the neurons and their mechanosensitive ciliary tips.

2.2.5 Johnston's organ ultrastructure seems rhodopsin-independent

Rhodopsins are known to be an integral part of the membrane of photoreceptors (Montell 1999), therefore I guess that, expressed in the Johnston's organ neurons, rhodopins are in cooperated into the membrane in these neurons. As a part of the membrane of Johnston's organ neurons, rhodopsins could be required for ultrastructural properties of scolopidia. To probe *Rh5*,*Rh6* double mutants for ultrastructural deficits I checked corresponding transmission electron micrographs for alterations.

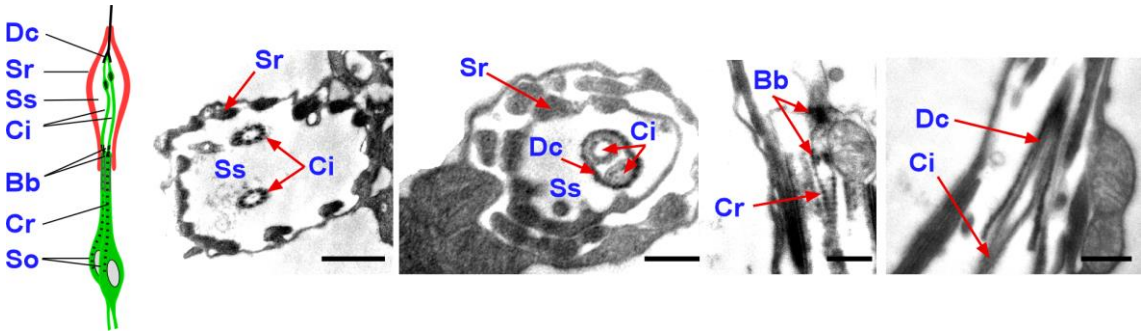

Figure 34: Johnston's organ ultrastructure of rhodopsin double mutant flies.

Left: Scheme of a scolopidium (Senthilan and Piepenbrock et al. 2012).
Right: Electron micrographs (scale bars: 0.5 µm) depict structures like: Dendritic cap (Dc), Scolopale rods (Sr), Scolopale space (Ss), Cilia (Ci), Basal bodies (Bb), and Ciliary rootlets (Cr) in *Rh5*,*Rh6* mutant flies. Samples were prepared by Margret Winkler (Senthilan and Piepenbrock et al. 2012).

Electron microscopy revealed normal auditory neuron and cilium structure for *Rh5*,*Rh6* double mutants.

2.3 Discussion

In this chapter I screened for genes known to be involved in the visual sense of *Drosophila* and their potential contribution to *Drosophila* hearing. Rhodopsin mutant flies have been shown to alter transducer gating and rhodopsin proteins have been localized to Johnston's organ neurons. In addition, physiological experiments have been presented that focus on the potential roles on temperature-control and the light-dependence of Johnston's organ function.

2.3.1 Genes of the phototransduction cascade impact *Drosophila* hearing

Mutations affecting genes of the *Drosophila* phototransduction cascade are shown to affect hearing in *Drosophila*. These genes have significant impact on the *Drosophila* auditory organ function and especially active antennal amplification. Four mutations are shown to 'severely impair' Johnston's organ function: *inaD, rh5, rh6,* and *Arr2*. The gene *inaD* encodes the scaffold protein 'inactivation no afterpotential D'. This protein forms a supramolecular signaling complex (signalplex) with phospholipase C, protein kinase C (encoded by *inaC*) and TRP ion channel (Wang and Montell 2007; Katz and Minke 2009). The gene *Arrestin 2* is known to be involved in deactivation of rhodopsin mediated signaling (Dolph et al. 1993; Alloway and Dolph 1999) and both Rhodopsins are light detectors (Salcedo et al. 1999).

'Moderately impaired' Johnston's organ function is a result of mutations in *TRP*, *ninaE*, *trpl*, *rh7, gl*, and *stops*. Mutation of *inaC* results in a significantly reduced gain but is in the category of normal hearing flies. Mutations in *Cam* lead to a 'hymperamplification' phenotype.

Eleven genes out of the phototransduction cascade significantly reduce the sensitivity gain. This may indicate that the whole phototransduction cascade is present in the *Drosophila* Johnston's organ. The hyper amplification of *Calmodulin* mutant flies indicates that Johnston's organ function is regulated by these phototransduction genes in both ways, negatively by *Cam* and positively by all others.

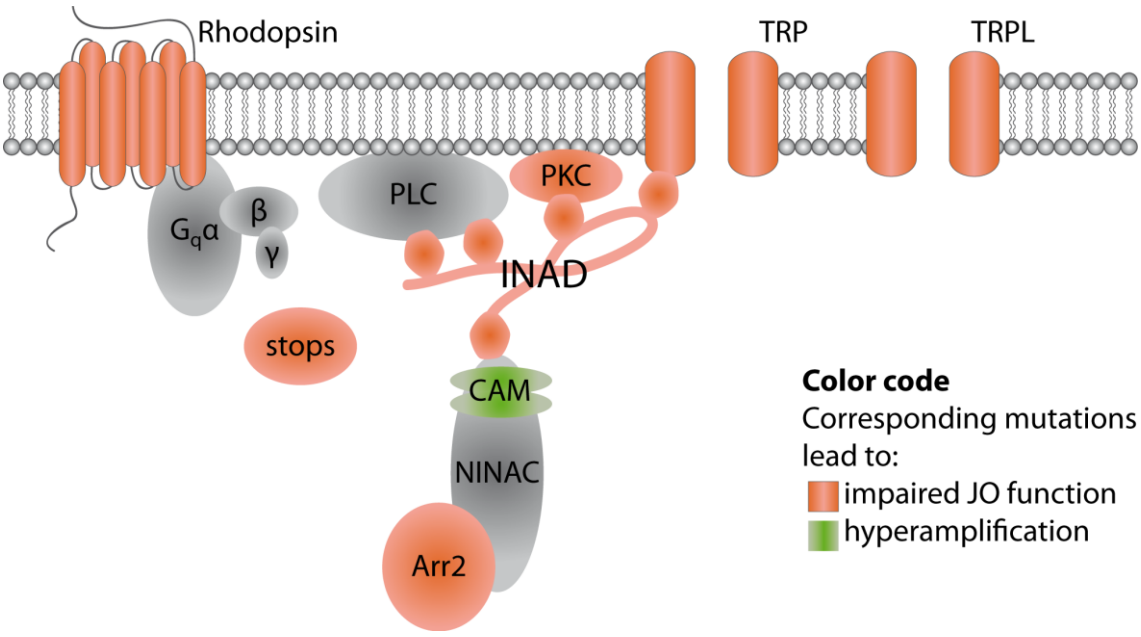

Figure 35: Scheme of the phototransduction cascade

Proteins of the phototransduction cascade as they are known from the *Drosophila* visual transduction. Corresponding mutations that affect *Drosophila* auditory transduction are highlighted in red (impaired JO function) or green (hyperamplification). Figure modified from: (Hardie 2012b).

2.3.2 Genes involved in eye morphogenesis are required for auditory organ function

The genes *glass* and *eyes absent* are involved in the development of the *Drosophila* compound eye (Moses et al. 1989; Tavsanli et al. 2004) and affect Johnston's organ function significantly. Mutations in the gene *glass* specifically remove photo-receptor cells (Moses et al. 1989). This mutation also results in 'moderately impaired' Johnston's organ function. Mutations in *eyes absent* lead to a 'hyperamplification' phenotype.

2.3.3 Auditory organ function is affected by beta-carotene

Rhodopsin, the light detector in the *Drosophila* eye, is composed of two parts, the protein opsin and its chromophore retinal, which, in *Drosophila*, is 3–OH–11–*cis*–retinal (Montell 2012; Wang et al. 2012). This retinal cannot be synthesized by the fly on its own but it is metabolized from its precursor beta-carotene (vitamin A), which is absorbed from the food (Wang et al. 2007). Here I show, that a mutation in *santa-maria*, a gene, that encodes a scavenger receptor that is required for beta-carotene uptake (Wang et al. 2007; Wang and Montell 2007), 'severely impairs' Johnston's organ function. In contrast to this very strong phenotype, mutations affecting genes in the downstream metabolic pathway do not affect Johnston's organ function or only very slightly (*ninaB*, *pintaA*). This is a first indication, that beta-carotene is required for Johnston's organ

function and not its product retinal, because only the uptake of beta-carotene but not the metabolic pathway affect Johnston's organ function. Analysis of mutations of the chromophore recycling pathway like *ninaG, rdhB, pdh* and *rdhb* should reveal if beta-carotene or 3–OH–11–*cis*–retinal is required for auditory organ function.

2.3.4 Rhodopsin is crucial for hearing in *Drosophila*

Rhodopsins are crucial for sensitive hearing in *Drosophila*. In the following I discuss results of mutations affecting rhodopsins.

2.3.4.1 Rhodopsin is required for hearing in *Drosophila*

Antibody staining indicates rhodopsin 5 and rhodopsin 6 expression in the sensory neurons of the Johnston's organ. More precisely these rhodopsins seem to be located in the ciliary tip of sensory neurons and in their somata. The specificity of this staining has been confirmed by absence of this staining pattern in respective mutant flies. Although rhodopsins might be located in these sensory neurons, its absence due to mutations in *Rh5* and *Rh6* does not alter the ultrastructural integrity of scolopidia, shown by electron micrographs.

Rhodopsins are functionally involved in nonlinear feedback amplification of the Johnston's organ. Mutations in *Rh5* and *Rh6* result in a 'severely impaired' Johnston's organ whereas flies with mutations in *ninaE* and *rh7* are 'moderately impaired'. Whereas rhodopsins are required for amplification, they appear not to confer a regulation to Johnston's organ function by e.g. light or temperature. Since *Drosophila* mating depends on the time of a day (Sakai and Ishida 2001), and the production and reception of the 'love song' is a part of this mating behavior, it could be worth to probe for circadian rhythm regulated Johnston's organ function.

First results indicate, that rhodopsins may function in a different way than in the eye. In the *Drosophila* eye rhodopsins are composed of the protein opsin in addition with its chromophore retinal, but neither retinal depletion nor interrupting the metabolic pathway that's forms the retinal does alter Johnston's organ function.

Only the very first metabolic step – the beta-carotene uptake via *santa-maria* – seems to be important for Johnston's organ function. This could be an indication, that rhodopsin may function without its chromophore 3–OH–11–*cis*–retinal in the *Drosophila* Johnston's organ or there is another metabolic pathway besides the known one (Wang et al. 2012).

2.3.4.2 Rhodopsin is crucial for transducer gating

Probing correlates of transducer gating revealed that transducing as well as nontransducing components are altered in *Rh6* and *Rh5,Rh6* mutants. The gating spring model, describing the event of transduction, is used to get insight on the molecular level of transduction. Approximated model parameters yielded differences between controls and rhodopsin mutants.

The count of insensitive transducers is decreased in *Rh6 and Rh5,Rh6* double mutants. As a result the maximum compound action potential amplitude and the combined gating spring stiffness (K_{GS}) decreases. Besides affecting the function of insensitive transducers, the *Rh6* mutation also decreases the single channel gating force of the sensitive transducers. As a result the sensitivity of the Johnston's organ declines because a lower gating force increase the probability of spontaneous channel gating and thus decrease the phase coupled response of the Johnston's organ. *Rh5,Rh6* double mutants have no sensitive transducers at all. There are two explanations. Either sensitive channels are not present in the Johnston's organ or antennal displacement does not lead to gating of this channels.

A decrease of the linear stiffness indicates alterations of nontransducing components. Both fly strains, single mutant *Rh6* and double mutant *Rh5,Rh6*, show a decrease in parallel stiffness. This data indicates that (a) neurons are lost or (b) the stiffness of neurons or other cells is reduced. Mechano-electrical transducers are directly gated via mechanical force. But coupling of transducers and antennal displacement depends on different aspects like: anchoring of transducers, initial tension of transducers and intrinsic properties of force conducting structures. Alteration in this coupling could explain that less transducers gate due to antennal deflections.

Comparing results of *Rh5,Rh6* mutant flies with *nompC* mutants (Effertz et al. 2012) reveals that they have similar phenotypes. Both mutants have higher best frequencies, reduced Johnston's organ system power, no sensitivity gain, high 'hearing thresholds' and antennal 'displacement thresholds' as well as no sensitive channels involved in transduction, but the parallel stiffness is different (K_{lin}). Whereas the parallel stiffness stays constant between *nompC* mutants and respective controls it is reduced between *Rh6* mutant*s,* *Rh5,Rh6* mutant*s* and *Rh6* rescues. This indicates that not just transducers are missing but also non transducing contributions are reduced in stiffness. That could be explained by an altered neuron stiffness or these neurons just do not exist. Until now a decrease in parallel stiffness is only documented for flies with ablated auditory neurons (Effertz et al. 2012).

The only difference of *nompC* mutants as well as flies with ablated auditory neurons and *Rh5,Rh6* double mutants is the antennal best frequency. Flies with ablated auditory neurons and *nompC* mutants have a higher best frequency of circa 500 Hz (Effertz et al. 2011) compared to *Rh5[2],Rh6[1]* (396 ± 49 Hz). This indicates that removing transducers increases the asymptotic stiffness of the Johnston's organ whereas mutations in rhodopsin influence this stiffness less. The auditory system of *Rh5,Rh6* double mutant flies has a higher best frequency than controls (*Canton S* and *Rh6* rescues), but a lower one than *nompC* mutants or flies with ablated auditory neurons. This could be explained by the drop of the parallel stiffness of *Rh5,Rh6* double mutant flies that result in a slightly less high best frequency. Ablated auditory neurons do not affect the best frequency differently than flies with no auditory transducers (*nompC* mutants). But flies whose auditory transducers do not gate because of altered parallel stiffness could have an intermediate best frequency (in between controls and *nompC* mutants). A drop in parallel stiffness is observed for flies with ablated auditory neurons as well but the change in parallel stiffness of *Rh5,Rh6* might arise if, for example, the membrane stiffness alters.

2.3.4.3 Rhodopsins may tune the stiffness of the antenna

Many genes that are known to be involved in the phototransduction cascade are found in the *Drosophila* Johnston's organ (Senthilan et al. 2012). Since transcription and expression of genes is costly for a cell one could expect that expressed proteins play a functional role in these cells. This study shows that many genes of the phototransduction cascade contribute to Johnston's organ function. In addition probing correlates of transducer gating revealed that transducing as well as non transducing components of the Johnston's organ are altered. This phenotype could be explained by an altered stiffness of Johnston's organ sensory neurons.

In the *Drosophila* eye rhodopsins are known to activate phospholipase C (PLC) via G–proteins, and PLC hydrolyzes the membrane lipid phosphatidylinositol 4,5-bisphosphate (PIP2). Roger C. Hardie and colleagues have shown that this hydrolyzation leads to a contraction of the microvilli that seem to activate TRP and TRP-like channels (Hardie & Franz, 2012).

Reversely, rhodopsin and proteins of the phototransduction cascade could tune the Johnston's organ stiffness via PIP_2 to provide best physical properties for sensitive hearing. This would need phototransduction proteins working as a functional unit in the Johnston's organ. This hypothesis could be probed by co–localization of these proteins, inhibiting the function of G-proteins and altering the concentration of PIP_2 in the Johnston's organ.

This hypothetical 'change in stiffness of sensory neurons' could explain both: (1) drop in passive Johnston's organ stiffness and (2) altered transduction. A weaker coupling of transducers and antennal receiver would decrease the Johnston's organ sensitivity. Furthermore stronger antenna displacement would be required to open transduction channel.

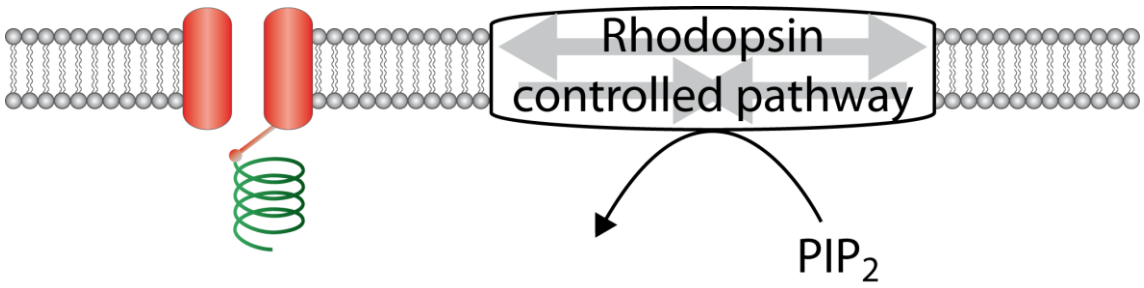

Figure 36: Scheme depicting the hypothetical role of rhodopsin in mechanotransduction

A rhodopsin regulated pathway controls stiffness of the Johnston's organ. The membrane stiffness is regulated by insertion or removal of PIP_2. This hypothetical function of rhodopsins in the Johnston's organ could tune antennal stiffness providing best biophysical properties for sensitive mechano-electrical transduction.

Rhodopsin 5 and 6 seem to play a partial non redundant role. They are required for the sensitivity of the Johnston's organ. Rhodopsins may function as a 'stiffness tuner' for Johnston's organ

neurons providing best biophysical properties for mechano-electrical transduction and feedback amplification.

To address this issue, rhodopsin mutant flies have to be checked for count of sensory neurons. Prior studies have shown that a decrease of the parallel stiffness can be explained by ablation of auditory Johnston's organ neurons (Effertz et al. 2012). *Rh5,Rh6* mutants have a decreased parallel stiffness as well but potentially without a loss of sensory neurons, just due to an altered neuron stiffness. If the count of sensory neurons is not altered in *Rh5,Rh6* mutant flies, it would support the hypothesis of a regulated membrane stiffness. This can be done by transmission electron micrography and fluorescence imaging to detect auditory neurons in the Johnston's organ (AB neurons).

In addition, one could check, if NOMPC proteins are present in rhodopsin mutant flies. If NOMPC is not present or dislocated due to mutations in rhodopsin, this would open another hypothetical explanation of rhodopsin and phototransduction proteins being involved in trafficking of NOMPC.

2.3.4.4 Other multiple roles of genes in sensory perception

As mentioned, it is likely, that vision operates via detour. First, light is transduced to a second messenger response, second, this second messengers alter the mechanical properties of rhabdomeric membranes, which result in contractions of photoreceptors, and lastly this mechanical stimulus is transduced to an electric response via TRP channels. In summary, this indicates that various transduction mechanisms work 'hand in hand'.

Moreover, genes, that are involved in sensory perception of sound in *Drosophila*, are already known to play a role in other senses. For example:

- The transient receptor potential vanilloid channel Inactive (IAV) is involved in thermotaxis (Kwon et al. 2010) and hearing (Gong et al. 2004; Göpfert et al. 2006).
- Nanchung (NAN) is located in the Johnston's organ neurons and hygroreceptors in the third antennal segment and involved in geotaxis, hearing (Sun et al. 2009) and the detection of dry air (Liu et al. 2007).
- The gene *touch insensitive larva B* (*tilB*) is involved in hearing (Eberl et al. 2000) and the temperature compensation of the circadian clock (Sehadova et al. 2009).
- The nuclear gene *technical knockout* (*tko*), encoding a mitochondrial protein, is involved in response of flies due to anesthetizing with CO_2 (Whelan et al. 2010) and flies with mutations in *tko* show an impaired behavioral response to sound (Toivonen et al. 2001).
- The gene *spalt major* (*salm*) is involved in compound eye morphogenesis contributing to the differentiation of photoreceptor cells (Mollereau et al. 2001), as well as in *Drosophila* hearing. Flies with mutations in the *spalt* gene are blind and deaf (Dong et al. 2002; Dong et al. 2003).
- Rhodopsin, which is known to be the light sensing protein in the *Drosophila* eye, is involved in temperature discrimination in *Drosophila* larvae (Shen et al. 2011).

- And *Drosophila* photoreceptors as well as chordotonal organs, like the ones in Johnston's organ are both developmentally specified by *atonal* (*ato*) a basis-helix-loop-helix transcription factor (Jarman et al. 1994; Jarman et al. 1995; Gupta and Rodrigues 1997).

With this in mind it does not surprise, that a huge number of genes, which are implicated in sensory perception of light, are functionally involved in hearing. Although there are major differences at the level of signal transduction between vision and hearing in *Drosophila*, I provided evidence that they share common genes.

3 Candidate gating spring: NOMPC ankyrin repeats

3.1 Introduction

NOMPC (no mechanoreceptor potential C = TRPN1) is a bona fide mechanotransduction (Walker et al. 2000; Göpfert et al. 2006; Kamikouchi et al. 2009; Effertz et al. 2011; Yan et al. 2013). NOMPC is expressed in Johnston's organ neurons, localizing to their ciliary tips (Lee et al. 2010; Liang et al. 2011). NOMPC consist of 1732 amino acids (Cheng et al. 2010) and contains 6 predicted transmembrane domains, a pore region and 29 ankyrin repeats (Cheng et al. 2010; Yan et al. 2013). These 29 ankyrin repeats form one turn of an intracellular helix and are proposed to function as the gating spring of the mechanotransducer (Howard and Bechstedt 2004).

3.1.1 Motivation: Function and identity of the gating spring

Mechanical force is transmitted via an elastic element, presumably the gating spring, to mechanical gated channels that transduce mechanical force to electrochemical signals (Corey and Hudspeth 1983; Howard and Hudspeth 1987; Howard and Hudspeth 1988; Effertz et al. 2012).

The transient receptor potential (TRP) channel NOMPC is a good candidate for the *Drosophila* auditory transduction channel (Walker et al. 2000; Göpfert et al. 2006; Kamikouchi et al. 2009; Lee et al. 2010; Effertz et al. 2011; Liang et al. 2011; Effertz et al. 2012). We found that loss-of-function mutations in the *nompC* gene disrupt the gating and the mechanical integrity of the fly's auditory transduction channel (Effertz et al. 2012), suggesting that NOMPC forms this channel and/or its gating spring. Forming a helix with one turn, the 29 ankyrin repeats of NOMPC form a molecular spring that might act as the gating spring that couples mechanical stimuli to the gate of

the channel (Howard and Bechstedt 2004; Zanini and Göpfert 2013). The aim of this study is to probe if NOMPC ankyrin repeats serve as the gating spring.

3.1.2 Objectives and approach: Manipulating the number of NOMPC ankyrin repeats

If the NOMPC ankyrin residue acts as gating spring, manipulating the number of ankyrin residues should alter the length and tension of native gating springs. To address this issue, Li E. Cheng (University of California) has generated transgenic flies that carry a *nompC* gene with a duplicated ankyrin residue. This construct comprises 58 instead of 29 repeats, under control of an upstream activating sequence (UAS) (Duffy 2002).

Doubling the length of a spring will reduce its stiffness by one-half, so replacing the native *nompC* gene with that construct should reduce the stiffness of the gating springs that are associated with the fly's auditory transduction channels accordingly. To test this, I have targeted the expression of the construct to the fly's auditory sensory cells using a *nompC-Gal4* driver in a *nompC* null mutant background. *nompC* nulls expressing a *UAS-nompC* construct with 29 ankyrin repeats in auditory Johnston's organ neurons were used as controls.

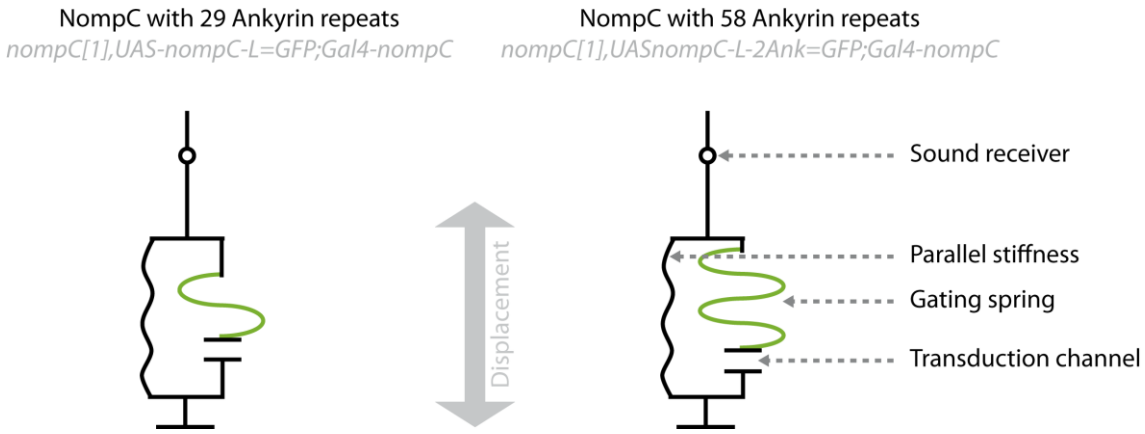

Figure 37: Model of mechano-electrical transducer gating spring

This model of a transducer consists of a sound receiver (top) whose movement activates mechanotransduction channels by altering the gating spring tension (Albert et al. 2007a). Black turns indicate the parallel stiffness that represents the linear elasticity of the fly's antennal joint and Johnston's organ, whereas green turns highlight the gating spring.
Left: Control flies, in which the native *nompC* gene is substituted with a *UAS-nompC-1ANK-GFP* construct with 29 ankyrin repeats.
Right: Flies with a duplicated ankyrin residue, in which the native *nompC* gene is substituted with a *UAS-nompC-2ANK-GFP* construct with 58 ankyrin repeats.

Crossing scheme 1: Flies with 58 NOMPC ankyrin repeats

$$♂\ \frac{Sb}{CyO};nompC-Gal4 \quad \times \quad ♀\ \frac{nompC[1]2Ank:GFP}{CyOweep};\frac{TM2}{TM6} \quad = \quad \frac{nompC[1]2Ank:GFP}{Sb};\frac{nompC-Gal4}{TM2\ or\ TM6}$$

$$♂\ \frac{nompC[1]2Ank:GFP}{Sb};\frac{nompC-Gal4}{TM2\ or\ TM6} \quad \times \quad ♀\ yw;\frac{CyO}{Sb};\frac{MKRS}{TM6b} \quad = \quad yw;\frac{nompC[1]2Ank=GFP}{CyO};\frac{nompC-Gal4}{MKRS}$$

$$♀\ yw;\frac{nompC[1]2Ank:GFP}{CyO};\frac{nompC-Gal4}{MKRS} \quad \times \quad ♂\ yw;\frac{nompC[1]2Ank:GFP}{CyO};\frac{nompC-Gal4}{MKRS} \quad = \quad yw;nompC[1]2Ank:GFP;nompC-Gal4$$

Crossing scheme 2: NOMPC controls, flies with 29 Ankyrin repeats

$$♂\ \frac{Sb}{CyO};nompC-Gal4 \quad \times \quad ♀\ \frac{nompC[1],UAS-nompC-L:GFP}{CyOGB} \quad = \quad \frac{nompC[1],UAS-nompC-L:GFP}{Sb};\frac{nompC-Gal4}{+}$$

$$♂\ \frac{nompC[1],UAS-nompC-L:GFP}{Sb};\frac{nompC-Gal4}{+} \quad \times \quad ♀\ \frac{nompC[1],UAS-nompC-L:GFP}{Sb};\frac{nompC-Gal4}{+} \quad = \quad nompC[1],UAS-nompC-L:GFP;nompC-Gal4$$

3.2 Results

3.2.1 NOMPC with doubled ankyrin length is expressed in the Johnston's organ neurons

Expression of NOMPC with 58 ankyrin repeats was confirmed via fluorescence microscopy. Fluorescence caused by the GFP-tagged construct was seen in the second antennal segment. Antibody staining against GFP and HRP (horseradish peroxidase) showed that the construct is expressed in Johnston's organ neurons. Due to a partial overlap between HRP staining, which labels Johnston's organ neurons, and GFP antibody, the NOMPC with 58 ankyrin repeats could be localized in sensory neurons.

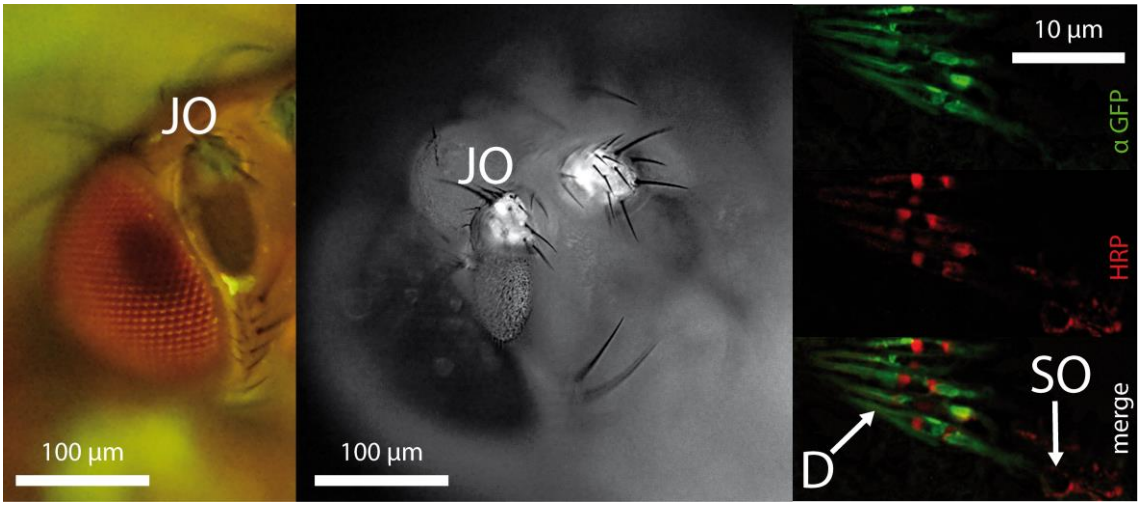

Figure 38: Expression pattern of NOMPC with 58 ankyrin repeats

Expression of NOMPC-2ANK-GFP in Johnston's organ, revealed by GFP expression.
Left and middle: GFP fluorescence in the Johnston's organ (JO) in the second segment of the antenna (Fluorescence stereoscope: left: Olympus SZX16, middle: Zeiss SteREO Lumar.V16).
Right: GFP expression in the dendrites (D) of Johnston's organ neurons. The neurons are counterstained with HRP antibody. Somata: (SO), Dendrites (D) of Johnston's organ neurons (Leica TCS SP2 confocal microscope).

Upon confirming the successful fly crossing, the antennal mechanics were probed.

3.2.2 Flies with 58 NOMPC ankyrin repeats have softer antennal receivers

nompC null mutant flies have impaired antennal mechanics (Effertz et al. 2011; Effertz 2011; Effertz et al. 2012). To test whether the construct with 29 and the one with 58 ankyrin repeats rescues auditory function, the antenna's free mechanical fluctuations, and sound-evoked vibration, were probed.

Both *nompC* ankyrin constructs have a best frequency and power spectral density, which is close to wild type flies (*Canton S* circa 250 Hz and 1500 nm²), and therefore rescue the mutant phenotype (*nompC* null circa 500 Hz and 100 nm² (Effertz 2011)). Flies with doubled count of NompC ankyrin repeats have a shifted maximum of the power spectra when compared to controls (flies with 29 ankyrin repeats). This shift indicates a reduced stiffness of the antennal receiver. Probing the mechanical response characteristic reveals a compressive nonlinearity for controls and flies with doubled ankyrin repeats.

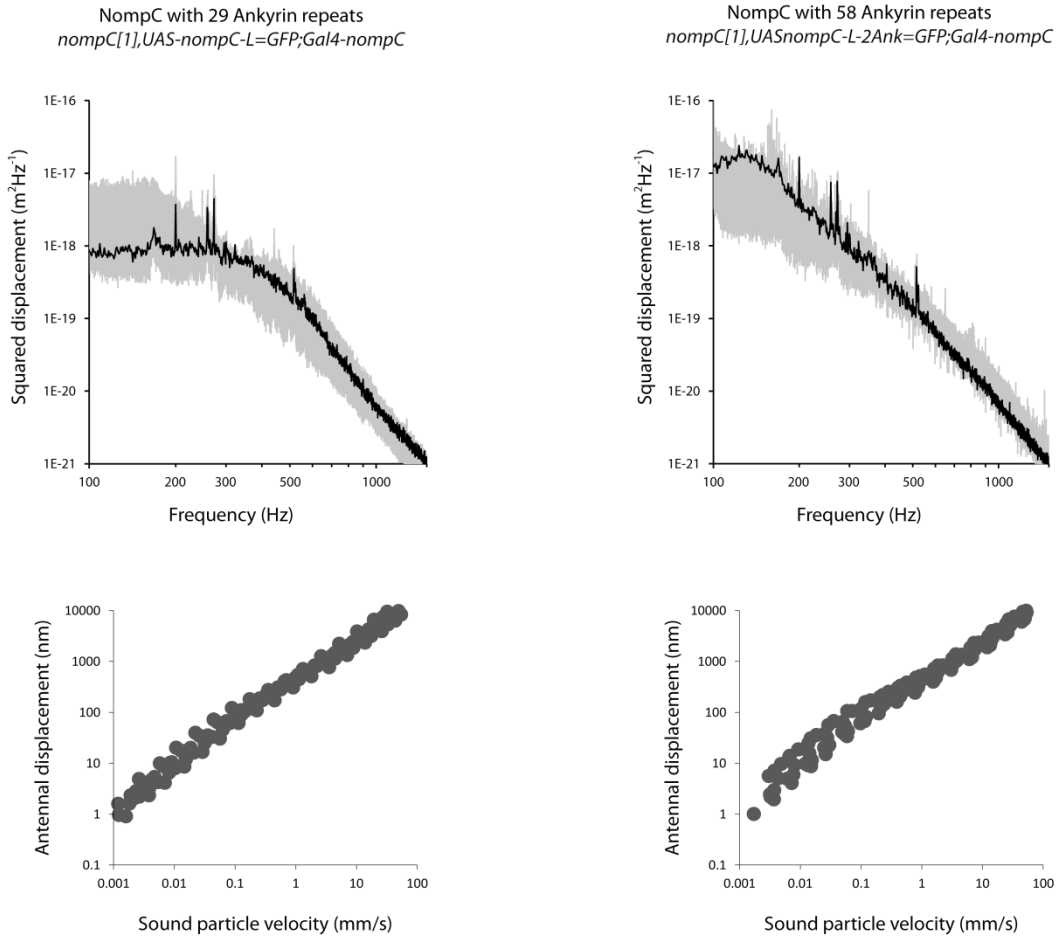

Figure 39: Mechanics of *Drosophila* antenna with doubled count of ankyrin repeats.

Upper plots: Free fluctuation recordings. Data are plotted as power spectra (x-axis: frequency, y-axis: squared displacement). Grey ghost traces show the range of individual recordings, N = 5 flies. One exemplary recording in each dataset is highlighted in black.
Lower plots: Mechanical response characteristics. Each dataset includes N = 5 flies.

To quantify the impact of ankyrin numbers on antennal mechanics I calculated the antennal best frequency, flutuation power and amplificaiton gain.

In flies with a duplicated NOMPC ankyrin residue, the antennal tuning is altered when compared to controls: in these flies, the antennal best frequency is 158 ± 56 Hz (mean ± 1 S.D., N = 5), which is significantly lower than in controls (272 ± 81 N = 5, $p < 0.05$, Mann-Whiney U-Test). The receiver's mechanical tuning reflects passive mechanical properties of the antenna and Johnston's organ as well as active properties of Johnston's organ neurons. Alterations in both properties may lower the best frequency of the receiver (Göpfert et al. 2005).

The fluctuation power of flies with 58 compared to those with 29 ankyrin repeats is increased ($p = 0.083$) by 708 nm². The amplification gain is slightly increased for flies with 58 ankyrin repeats when compared to controls (7.1 ± 2.9 for 58 ankyrin repeats and 5.9 ± 2.2 for 29 ankyrin repeats).

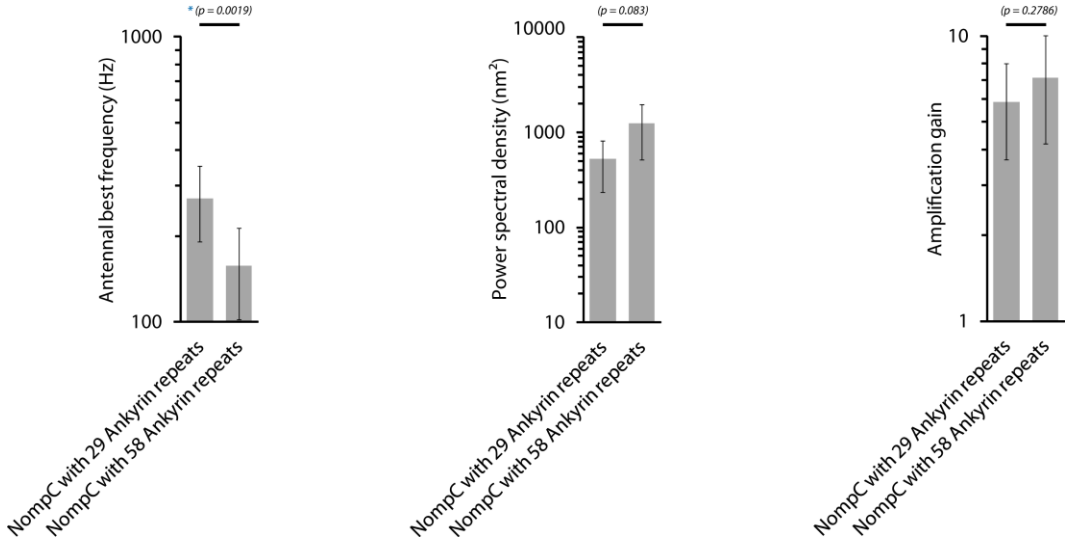

Figure 40: Quantitative results of antenna mechanics of flies with single and flies with doubled count of ankyrin repeats.

Data are presented as mean values ± 1 standard deviation. N = 5 flies per strain were probed. Statistical differences where probed by two-tailed Mann-Whitney U test, $p < 0.05$.
Left: Sound receiver best frequencies differ significantly between flies with 29 to flies with 58 NOMPC ankyrin repeats.
Middle: Johnston's organ power as power spectral density (nm²), slight difference was observed ($p = 0.083$).
Right: Mechanical amplification gains of flies with 29 NOMPC ankyrin repeats 5.9 ± 2.2 to flies with 58 NOMPC ankyrin repeats 7.1 ± 2.9

This results show that the antennal mechanics is changed due to different count of NOMPC ankyrin repeats. It may indicate that mechano-electrical signal transduction is altered.

3.2.3 NOMPC with doubled ankyrin repeats make a functional mechano-electrical transducer

To access mechano-electrical signal transduction, extracellular recordings of the antennal nerve of flies with altered ankyrin repeats were done. *nompC* mutant flies show only a remnant nerve response, to auditory stimuli (Effertz et al. 2011; Effertz 2011; Effertz et al. 2012)

Plotting relative CAP amplitudes against the sound particle velocity revealed a dynamic range of 0.08 to 2 mm/s for both flies with 29 and 58 ankyrin repeats.

When the CAP amplitudes were plotted against the antennal displacement, no differences were observed. The dynamic range for the antennal displacement is between 80 nm and 600 nm arista tip displacement.

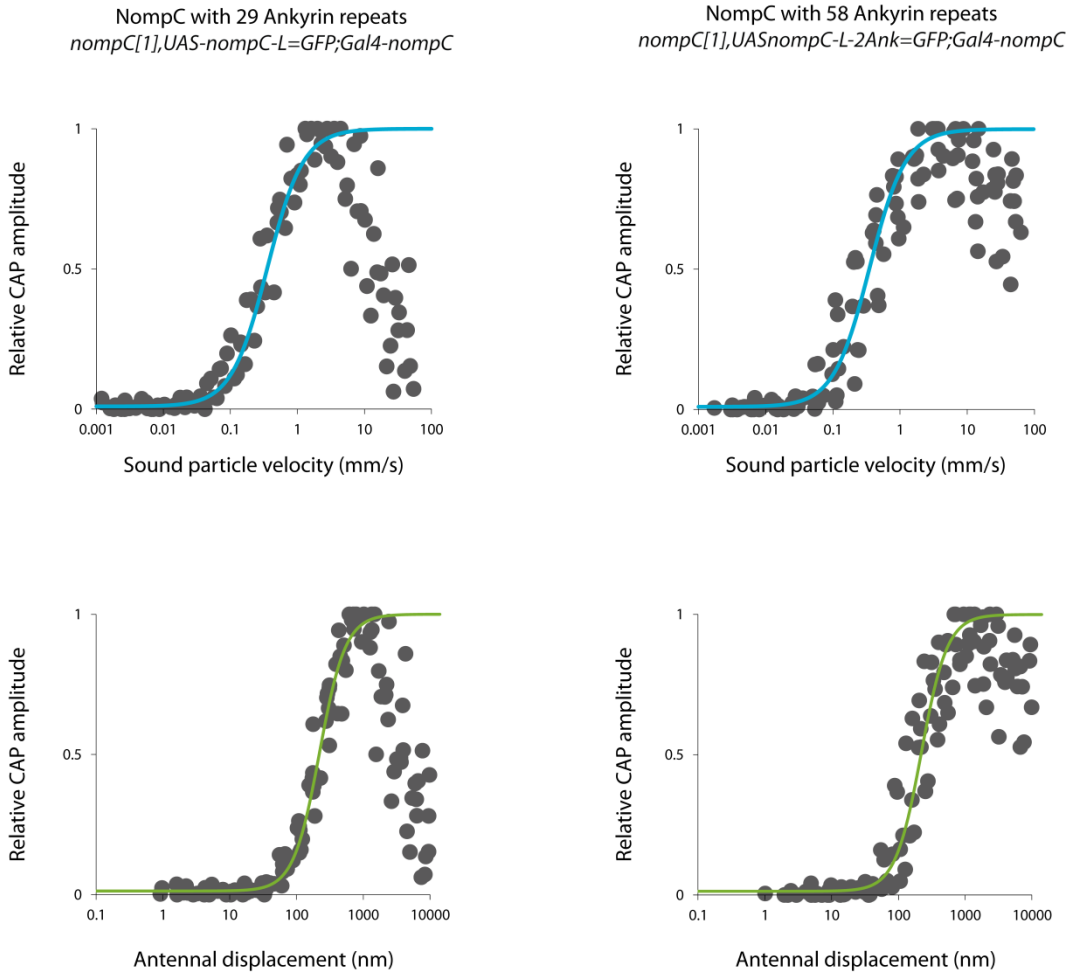

Figure 41: Compound action potential response characteristic of flies with altered NOMPC ankyrin repeats

Upper plots: Compound action potential response as a function of sound particle velocity. Each dataset includes N = 5 flies. Blue trace is the Hill-fit of flies with 29 NOMPC ankyrin repeats.
Lower plots: Compound action potential response as a function of arista displacement. Each dataset includes N = 5 flies. Green trace is the Hill-fit of flies with 29 NOMPC ankyrin repeats.

Quantifying the sound evoked antennal compound action potential confirms the first impression, that flies with 29 and 58 ankyrin repeats look the same. The maximum CAP amplitudes observed in flies with 58 ankyrin repeats was 28.5 ± 10.8 µV and those with 28 ankyrin repeats is 28.1 ± 19.5 µV. These values are substantially higher than those reported for *nompC* nulls (< 5 µV) (Effertz et al. 2011).

The 'hearing threshold' were 84 ± 47 µm/s for flies with 29 ankyrin residues and 79 ± 25 for flies with a duplicated NOMPC ankyrin domain. And the 'displacement threshold' was at 79 ± 25 for 58 ankyrin repeats, and at 77 ± 19 for flies with 29 ankyrin repeats.

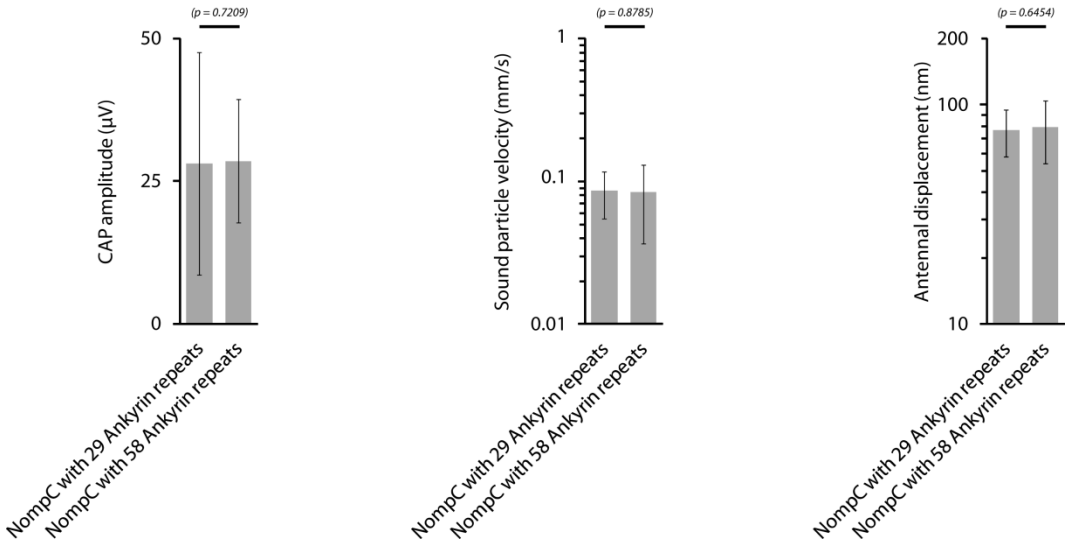

Figure 42: Quantitative results of compound action potential (CAP) of flies with single and flies with doubled count of ankyrin repeats.

Data are presented as mean values ± 1 standard deviation. N = 5 flies per strain. Statistical differences were assessed with two-tailed Mann-Whitney U tests, $p < 0.05$.
Left: Maximum amplitudes of sound-evoked compound action potentials.
Middle: 'hearing threshold'
Right: 'displacement threshold'

No significant alterations between flies with 29 compared to those with 58 NOMPC ankyrin repeats could be observed. The maximum compound action potential, 'hearing threshold' and 'displacement threshold' of both fly strains is similar to wild-type flies (*Canton S* maximum CAP: 41 µV, 'hearing threshold' 50 µm/s, 'displacement threshold' 100 nm).

Is there a change in transducer gating, despite the fact that the antennal nerve response does not change?

3.2.4 Gating compliance recordings of flies with single and doubled ankyrin repeats

To test, whether the best frequency shift, the increase in power spectral density and the slight alteration in amplification gain indeed reflect a drop in antennal stiffness, I probed the receiver's gating compliance.

I used this compliance to quantify the gating spring stiffness in flies carrying the construct and compare it to that of *nompC* null mutants that express a *nompC* construct with the normal number of 29 ankyrins.

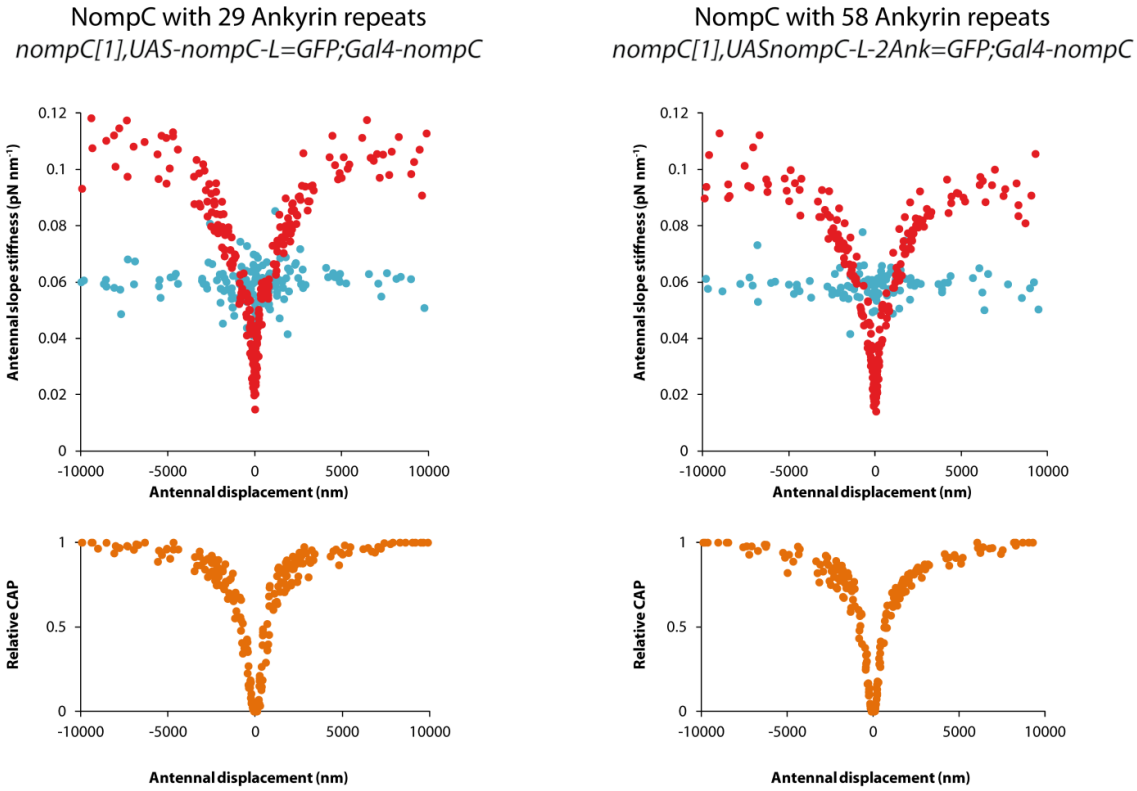

Figure 43: Correlates of mechano–electrical transducer gating of flies with single and doubled count of ankyrin repeats.

The dataset of flies with 29 ankyrin repeats includes N = 9 flies and for those with 58 ankyrin repeats N = 8. First row: The plots show the peak slope stiffness (red) of the antennal ear as a function of antennal displacement and in blue the steady state slope stiffness. Second row: relative compound action potential amplitude for different antennal displacements.

The gating spring model predict a change of gating spring stiffness K_{GS}, a change of the asymptotic stiffness (K_∞) and a change of the width of the gating compliance for changes in the gating spring (Albert et al. 2006).

To quantify receiver mechanics, I fitted the gating compliance with a four-state gating spring model (for details see: Methods – Correlates of mechano-electrical transducer gating of the *Drosophila*

antenna). The fits of flies with 29 compared to those with 58 ankyrin repeats look very similar, with a slight decrease in the overall receiver stiffness for flies with 58 ankyrin repeats (Figure 40, highlighted with blue arrow).

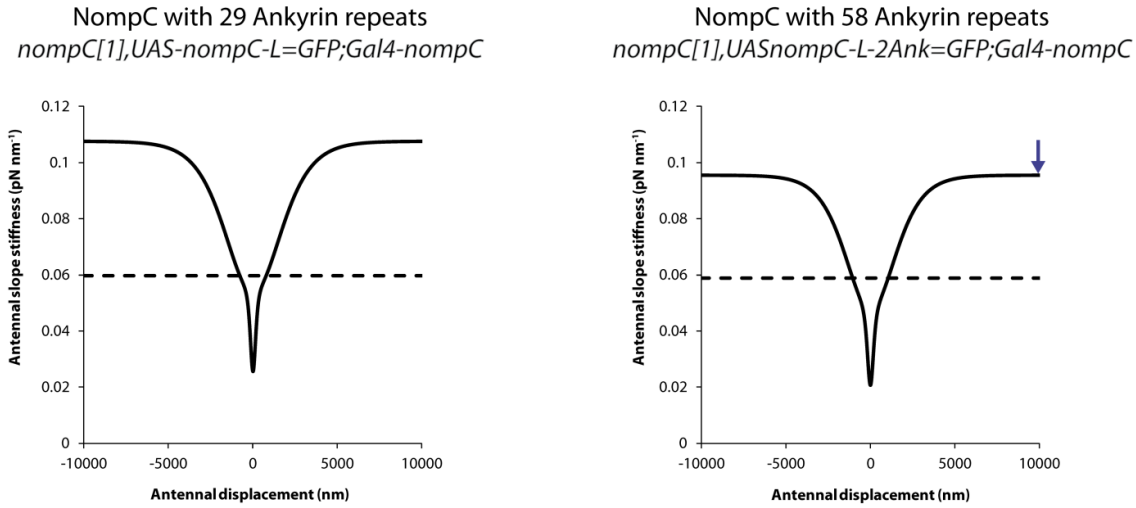

Figure 44: Fits of gating spring models of flies with single and doubled count of ankyrin repeats.

Flies with 29 and those with 58 NOMPC ankyrin repeats are analyzed with the gating spring model consisting of sensitive (N_s) and insensitive (N_i) channels. This fit reveals that flies with 58 ankyrin repeats have a reduced K_∞, highlighted with blue arrows.

Fits of the gating spring model, on pooled datasets of each fly strain, reveal a decrease of the receivers asymptotic stiffness (K_∞) by 12 µN/m for flies with 58 NOMPC ankyrin repeats compared to those with 29 ankyrin repeats. Corresponding linear stiffness stays virtually constant (drop of 1 µN/m). The calculated combined gating spring stiffness drops by 11 µN/m.

By taking the confidence bounds into consideration (no overlap of parameter bounds), the model suggests, that the number of the sensitive transducers, the single channel gating force of sensitive and insensitive channels, and the linear stiffness all stay constant. A change is only observed in the asymptotic stiffness (K_∞), due to a reduced gating spring stiffness (K_{GS}), and the reduced number of insensitive transducers.

	N_s			z_s (fN)			N_i			z_i (fN)			K_∞ (µN/m)			K_{lin} (µN/m)			K_{GS} (µN/m)	Number of flies
	Coefficient	95 % confidence bounds		Coefficient	95 % confidence bounds		Coefficient	95 % confidence bounds		Coefficient	95 % confidence bounds		Coefficient	95 % confidence bounds		Coefficient	95 % confidence bounds		K_∞ - K_{lin}	
Ankyrin rescue	291	162	419	40	32	48	65840	55650	76030	3.7	3.4	4.0	108	106	110	60	59	61	48	9
Ankyrin double	365	191	540	35	27	42	46480	38730	54240	4.1	3.7	4.5	96	94	97	59	58	60	37	8

Table 6: Gating spring model parameter values of flies with doubled NOMPC ankyrin repeats

Data are presented as fit coefficients (with lower and upper confidence bounds), deduced by fitting receiver mechanics with gating spring model consisting of two different channels (sensitive and insensitive). N = 9 flies with 29 ankyrin repeats and N = 8 flies with 59 ankyrin repeats where recorded. R^2 for *ankyrin rescue* (29 repeats) = 0.9484 and *ankyrin double* (58 repeats) = 0.9461.

Table 7 compares all parameters of flies with 29 to those with 58 ankyrin repeats. The double count of ankyrin repeats lead to antennae with significantly reduced best frequencies. In addition the confidence bounds of the asymptotic stiffness (K_∞), the combined gating spring stiffness (K_{GS}) and number of insensitive transducers do not overlap.

Parameters	***29 ankyrin repeats***	***58 ankyrin repeats***
Best frequency (Hz)	272	↓ 158
Power spectral density (nm^2)	529	– 1237
Sensitivity gain	5.9	– 7.1
Maximum CAP (µV)	28.1	– 28.5
'Hearing threshold' (µm/s)	86.6	– 84.1
Threshold of antennal displacement (nm)	76.7	– 79.3
K_{inf} (µN/m)	108	↓ 96
K_{lin} (µN/m)	60	– 59
K_{GS} (µN/m)	48	↓ 37
N_s	291	– 365
z_s (fN)	40	– 35
N_i	65840	↓ 46480
z_i (fN)	3.7	– 4.1

Table 7: Comparing control flies with flies that have NOMPC with 58 ankyrin repeats

Difference of flies with 58 ankyrin repeats compared to controls (29 ankyrin repeats) is highlighted with an arrow if significant or if confidence bounds do not overlap.

These results show that duplicating NOMPC ankyrin residues softens the fly`s antenna and also gating springs.

3.3 Discussion

The TPR channel NOMPC is a bona fide mechanotransduction channel (Yan et al. 2013), and there is growing evidence, that NOMPC ankyrin repeats are good candidates for being gating springs (Liang et al. 2013). The main question now is: Do NOMPC ankyrin repeats serve as gating springs (Zanini and Göpfert 2013)?

To answer this question, fly strains where made with 58 NOMPC ankyrin repeats. Doubling the length of the ankyrin residues is expected to alter the mechanics of the fly antenna.

GFP expression indicated that the transgenic NOMPC, with twice the number of ankyrin repeats, is properly expressed in the Johnston's organ. Probing Johnston's organ function revealed significant differences between flies with normal, and those with twice the number of NOMPC ankyrin repeats. Both *nompC* ankyrin constructs rescue the *nompC* null mutant phenotype, indicating that the constructs lead to fully functional mechano-electrical transducers. However, the results just partially met our expectations. The gating spring model predicted the gating compliance for varying gating spring stiffness's. Doubling the length of the gating spring should result, in a decreased K_{inf} (asymptotic stiffness), because K_{GS} (gating spring stiffness) is altered (Albert et al. 2007a).

We did not expect to see alterations in the number of insensitive channels, which are proposed to be NOMPC independent. This unexpected decrease of insensitive transducers cannot be explained by a prolonged gating spring, of NOMPC dependent, sensitive transducers. Altered expression and function of insensitive transducers could compensate the effects of altered spring stiffness of sensitive transducers. It would be conceivable, that expression and function of sensitive and insensitive transducers regulate each other. Adaptation processes, which regulate the tension on the gating spring and the transduction channel, could compensate a decrease of the gating spring stiffness as well. Compensatory effects would make it more difficult to reveal the impact of ankyrin repeats in mechano-electrical transduction.

The expected decrease of the gating spring stiffness, can be observed at least as a trend towards a decreased single channel gating force of the sensitive transducers (fit coefficients with lower and upper confidence bounds for 29 ankyrin repeats: 40 [32, 48] fN, for 58 ankyrin repeats 35 [27, 42] fN). The combined gating spring stiffness of sensitive and insensitive channels reads: $K_{GS} = K_{GS_s} + K_{GS_i}$. The gating spring stiffness for both transducers is defined as: $K_{GS} = \kappa N \gamma^2$ whereas κ is the spring constant, N the number of channels, and γ a factor to geometrical scale between sound receiver displacement and neurons (Albert et al. 2007a). The observed reduction of K_{GS} can thus be partially explained by a reduced number of insensitive channels, and the lowered single channel gating force of sensitive transducers (z_s). The single channel gating force reads: $z = \gamma\kappa d$. The scaling factor γ and the gating swing are expected to stay constant, whilst the spring constant κ should be reduced (Albert et al. 2007a). This reduced spring constant could be the reason for the lowered single channel gating force of the sensitive transducers.

Additional experiments will be required to answer finally the question, whether NOMPC ankyrin repeats serve as the gating spring. Tripling and quadrupling the count of ankyrin repeats could lead to a more distinct phenotype. Such data should help to judge, whether the phenotype is only due to an altered number of channels, or if it is due to the altered gating force.

Direct examination of the length of tagged ankyrin repeats, via electron microscopy, would solve the question, whether additional ankyrin repeats lead to differences in Johnston's organ neuron structure.

My physiological results of antennal fluctuations and the gating compliance strengthen the hypothesis, that ankyrin repeats are candidates for the gating spring. The hypothesis suggested, that a different length of the gating spring should result in a softer *Drosophila* antenna. This is shown by a decreased antennal best frequency, increased fluctuation power and decreased asymptotic stiffness (K_{inf}).

4 Appendix

4.1 List of abbreviations

Abbreviation	Explanation
AIC	Akaike information criterion
AICc	Akaike information criterion with correction for finite sample size
bf	best frequency
CAP	compound action potential
GAL4	transcriptional activator (galactose)
GO	Gene Ontology
JO	Johnston's organ
PSD	power spectral density
UAS	upstream activating sequence

4.2 List of figures

4.3 List of tables

4.4 Bibliography

Adams, M. D., S. E. Celniker, R. A. Holt, C. A. Evans, J. D. Gocayne, P. G. Amanatides, S. E. Scherer, et al. 2000. The genome sequence of Drosophila melanogaster. Science 287:2185–2195.

Albert, J. T. 2006. Mechanical tracing of protein function in the Drosophila ear. Nature Neuroscience Protocols 10.1038/np.

Albert, J. T., B. Nadrowski, and M. C. Göpfert. 2007a. Drosophila mechanotransduction - linking proteins and functions. Fly (Austin) 1:238–241.

Albert, J. T., B. Nadrowski, and M. C. Göpfert. 2007b. Mechanical signatures of transducer gating in the Drosophila ear. Current biology: CB 17:1000–6.

Albert, J. T., B. Nadrowski, A. Kamikouchi, and M. C. Göpfert. 2006. Mechanical tracing of protein function in the Drosophila ear. Nat Protocol doi:10.103.

Alloway, P. G., and P. J. Dolph. 1999. A role for the light-dependent phosphorylation of visual arrestin. Proceedings of the National Academy of Sciences of the United States of America 96:6072–6077.

Ashburner, M., C. A. Ball, J. A. Blake, D. Botstein, H. Butler, J. M. Cherry, A. David, et al. 2000. Gene ontology: tool for the unification of biology. The Gene Ontology Consortium. Nat Gene 25:25–29.

Bettencourt Da Cruz, A., M. Schwärzel, S. Schulze, M. Niyyati, M. Heisenberg, and D. Kretzschmar. 2005. Disruption of the MAP1B-related protein FUTSCH leads to changes in the neuronal cytoskeleton, axonal transport defects, and progressive neurodegeneration in Drosophila. Molecular Biology of the Cell 16:2433–2442.

Burnham, K. P., and D. R. Anderson. 2002. Model Selection and Multimodel Inference: a Practical Information-theoretic Approach, 2nd edn. Springer-Verlag, New York. New York Springer (Vol. 60, p. 488).

Caldwell, J. C., and D. F. Eberl. 2002. Towards a molecular understanding of Drosophila hearing. J Neurobiol 53:172–189.

Cheng, L. E., W. Song, L. L. Looger, L. Y. Jan, and Y. N. Jan. 2010. The role of the TRP channel NompC in Drosophila larval and adult locomotion. Neuron 67:373–80.

Chou, W. H., K. J. Hall, D. B. Wilson, C. L. Wideman, S. M. Townson, L. V Chadwell, and S. G. Britt. 1996. Identification of a novel Drosophila opsin reveals specific patterning of the R7 and R8 photoreceptor cells. Neuron 17:1101–15.

Corey, D. P., and A. J. Hudspeth. 1983. Kinetics of the receptor current in bullfrog saccular hair cells. J Neurosci 3:962–976.

Dolph, P. J., R. Ranganathan, N. J. Colley, R. W. Hardy, M. Socolich, and C. S. Zuker. 1993. Arrestin function in inactivation of G protein-coupled receptor rhodopsin in vivo. Science 260:1910–6.

Dong, P. D. S., J. S. Dicks, and G. Panganiban. 2002. Distal-less and homothorax regulate multiple targets to pattern the Drosophila antenna. Development Cambridge England 129:1967–1974.

Dong, P. D. S., S. V Todi, D. F. Eberl, and G. Boekhoff-Falk. 2003. Drosophila spalt/spalt-related mutants exhibit Townes-Brocks' syndrome phenotypes. PNAS 100:10293–10298.

Eberl, D. F. 1999. Feeling the vibes: chordotonal mechanisms in insect hearing. Current opinion in neurobiology 9:389–93.

Eberl, D. F., G. M. Duyk, and N. Perrimon. 1997. A genetic screen for mutations that disrupt an auditory response in Drosophila melanogaster. Proc Natl Acad Sci U S A 94:14837–14842.

Eberl, D. F., R. W. Hardy, and M. J. Kernan. 2000. Genetically similar transduction mechanisms for touch and hearing in Drosophila. J Neurosci 20:5981–5988.

Effertz, T. 2011. *Candidate mechanosensitive transduction channels in Drosophila melanogaster.* Georg-August University of Göttingen - PhD thesis.

Effertz, T., B. Nadrowski, D. Piepenbrock, J. T. Albert, and M. C. Göpfert. 2012. Direct gating and mechanical integrity of Drosophila auditory transducers require TRPN1. Nature neuroscience 15:1198–200.

Effertz, T., R. Wiek, and M. C. Göpfert. 2011. NompC TRP Channel Is Essential for Drosophila Sound Receptor Function. Current biology: CB 21:592–7.

Ernst, M. O., and H. H. Bülthoff. 2004. Meging the senses into a robust percept. Trends in Cognitive Sciences 8:162–169.

Ewing, A. W. 1978. The antenna of Drosophila as a love song receptor. Physiol. Entomol. 3:33–36.

Fettiplace, R., and C. M. Hackney. 2006. The sensory and motor roles of auditory hair cells. Nat Rev Neurosci 7:19–29.

Golldamm, J. 2010. *Elektrophysiologie des Hörens in Drosophila melanogaster - Die Erforschung der Taubheitsgene als Grundstein zur Analyse des auditorischen Systems.* Georg-August University of Göttingen - Bachelor thesis.

Gong, Z., W. Son, Y. D. Chung, J. Kim, D. W. Shin, C. A. McClung, Y. Lee, et al. 2004. Two interdependent TRPV channel subunits, inactive and Nanchung, mediate hearing in Drosophila. J Neurosci 24:9059–9066.

Göpfert, M. C., J. T. Albert, B. Nadrowski, and A. Kamikouchi. 2006. Specification of auditory sensitivity by Drosophila TRP channels. Nature neuroscience 9:999–1000.

Göpfert, M. C., A. D. L. Humphris, J. T. Albert, D. Robert, and O. Hendrich. 2005. Power gain exhibited by motile mechanosensory neurons in Drosophila ears. Proceedings of the National Academy of Sciences of the United States of America 102:325–30.

Göpfert, M. C., and D. Robert. 2001. Turning the key on Drosophila audition. Nature 411:908.

Göpfert, M. C., and D. Robert. 2002. The mechanical basis of Drosophila audition. The Journal of experimental biology 205:1199–208.

Göpfert, M. C., and D. Robert. 2003. Motion generation by Drosophila mechanosensory neurons. Proc Natl Acad Sci U S A 100:5514–5519.

Göpfert, M. C., D. Robert, a D. L. Humphris, J. T. Albert, and O. Hendrich. 2003. Motion generation by Drosophila mechanosensory neurons. Proceedings of the National Academy of Sciences of the United States of America 102:325–30.

Grätsch, S. 2010. *Genetic Hearing Defects in Drosophila melanogaster*. Georg-August University of Göttingen - Bachelor thesis.

Gregory, S. G., K. F. Barlow, K. E. McLay, R. Kaul, D. Swarbreck, A. Dunham, C. E. Scott, et al. 2006. The DNA sequence and biological annotation of human chromosome 1. Nature 428:529–535.

Gupta, B. P., and V. Rodrigues. 1997. Atonal is a proneural gene for a subset of olfactory sense organs in Drosophila. Genes Cells 2:225–233.

Hardie, R. C. 2012a. Polarization vision: Drosophila enters the arena. Current biology: CB 22:R12–4.

Hardie, R. C. 2012b. Phototransduction mechanisms in Drosophila microvillar photoreceptors. Wiley Interdisciplinary Reviews: Membrane Transport and Signaling 1:162–187.

Held, L. I. 1991. Bristle patterning in Drosophila. BioEssays news and reviews in molecular cellular and developmental biology 13:633–640.

Henry, C., R. Overbeek, and R. L. Stevens. 2010. Building the blueprint of life. Biotechnology Journal 5:695–704.

Howard, J., and S. Bechstedt. 2004. Hypothesis: A helix of ankyrin repeats of the NOMPC-TRP ion channel is the gating spring of mechanoreceptors. Current Biology 14:224–226.

Howard, J., and A. J. Hudspeth. 1987. Mechanical relaxation of the hair bundle mediates adaptation in mechanoelectrical transduction by the bullfrog's saccular hair cell. Proc Natl Acad Sci U S A 84:3064–3068.

Howard, J., and A. J. Hudspeth. 1988. Compliance of the hair bundle associated with gating of mechanoelectrical transduction channels in the bullfrog's saccular hair cell. Neuron 1:189–199.

Hudspeth, A. J. 1989. How the ear's works work. Nature 341:397–404.

Hummel, T., K. Krukkert, J. Roos, G. Davis, and C. Klämbt. 2000. Drosophila Futsch/22C10 is a MAP1B-like protein required for dendritic and axonal development. Neuron 26:357–370.

Jarman, A. P., E. H. Grell, L. Ackerman, L. Y. Jan, and Y. N. Jan. 1994. Atonal is the proneural gene for Drosophila photoreceptors. Nature 369:398–400.

Jarman, A. P., Y. Sun, L. Y. Jan, and Y. N. Jan. 1995. Role of the proneural gene, atonal, in formation of Drosophila chordotonal organs and photoreceptors. Development Cambridge England 121:2019–2030.

Jemc, J., and I. Rebay. 2007. The eyes absent family of phosphotyrosine phosphatases: properties and roles in developmental regulation of transcription. Annual review of biochemistry 76:513–38.

Jonsson, T., E. a. Kravitz, and R. Heinrich. 2011. Sound production during agonistic behavior of male Drosophila melanogaster. Fly 5:29–38.

Kamikouchi, A., H. K. Inagaki, T. Effertz, O. Hendrich, A. Fiala, M. C. Göpfert, and K. Ito. 2009. The neural basis of Drosophila gravity-sensing and hearing. Nature 458:165–171.

Kamikouchi, A., T. Shimada, and K. E. I. Ito. 2006. Comprehensive classification of the auditory sensory projections in the brain of the fruit fly Drosophila melanogaster. J Comp Neurol 499:317–356.

Katz, B., and B. Minke. 2009. Drosophila photoreceptors and signaling mechanisms. Frontiers in cellular neuroscience 3:2.

Kernan, M., D. Cowan, and C. Zuker. 1994. Genetic dissection of mechanosensory transduction: mechanoreception-defective mutations of Drosophila. Neuron 12:1195–206.

Kwon, Y., W. L. Shen, H.-S. Shim, and C. Montell. 2010. Fine thermotactic discrimination between the optimal and slightly cooler temperatures via a TRPV channel in chordotonal neurons. The Journal of neuroscience : the official journal of the Society for Neuroscience 30:10465–71.

Lee, J., S. Moon, Y. Cha, and Y. D. Chung. 2010. Drosophila TRPN(=NOMPC) channel localizes to the distal end of mechanosensory cilia. PloS one 5:e11012.

Liang, X., J. Madrid, R. Gärtner, J.-M. Verbavatz, C. Schiklenk, M. Wilsch-Bräuninger, A. Bogdanova, et al. 2013. A NOMPC-dependent membrane-microtubule connector is a candidate for the gating spring in fly mechanoreceptors. Current biology : CB 23:755–63.

Liang, X., J. Madrid, H. S. Saleh, and J. Howard. 2011. NOMPC, a member of the TRP channel family, localizes to the tubular body and distal cilium of Drosophila campaniform and chordotonal receptor cells. Cytoskeleton (Hoboken, N.J.) 68:1–7.

Lindsley, D. L., and G. G. Zimm. 1992. The genome of Drosophila melanogaster. Annual Review of Genomics and Human Genetics 4:89–117.

Liu, L., Y. Li, R. Wang, C. Yin, Q. Dong, H. Hing, C. Kim, et al. 2007. Drosophila hygrosensation requires the TRP channels water witch and nanchung. Nature 450:294–298.

Meyer-Jürgens, S. 2012. *New auditory relevant genes in Drosophila melanogaster*. Georg-August University of Göttingen - Bachelor thesis.

Minke, B., and M. Peters. 2011. Cell biology. Rhodopsin as thermosensor? Science (New York, N.Y.) 331:1272–3.

Mollereau, B., M. Dominguez, R. Webel, N. J. Colley, B. Keung, J. F. De Celis, and C. Desplan. 2001. Two-step process for photoreceptor formation in Drosophila. Nature 412:911–913.

Montell, C. 1999. Visual transduction in Drosophila. Annual review of cell and developmental biology 15:231–68.

Montell, C. 2012. Drosophila visual transduction. Trends in neurosciences 35:356–63.

Moreira, S., S. Breton, and G. Burger. 2012. Unscrambling genetic information at the RNA level. Wiley interdisciplinary reviews RNA 3:213–28.

Moses, K., M. C. Ellis, and G. M. Rubin. 1989. The glass gene encodes a zinc-finger protein required by Drosophila photoreceptor cells. Nature 340:531–536.

Munkong, R., and B.-H. J. B.-H. Juang. 2008. Auditory perception and cognition. IEEE Signal Processing Magazine 25:98–117.

Nadrowski, B., J. T. Albert, and M. C. Göpfert. 2008. Transducer-based force generation explains active process in Drosophila hearing. Current biology : CB 18:1365–72.

Nadrowski, B., and M. C. Göpfert. 2009. Modeling auditory transducer dynamics. Curr Opin Otolaryngol Head Neck Surg 17:400–406.

Olson, E. S., H. Duifhuis, and C. Steele. 2012. Von Békésy and cochlear mechanics. Hearing Research 1–13.

Pielage, J., L. Cheng, R. D. Fetter, P. M. Carlton, J. W. Sedat, and G. W. Davis. 2008. A presynaptic giant ankyrin stabilizes the NMJ through regulation of presynaptic microtubules and transsynaptic cell adhesion. Neuron 58:195–209.

Piepenbrock, D. 2009. *Identifying and Characterizing Genetic Hearing Defects in Drosophila melanogaster*. Georg-August University of Göttingen - Diploma thesis.

Renfranz, P. J., and S. Benzer. 1989. Monoclonal antibody probes discriminate early and late mutant defects in development of the Drosophila retina. Developmental biology 136:411–29.

Riabinina, O., M. Dai, T. Duke, and J. T. Albert. 2011. Active process mediates species-specific tuning of Drosophila ears. Current biology : CB 21:658–64.

Rister, J., and C. Desplan. 2011. The retinal mosaics of opsin expression in invertebrates and vertebrates. Developmental neurobiology 71:1212–1226.

Roos, J., T. Hummel, N. Ng, C. Klämbt, and G. W. Davis. 2000. Drosophila Futsch regulates synaptic microtubule organization and is necessary for synaptic growth. Neuron 26:371–82.

Roy, M., E. Sivan-Loukianova, and D. F. Eberl. 2013. Cell-type-specific roles of Na+/K+ ATPase subunits in Drosophila auditory mechanosensation. Proceedings of the National Academy of Sciences of the United States of America 110:181–6.

Rüdiger, W., and G. Walter. 2007. Zoologie (24. Auflag., p. 954). Thieme Verlag KG, Stuttgart.

Sakai, T., and N. Ishida. 2001. Time, love and species. Neuro endocrinology letters 22:222–8.

Salcedo, E., A. Huber, S. Henrich, L. V Chadwell, W. H. Chou, R. Paulsen, and S. G. Britt. 1999. Blue- and green-absorbing visual pigments of Drosophila: ectopic expression and physiological characterization of the R8 photoreceptor cell-specific Rh5 and Rh6 rhodopsins. The Journal of neuroscience : the official journal of the Society for Neuroscience 19:10716–26.

Schmitz, J. 2010. *Hearing and gravitaxis in Drosophila melanogaster*. Georg-August University of Göttingen - Bachelor thesis.

Sehadova, H., F. T. Glaser, C. Gentile, A. Simoni, A. Giesecke, J. T. Albert, and R. Stanewsky. 2009. Temperature entrainment of Drosophila's circadian clock involves the gene nocte and signaling from peripheral sensory tissues to the brain. Neuron 64:251–266.

Senthilan, P. 2010. *Identification and characterization of deafness genes in drosophila melanogaster*. Georg-August University of Göttingen - PhD thesis.

Senthilan, P. R., Q. Lu, and M. C. Göpfert. 2010. Grundlagen des Hör- und Gleichgewichtssystems. Plinkert PK, Klingmann C: Hören und Gleichgewicht im Blick des gesellschaftlichen Wandels (pp. 3–8). Springer.

Senthilan, P. R., D. Piepenbrock, G. Ovezmyradov, B. Nadrowski, S. Bechstedt, S. Pauls, M. Winkler, et al. 2012. Drosophila Auditory Organ Genes and Genetic Hearing Defects. Cell 150:1042–1054.

Shen, W. L., Y. Kwon, A. a Adegbola, J. Luo, A. Chess, and C. Montell. 2011. Function of rhodopsin in temperature discrimination in Drosophila. Science (New York, N.Y.) 331:1333–6.

Sukharev, S., and F. Sachs. 2012. Molecular force transduction by ion channels - diversity and unifying principles. Journal of Cell Science d.

Sun, Y., L. Liu, Y. Ben-Shahar, J. S. Jacobs, D. F. Eberl, and M. J. Welsh. 2009. TRPA channels distinguish gravity sensing from hearing in Johnston's organ. Proceedings of the National Academy of Sciences of the United States of America 106:13606–11.

Tavsanli, B. C., E. J. Ostrin, H. K. Burgess, B. W. Middlebrooks, T. A. Pham, and G. Mardon. 2004. Structure-function analysis of the Drosophila retinal determination protein Dachshund. Developmental Biology 272:231–247.

Tian, Y., W. Hu, H. Tong, and J. Han. 2011. Phototransduction in Drosophila. Science China. Life sciences 55:27–34.

Toivonen, J. M., K. M. O'Dell, N. Petit, S. C. Irvine, G. K. Knight, M. Lehtonen, M. Longmuir, et al. 2001. Technical knockout, a Drosophila model of mitochondrial deafness. Genetics 159:241–254.

Tootoonian, S., P. Coen, R. Kawai, and M. Murthy. 2012. Neural representations of courtship song in the Drosophila brain. The Journal of neuroscience : the official journal of the Society for Neuroscience 32:787–98.

Wahl, H.-W., V. Heyl, P. M. Drapaniotis, K. Hörmann, J. B. Jonas, P. K. Plinkert, and K. Rohrschneider. 2013. Severe Vision and Hearing Impairment and Successful Aging: A Multidimensional View. The Gerontologist.

Walker, R. G., A. T. Willingham, and C. S. Zuker. 2000. A Drosophila Mechanosensory Transduction Channel. Science 287:2229–2234.

Wang, T., Y. Jiao, and C. Montell. 2007. Dissection of the pathway required for generation of vitamin A and for Drosophila phototransduction. The Journal of cell biology 177:305–16.

Wang, T., and C. Montell. 2007. Phototransduction and retinal degeneration in Drosophila. Pflügers Archiv : European journal of physiology 454:821–47.

Wang, T., X. Wang, Q. Xie, and C. Montell. 2008. The SOCS box protein STOPS is required for phototransduction through its effects on phospholipase C. Neuron 57:56–68.

Wang, T., H. Xu, J. Oberwinkler, Y. Gu, R. C. Hardie, and C. Montell. 2005. Light activation, adaptation, and cell survival functions of the Na+/Ca2+ exchanger CalX. Neuron 45:367–78.

Wang, X., T. Wang, J. D. Ni, J. von Lintig, and C. Montell. 2012. The Drosophila Visual Cycle and De Novo Chromophore Synthesis Depends on rdhB. The Journal of neuroscience : the official journal of the Society for Neuroscience 32:3485–91.

Whelan, J., B. Burke, A. Rice, M. Tong, and D. Kuebler. 2010. Sensitivity to seizure-like activity in Drosophila following acute hypoxia and hypercapnia. Brain Research 1316:120–128.

Wiek, R. J. 2013. *A Functional Characterization of Drosophila Chordotonal Organs.* Georg-August University of Göttingen - PhD thesis.

Yack, J. E. 2004. The structure and function of auditory chordotonal organs in insects. Microscopy research and technique 63:315–37.

Yamada, T., Y. Takeuchi, N. Komori, H. Kobayashi, Y. Sakai, Y. Hotta, and H. Matsumoto. 1990. A 49-kilodalton phosphoprotein in the Drosophila photoreceptor is an arrestin homolog. Science (New York, N.Y.) 248:483–6.

Yan, Z., W. Zhang, Y. He, D. Gorczyca, Y. Xiang, L. E. Cheng, S. Meltzer, et al. 2013. Drosophila NOMPC is a mechanotransduction channel subunit for gentle-touch sensation. Nature 493:221–5.

Yorozu, S., A. Wong, B. J. Fischer, H. Dankert, M. J. Kernan, A. Kamikouchi, K. Ito, et al. 2009. Distinct sensory representations of wind and near-field sound in the Drosophila brain. Nature 458:201–5.

Zanini, D., and M. C. Göpfert. 2013. Mechanosensation: tethered ion channels. Current biology : CB 23:R349–51.

4.5 Methods and experimental procedure

4.5.1 Fly husbandry

Drosophila melanogaster fly strains were obtained from the Bloomington Stock Centre and the Exelixis Collection at Harvard Medical School. Fly strains where maintained under normal conditions: 12 hours light : 12 hours dark rhythm at 18°C, with 60 % humidity. To facilitate fly crossing they were kept at 25°C for period of crossing, and then stored at 18°C. Flies were grown on standard fly food made of agar, soy bean flour, yeast, maize meal and treacle.

Dietary fly food was made according to "Function of Rhodopsin in Temperature Discrimination in *Drosophila*", supporting online material (Shen et al. 2011). Vitamin A depleted medium: water, yeast, glucose, rice powder, cholesterol, butyl p-hydroxybenzoate and propionic acid. Retinal was obtained from Sigma (#R2500), and added to the dietary fly food (dissolved in ethanol).

4.5.2 Statistical evaluation

For statistical data evaluation, the two-tailed rank sum Mann-Whitney U test ($p < 0.05$), with correction for multiple comparisons, using the Benjamini and Yekutieli procedure for control of the false discovery rate, was performed (Matlab R2010b ranksum (x,y) and the Benjamini & Yekutieli procedure for controlling the false).

4.5.3 Electron micrography: Probing the ultrastructural integrity of Johnston's organ neurons

Electron microscopy was carried out on ultrathin sections (Reichert-Jung Ultracut E, Diatom diamond knife) using a Zeiss EM900 transmission electron microscope, and a JEOL electron microscope (JEM 1011), equipped with Gatan Orius 1200A camera.

Day 1	Fixation	24 hours	KK
	2 % Paraformaldehyde		
	2.5 % Glutardialdehyd		
	in 0.1 M Nacacodylatpuffer		
	pH 7.4		
Day 2	Washing step	3 x 5 minutes	RT
	in 0.05 Nacaco		
	Osmierung	4 hours	KK
	2% OsO_4 in buffer		
	Washing step	Short	RT
	In buffer		
	Dehydrate		
	30 – 96 % ETOH	2 x 7 minutes	RT
	Uranylacetat in 70% ETOH	1 x 30 minutes	
	100 % ETOH	2 x 10 minutes	
	Propylenoxid	2 x 10 minutes	
	Intermedien		
	Propylenoxid/Durcupan 3:1	1 hour	RT
	Propylenoxid/Durcupan 1:1	Overnight	
Day 3	Propylenoxid/Durcupan1:3	1 hour	
	Embedding: Durcupan 48 h bei 650	48 hours	oven

Table 8: EM protocol for sample fixation.

Fixation protocol to prepare *Drosophila* second antennal segments, for transmission electron microscopy. Reported and carried out by Margret Winkler

4.5.4 Antibody staining and confocal microscopy

Confocal microscopy was carried out using a Leica TCS SP2 microscope. Samples were prepared according to the protocol (see below). Post processing, z-projection and brightness adjustment with ImagJ 1.47g. Antibodies used: Rhodopsin 5 and Rhodopsin 6 from Steven Britt (Chou et al. 1996), antiGFP (GenTex GTX13970), antiHRP(Sigma P5774).

Fixation of *Drosophila* heads	
In 4 % paraformaldehyd	
Embedding in albumin gelatin and postfixation in 6% paraformaldehyd	Overnight
Cutting slices (vibratom): 30 µm	
Washing step: 1 % PBST	
Blocking in 10 % normal goat serum: 0.25 % BSA in 1 % PBST	2 hours
Staining with rhodopsin antibody 1:100 and HRP 1:300 in blockinsolution on shaker	Overnight
Washing step PBSt 1 %	3x
Second antibodies:	2 hours on shaker, in room temperature
Anti rabbit 488 (HRP) 1:300	
Anti mouse 546 (Rhodopsin)1:300	
Phalloidin 633 1:40	
Washing step: PBS 4x	
Cover the sections with DABCO	

Table 9: Protocol to prepare *Drosophila* JO samples for confocal microscopy.

Reported and carried out by Stephanie Pauls.

4.5.5 Cross santa-maria

Fly cross to obtain *santa-maria* rescue flies. This flies express in all Johnston's organ neurons (under the control of NP0761 (Kamikouchi et al. 2006)) an intact copy of the *santa-maria* gene.

$$w^{*}; santa-maria^{1}; P\{w^{+mC} = UAS-santa-maria.W\}3 \times w; \frac{Sp}{SM1}; \frac{NP0761}{TM65b,Tb} = w; \frac{santa-maria^{1}}{Sm1}; \frac{P\{w^{+mC} = UAS-santa-maria.W\}3}{NP0761}$$

$$w; \frac{santa-maria^{1}}{Sm1}; \frac{P\{w^{+mC} = UAS-santa-maria.W\}3}{NP0761} \times w; \frac{santa-maria^{1}}{Sm1}; \frac{P\{w^{+mC} = UAS-santa-maria.W\}3}{NP0761} = w; santa-maria^{1}; \frac{P\{w^{+mC} = UAS-santa-maria.W\}3}{NP0761}$$

4.6 Quotation

National Human Genome Research Institute

National Institutes of Health
U.S. Department of Health and Human Services

National Human Genome Research Institute
National Institutes of Health
Department of Health and Human Services
and
Office of Science
U.S. Department of Energy

The Human Genome Project Completion: Frequently Asked Questions

On April 14, 2003 the National Human Genome Research Institute (NHGRI), the Department of Energy (DOE) and their partners in the International Human Genome Sequencing Consortium announced the successful completion of the Human Genome Project.

Unquoted text is skipped.
...
..
.

What will the next 50 years of medical science look like?

Having the essentially complete sequence of the human genome is similar to having all the pages of a manual needed to make the human body. The challenge to researchers and scientists now is to determine how to read the contents of all these pages and then understand how the parts work together and to discover the genetic basis for health and the pathology of human disease. In this respect, genome-based research will eventually enable medical science to develop highly effective diagnostic tools, to better understand the health needs of people based on their individual genetic make-ups, and to design new and highly effective treatments for disease.

Individualized analysis based on each person's genome will lead to a very powerful form of preventive medicine. We'll be able to learn about risks of future illness based on DNA analysis. Physicians, nurses, genetic counselors and other health-care professionals will be able to work with individuals to focus efforts on the things that are most likely to maintain health for a particular individual. That might mean diet or lifestyle changes, or it might mean medical surveillance. But there will be a personalized aspect to what we do to keep ourselves healthy. Then, through our understanding at the molecular level of how things like diabetes or heart disease or schizophrenia come about, we should see a whole new generation of interventions, many of which will be drugs that are much more effective and precise than those available today.

Figure 45: Quotation from paragraph '1.1.1 Motivation: Identifying *Drosophila* hearing genes'

4.7 Acknowledgements

Nach nun über drei Jahren Wissen schaffen möchte ich mich ganz herzlich bei meinem Doktorvater Martin Göpfert bedanken. Danke für die Möglichkeit, eigenständig Projekte zu entwerfen, zu bearbeiten, Bachelorarbeiten zu betreuen, sowie für deine engagierte Unterstützung.

Vielen Dank an Tobias Moser und André Fiala, die meine Promotion als ‚Thesis Committee' auf Meetings sowie Retreats nach St. Andreasberg, Eisennach, Hiddensee sowie in die Alpen begleitet haben.

Danken möchte ich allen, mit denen ich intensiv an gemeinsamen Projekten gearbeitet habe: Thomas und Christian (transducer gating), Pingkalai (screen), Margret (electron micrography), Steffi (immunohistochemistry), Uwe (reception of electric fields in bees) und Fabien (‚*hemingway*'), sowie meinen Bachelorstudierenden: Swantje, Joscha, Julia und Sandra.

Bei Robert und Ralf möchte ich mich für eine sehr erfolgreiche Zusammenarbeit sowie gemeinsames Rennradfahren und diverse sportliche Ereignisse – Tour d'Energie und Göttinger Volkstriathlon – bedanken. Philipp danke ich für die exzellente gemeinsame Organisation des „Neurobiology Doctoral Students Workshop 2013" sowie für seine konstruktive Hilfe. Bei Sophia bedanke ich mich für die schönen Fotos des LDV-setup sowie die große Unterstützung in der Endphase meiner Promotion.

Für interessante Diskussionen sowie Korrekturen gebe ich meinen Dank weiter an: Judith, Helen, Hilde, Bart, Georg, Björn, Kathi, Krissy, Radek und Paule.

Ich danke zudem allen weiteren Personen meiner Arbeitsgruppe, die mich während der Promotion unterstützt und begleitet haben: Gudrun, Damiano, Somdatta, Seol-hee, Marta, Maike, Andreas, Mit, Heribert, Silvia und Natasa.

Die ideelle sowie finanzielle Förderung erhielt ich durch die Studienstifung des deutschen Volkes – Göttinger Graduiertenschule für Neurowissenschaften, Biophysik und Molekulare Biowissenschaften – sowie der Georg-August-Universität Göttingen. Ich bedanke mich dafür herzlich.

David Piepenbrock